2005-07-27

Characterization of JNK Binding Proteins: A Dissertation

Jeffrey Scott Rogers
University of Massachusetts Medical School

Characterization of JNK Binding Proteins

A Dissertation Presented

By

Jeffrey Scott Rogers

Submitted to the Faculty of the

University of Massachusetts Graduate School of Biomedical Sciences, Worcester

In partial fulfillment of the requirement for the degree of:

DOCTOR OF PHILOSOPHY

July 27th, 2005

Interdisciplinary Graduate Program

Characterization of JNK Binding Proteins

A Dissertation Presented
By

Jeffrey Scott Rogers

Approved as to style and content by:

Craig Peterson, Ph.D., Chair of Committee

Lan Xu, Ph.D., Member of Committee

Kendall Knight, Ph.D., Member of Committee

Craig Mello, Ph.D., Member of Committee

John Blenis, Ph.D., Member of Committee

Roger J. Davis, Ph.D., Thesis Advisor

Anthony Carruthers, Ph.D.,
Dean, Graduate School of Biomedical Sciences

Interdisciplinary Graduate Program

July 27th, 2005

Portions of this dissertation appear in the following publications:

Dickens, M., **Rogers, JS.,** Cavanagh, J., Raitano, A., Xia, Z., Halpern, JR., Greenberg, ME., Sawyers, CL., Davis, RJ. A cytoplasmic inhibitor of the JNK signal transduction pathway. *Science* 1997 Aug 1;227(5326): 693-6

Raingeaud, J., Gupta, S., **Rogers, JS.,** Dickens, M., Han, J., Ulevitch, RJ., Davis, RJ., Pro-inflammatory cytokines and environmental stress cause p38 mitogen-activated protein kinase activation by dual phosphorylation on tyrosine and theonine. *J. Biol. Chem.* 1995 Mar 31;270 (13): 7420-6

The following work has been submitted for publication:

Rogers, JS., Dickens, M., Davis, RJ., Characterization of a novel JNK binding protein, JMP1.

Rogers, JS., Davis, RJ., Analysis of a breeding defect in *Jnk3*$^{-/-}$ male mice.

DEDICATION

This work is dedicated to my parents,

Frank and Sharon Rogers

Your unconditional love, support and unwavering faith have kept me on this path,

many times after I would've turned away.

None of this would have been possible without the both of you.

ACKNOWLEDGEMENTS

I would like to thank my thesis research mentor, Dr. Roger J. Davis, for his encouragement, leadership and support during the course of my graduate career and his guidance while preparing this dissertation. I am grateful for the patience, help and time of my thesis research advisory council, Drs. Craig Peterson, Kendall Knight, Lan Xu and Craig Mello. I would like to thank both past and present members of the Davis laboratory group for their invaluable assistance and peership along the way. I gratefully acknowledge the help of Drs. Gregory Viglianti and David Schmidt for their scientific mentoring. My appreciation goes to Dr. Eric A. Schon of Columbia University for providing the spark. To my former bench-mate, roommate and colleague, Dr. Mark A. Wysk for the friendship, sushi, single-malt and numerous pints we've shared together. A special thanks to Dr. Claire Weston for her friendship and encouragement. Many thanks go to Drs. Stephen Doxsey, Martin Dickens, Victor Lazaron, Diane Casey, Ralph Zottola, David Lapointe, Laxman Gangwani, Gregory Pazour and David Raden, as well as Tamera Barrett, Beth Doran, Judy Reilly and Julie Cavanagh. Finally, to my friends and family: Laura Rogers, Lonnie DiNello, the Sward and Fries families, Andy & Michelle Debatis, Jeffery Eddy, Will Sanborn, Shawn Reed, Jen Seng, Bill McInnich, Melinda Berkman, Judy Masucci, Jim Sadlock... and the many rest of you that I have not listed by name, but will always have in mind, thank you for being there.

"Every honest researcher I know admits he's just a professional amateur. He's doing whatever he's doing for the first time. That makes him an amateur. He has sense enough to know that he's going to have a lot of trouble, so that makes him a professional."

-- Charles Franklin Kettering (1876-1958) U. S. Engineer and Inventor

ABSTRACT

The JNK signal transduction pathway mediates a broad, complex biological process in response to inflammatory cytokines and environmental stress. These responses include cell survival and apoptosis, proliferation, tumorigenesis and the immune response. The divergent cellular responses caused by the JNK signal transduction pathway are often regulated by spatial and cell type contexts, as well as the interaction with other cellular processes. The discovery of additional components of the JNK signal transduction pathway are critical to elucidate the stress response mechanisms in cells.

This thesis first discusses the cloning and characterization of two novel members of the JNK signal transduction pathway. JIP1 and JMP1 were initially identified from a murine embryo library through a yeast Two-Hybrid screen to identify novel JNK interacting proteins. Full length cDNAs of both genes were cloned and analyzed. JIP1 represents the first member of the JIP group of JNK scaffold proteins which were characterized. The JNK binding domain (JBD) of JIP1 matches the D-domain consensus of other JNK binding proteins, and it demonstrates JNK binding both *in vitro* and *in vivo.* This JNK binding was demonstrated to inhibit JNK signal transduction and over-expression of JIP1 inhibits the JNK mediated pre-B cell transformation by *bcr-abl.* Over-expressed JIP1 also sequesters JNK in the cytoplasm, which may be a mechanism of the inhibition of JNK signaling. A new, high-resolution digital imaging microscopy

technique using deconvolution demonstrated the absence of JNK1 in the nucleus of co-transfected JIP1 and JNK1 cells.

The other protein discussed in this thesis is JMP1, a novel JNK binding, microtubule co-localized protein. There is a JBD in the JMP1 carboxyl end and a consensus D-domain within this region. The JMP1 JBD demonstrates an increased association with phospho-JNK from UV irradiated cells compared to un-irradiated cells *in vivo.* JMP1 also has 12 WD-repeat motifs in its amino terminal end which are required for microtubule co-localization. JMP1 demonstrates a cell cycle specific localization at the mitotic spindle poles. This co-localization is dependent on intact microtubules and the amino-terminal WD-repeats are required for this localization. JMP1 mRNA is highly expressed in testis tissues. Immunocytochemistry on murine testis sections using an affinity purified anti-JMP1 antibody demonstrates JMP1 protein in the lumenal compartment of the seminiferous tubules. JMP1 protein is expressed in primary and secondary spermatocytes, cells which are actively undergoing meiosis.

The results obtained from the localization of JMP1 in meiotic spermatocytes led to an investigation of the roles of JNK signal transduction in the testis. The testis is an active region of cellular proliferation, apoptosis and differentiation, which make it an appealing model for studying JNK signal transduction. However, the roles JNK signaling have in the testis are poorly understood. I investigated the reproduction capability of *Jnk3*$^{-/-}$ male mice and discovered older *Jnk3*$^{-/-}$ males had a reduced capacity to impregnate females

compared to younger animals and age-matched wild type controls. The testis morphology and sperm motility of these animals were similar to wild-type animals, and there was no alteration of apoptosis in the testis. The final section of this thesis involves the study of this breeding defect and investigating for cellular defects that might account for this age-related *Jnk3*$^{-/-}$ phenotype.

TABLE OF CONTENTS

LIST OF FIGURES

LIST OF ABBREVIATIONS

α_2-MG	α_2-Macroglobulin
AKAP	A-Kinase Anchoring Protein
AP1	Activator Protein-1
ASK1	Apoptosis Signal-regulating Kinase 1
ATP	Adenosine Triphosphate
Asp	Aspartic Acid
BCIP	5-bromo-4-chloro-3-indoyl Phosphate
Bcl2	B-cell CLL/Lymphoma 2
BSA	Bovine Serum Albumin
BTB	Blood-Testis Barrier
CHOP	C/EBP-Homologous Protein
CREB	cAMP Response Element-Binding protein
DMSO	Dimethylsulfoxide
DNA	Deoxyribonucleic Acid
EGF	Epidermal Growth Factor
ERK	Extracellular signal Related Kinase
ES	Embryonic Stem cells
FADD	Fas Associated Death Domain
γ-TuRC	Gamma Tubulin Ring Complexes
Gly	Glycine
GST	Glutathione-S-Transferase

GTP	Guanosine Triphosphate
HA	Hemagglutinin
HEPES	(N-[2-Hydroxyethyl]piperazine-N'-[2-ethanesulfonic acid])
I_KB	Inhibitor of kappa B
IKK	I_KB Kinase complex (IKKα, β, γ)
IL-1	Interleukin 1
JBD	JNK Binding Domain
JIP	JNK Interacting Protein
JMP1	JNK binding, Microtubule associated Protein-1
JNK	c-Jun N-terminal Kinase
Leu	Leucine
Lys	Lysine
MAP	Microtubule Associated Protein
MAPK	Mitogen Activated Protein Kinase
MAPKK	Mitogen Activated Protein Kinase Kinase (MAP2K)
MAPKKK	Mitogen Activated Protein Kinase Kinase Kinase (MAP3K)
MEF	Mouse Embryonic Fibroblast
MEKK	MAP/ERK Kinase Kinase
MIA	Microtubule Inhibitory Agent
MKK	MAPK Kinase
MLK2	Mixed Lineage Protein Kinase 2
MLK3	Mixed Lineage Protein Kinase 3

MT	Microtubule
MTOC	Microtubule Organizing Center
NBT	Nitro-blue tetrazolium
NLS	Nuclear Localization Sequence
NFAT	Nuclear Factor of Activated T-cells
NF-KB	Nuclear factor kappa-B
ORF	Open Reading Frame
PCM	Pericentriolar Material
PEG	Polyethylene Glycol
Phe	Phenylalanine
PIPES	Piperazine-N,N'-bis[2-ethanesulfonic acid]
PKA	cAMP-dependent Protein Kinase A
PKC	Protein Kinase C
POSH	Plenty of SH3s
Pro	Proline
PTK	Protein Tyrosine Kinase
SAPK	Stress Activated Protein Kinase
Ser	Serine
SH3	Src-homology 3
SRF	Serum Response Factor
Thr	Threonine
TJ	Tight Junctions

TNF	Tumor Necrosis Factor
TNFα	Tumor Necrosis Factor alpha
TPL2	Tumor progression locus-2
TRAF	TNF Receptor Associated Factor
TUNEL	Terminal deoxynucleotidyl Transferase Biotin-dUTP Nick End Labeling
Tyr	Tyrosine
UV	Ultraviolet light
X-Gal	5-bromo-4-chloro-3-indolyl-βD-galactoside

CHAPTER I

INTRODUCTION

The JNK signal transduction pathway mediates broad and complex biological processes in response to external cellular stress. The biological results of JNK activation range from cell survival, apoptosis, proliferation, tumorigenesis and the immune response. Such processes are important not only in response to stress, but for the maintainance of homeostasis during cell proliferation and differentiation. In order to understand this complex signaling mechanism, it is critical to discover new proteins that are part of the JNK signal transduction pathway and understand their roles within cell signaling.

Mitogen--Activated Protein Kinases (MAPKs)

The Mitogen-Activated Protein Kinases (MAPK) are a family of evolutionary conserved serine/threonine kinases that play a regulatory role by the exposure of cells to growth factors, extracellular stimuli, cytokines and the extracellular matrix. This pathway coordinates signals from the cell surface to nuclear transcription factors, the cytoskeletal matrix and other downstream targets. The MAPK pathway is activated by a kinase cascade reaction where an activation signal is transduced by an upstream kinase which phosphorylates and activates a downstream kinase. The MAPK system is organized as a three-tiered kinase cascade that results in downstream phosphorylation events. The MAPK signal transduction pathway mediates a broad range of biological

responses by phosphorylation which activate and deactivate target substances, and is generally regulated by a concerted mechanism of phosphorylation and de-phosphorylation events. The rate at which the kinase cascade transduces the signal is partially controlled by specific protein-protein interactions and the understanding of how this is done is constantly evolving as new components of this pathway are discovered. There are three major MAPK subfamilies, the extra-cellular related kinases (ERKs) and the two stress-activated protein kinases (SAPKs); the c-Jun N-terminal kinases (JNKs) and the p38 kinases (Schaeffer and Weber, 1999)

c-Jun N-Terminal Kinase (JNK)

The JNK group of MAP kinases are activated by exposure to inflammatory cytokines, genotoxic agents, and environmental stress. Activated JNK phosphorylates amino terminal residues of the JunB, JunD and c-Jun family members of the AP-1 transcription factor. These activated transcription factors modulate gene expression for various biological processes involving cell proliferation and differentiation, apoptosis and cell motility (Davis, 2000).

The mammalian JNKs are encoded by three alternatively spliced genes, *Jnk1*, *Jnk2* and *Jnk3*. *Jnk1* and *Jnk2* are ubiquitously expressed while *Jnk3* has a more restricted expression limited to the brain, heart and testis. The alternative splicing creates ten different JNK isoforms with a common alternative splicing that occurs in the 3' coding region that results in the expression of both 46kDa and 55kDa protein kinases. However, there is also an alternative splicing which

is unique to both *Jnk1* and *Jnk2* between two exons within the kinase domain. This alternative splicing influences substrate specificity by altering how JNK interacts with the docking sites on substrates. (Gupta et.al. 1996). JNK docking sites are present in MAPK kinases, MAPK phosphatases as well as JNK substrates, and appear to mediate interactions through a common JNK docking sequence motif (Tanoue et al., 2000). Although there seems to be significant redundancy between each of the *Jnk* genes, the analysis of *Jnk* gene disruptions in transgenic mice indicate there are tissue specific defects in the signal transduction that might reflect the different *Jnk* isoforms expressed within these tissues (Davis, 2000).

MAPK/JNK Signal Transduction Pathways

The JNK signal transduction pathway is regulated by the concerted activity of upstream activating kinases and inactivating phosphatases requiring protein-protein interactions. JNK is activated by dual phosphorylation on Thr-183 and Tyr-185 within a conserved tripeptide (TPY) motif located within its activation domain (T-loop) by MAPKKs. Similarly, JNK is inactviated by a group of phosphatases which includes the Ser/Thr and Tyr phosphatases as well as dual specificity phosphatases (Keyse, 2000). The activation pathway involves a three-tiered protein kinase cascade involving MAPK kinase kinases (MAP3K), MAPK kinases (MAP2K) and MAPK (Fig. 1-1).

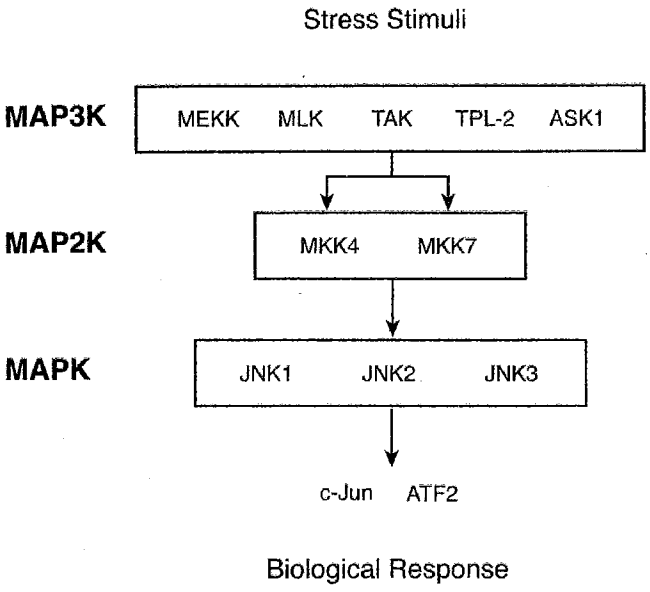

Figure 1-1 The MAPK signal transduction pathway showing the "three tiered" signaling structure involved in the kinase cascade.

There are two well characterized MAPKK that phosphorylate all ten JNK isoforms. *Mkk4* (Derijard et al., 1995) and *Mkk7* (Tournier et al., 1997) are alternatively spliced to generate multiple isoforms, though *Mkk7* isoforms are also expressed from alternative promoters (Tournier et al., 1999). MKK4 and MKK7 differ in their activation patterns based on the type of external stimuli (Tournier et al., 2001). MKK4 demonstrates stimuli-specific cross activation of the p38 MAPK pathway (Brancho et al., 2005). However, MKK7 seems to activate the JNK signal pathway exclusively (Yang et al., 1997a) (Tournier et al., 2001). While JNK activation requires a dual phosphorylation event, MKK4 seems to preferentially phosphorylate Tyr-185 and MKK7 favors Thr-183 within the JNK T-loop activation domain (Lawler et al., 1998). However, MKK4 and MKK7 act

synergistically for optimal JNK activation (Tournier et al., 2001). In studies of mouse embryo fibroblast cells with either *Mkk4* or *Mkk7* disrupted, there was a partial reduction of JNK activation in response to stress stimuli, and no JNK activity in cells with both MAPKKs disrupted (Tournier et al., 2001). Consequently, MKK4 (Ganiatsas et al., 1998; Nishina et al., 1999) and MKK7 (Wada et al., 2004) are essential for murine embryonic development as their disruprtion is embryonic lethal, but the mechanism is unclear (Dong et al., 2000b; Swat et al., 1998).

MKK4 and MKK7 are regulated by Ser/Thr phosphorylation within a conserved domain on the kinase's activation loop. There are a heterogeneous group of upstream kinases, the MAPKKKs (MAP3K), that are characterized in broad groups of highly divergent families (Davis, 2000; Kyriakis et al., 1994). These diverse families include the MEK kinase (MEKK) family including MEKK1-4, the mixed lineage kinases (MLK1-4, DLK, ZAK and LZK), TGF-β-activated kinase-1 (TAK1), Tumor Progression locus-2 (TPL2) and the apoptosis stimulating kinases (ASK1-2). Several of these MAPKKK members were identified as JNK activators using transfection assays (Fanger et al., 1997) but their physiological roles as JNK activators *in vivo* are still unclear. Gene disruption studies of the *Mekk* family member *Mekk1* in mice reveals that this gene is not essential (Xia et al., 2000; Yujiri et al., 1998; Yujiri et al., 2000). However, MEKK1 activity is apparently essential for TNF induced JNK activation in murine embryonic stem cells (Xia et al., 2000) indicating MEKK1 is likely a

physiological regulator of JNK signal transduction. Similarly, gene targeting studies reveal that MEKK2 is essential for JNK activation by Kit ligand and IgE in mast cells differentiated from embryonic stem cells (Garrington et al., 2000) and MEKK2 is essential for FGF-2 induced JNK activation in mouse embryonic fibroblast cells (Kesavan et al., 2004). MEKK3 is not essential for JNK signal transduction activation by TNF in fibroblasts derived from null embryos (Yang et al., 2001). However, the interpretation of these studies is particularly complex due to the inherent redundancy among the different MAPKKKs and their promiscuity of function.

Additional levels of complexity are added to this system by the upstream signaling that activates MAPKKKs. The MAPKKKs are activated by another highly diverse group of MAPKKKKs (MAP4K) (Minden et al., 1995) that include the Ste20 homologs p21-activated kinase (PAK), germinal center kinase (GCK), GCK-like kinase (GLK) and hematopoietic progenitor kinase (HPK) (Fanger et al., 1997). These variable cellular inputs must be integrated into the different MAPK signaling modules in order to mount an efficient biological response.

JNK Scaffold Proteins

The three-tiered structure of the MAPK activation kinase cascade has an inherent complexity that involves the integration of external stimuli through diverse numbers of upstream regulators. A key issue for stressed cells to regulate this complexity is to achieve a rapid signal specificity that is critical for efficient signal transduction. Scaffold proteins provide an organizational structure

that allows discrete clusters of signaling molecules to associate by increasing their local concentration within the cell. This organizational structure utilizes spatial and temporal regulation of the signalling process.

Scaffold proteins for the JNK signaling system have been identified that coordinate stress activated signal transduction. Known scaffold proteins include the JNK interacting proteins (JIP1-4), β-Arrestin-2, filamin, CrkII, IKK complex associated protein (IKAP), MAP kinase phosphatase X (MKPX), plenty of SH3 protein (POSH), and the SAPK pathway regulating phosphatase 1 (SKRP1) (Morrison and Davis, 2003; Weston and Davis, 2002).

The JIP proteins are the best characterized members of the JNK scaffolding proteins. JIP1 was originally identified as an inhibitor of the JNK signal transduction pathway, but this inhibition reflects the nature of the over-expression studies originally done. The signaling inhibition is apparently a result of the disruption of the normal signaling component stoichiometry and sequestration of JNK from critical upstream activation kinases and nuclear translocation (Dickens et al., 1997). Subsequent studies involving additional members of the JNK signal cascade revealed rapid and specific JNK activation. This activation was facilitated by MLK3 and MKK7 (Kelkar et al., 2000; Whitmarsh et al., 1998; Whitmarsh et al., 2001; Yasuda et al., 1999).

Scaffold proteins for the MAP-kinase modules in *S. cerevisiae* have been extensively studied. The yeast Ste5p scaffold binds components of the pheromone mating-response. Distinct regions of the Ste5p scaffold interact with

the MAP3K Ste11p, the MAP2K Ste7p and MAP kinases Fus3p and Kss1p. The activated MAP kinases initiate cellular pathways necessary for mating and filamentous growth. A second scaffold protein found in yeast, the MKK Pbs2p, also has distinct binding interactions with Ste11p and the MAP kinase Hog1p. This scaffold complex directs cellular processes involved with glycerol synthesis in response to osmotic stress. Both the Ste5p and Pbs2p represent two different MAP kinase scaffolding systems found in mammalian cells. The mammalian JIP scaffold structure most closely resembles the yeast Ste5p scaffolding mechanism (Fig. 1-2).

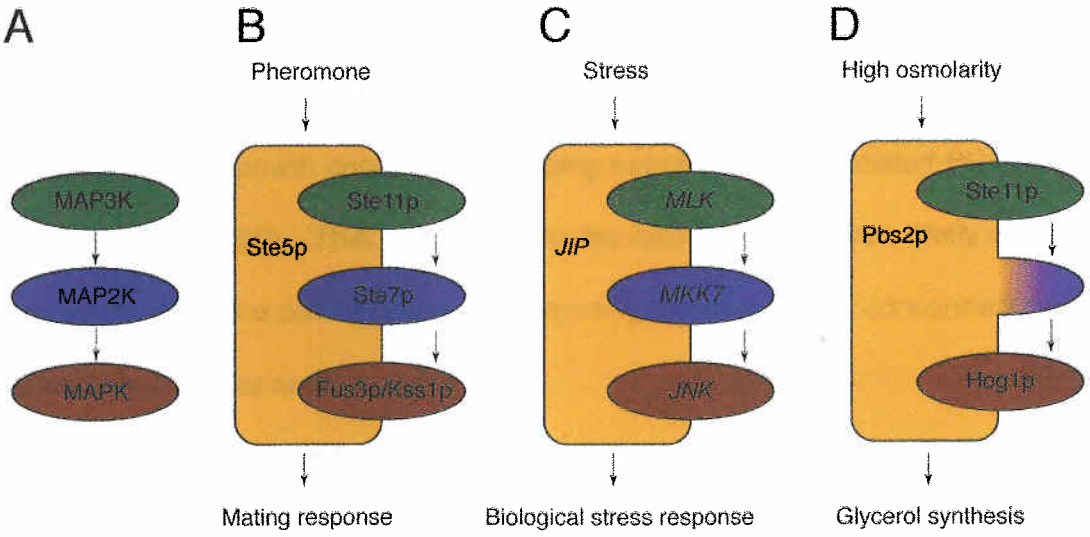

Figure 1-2. The JIP mammalian scaffold structure resembles the *S. cerevisiae* Ste5 scaffold. (A) The general MAP kinase three-tiered module. (B) The Ste5 MAP kinase scaffold structure involved with the pheromone mating response in *S. cerevisiae*. (C) The mammalian JIP scaffold structure involved with stress-mediated JNK signal transduction. (D) The Pbs2 scaffold structure involved with the glycerol synthesis response to high osmolar environmental conditions.

JIP might also coordinate the activation of opposing JNK inactivation pathways. JIP1 not only binds MLK3, MKK7 and JNK in an activation pathway, it has been shown to bind MKP7, a MAPK phosphatase that selectively

dephosphorylates JNK (Willoughby et al., 2003). In addition, there appears to be cross-talk with JIP in other stress-activated MAPK signal transduction pathways. JIP2 has been demonstrated to have cross activity with p38 signaling pathways (Buchsbaum et al., 2002; Schoorlemmer and Goldfarb, 2001). Likewise, JIP4 appears to preferentially activate the p38 MAPK kinase pathway (Kelkar et al., 2005).

The JIPs have been demonstrated to interact with the TPR tripeptide repeat domain of kinesin light chain, which is a component of the well characterized microtubule motor protein complex (Bowman et al., 2000; Verhey et al., 2001; Whitmarsh et al., 2001). This binding apparently contributes to the sub-cellular localization of JNK signaling components, as JIP1-3 have been localized to the growth cones of developing neurites in differentiated PC12 cells (Kelkar et al., 2000). This localization to the microtubule network likely adds to the efficiency of the cell response by increasing the local kinase concentrations to specific subcellular regions.

Although the JIPs are well characterized JNK scaffolding proteins, there are other scaffold proteins that interact with the JNK signaling pathway that have diffferent structures and functions than the JIP group (Morrison and Davis, 2003; Weston and Davis, 2002). The diversity seen amongst these other known scaffold proteins suggests that there are other scaffold proteins that have yet to be discovered.

JNK Signal Transduction Substrates

The JIP group of scaffold proteins mediate an efficient and rapid JNK signaling cascade. Because the activation of this module is critical for diverse cellular responses, which include stress-induced apoptosis, cell survival and oncogenic transformation, the identification of new JNK interacting proteins and phospho-substrates is crucial to understanding the biology of JNK signal transduction. There is a broad list of potential JNK substrates that include transcription factors, tumor suppressors and apoptosis regulating components. The first characterized JNK substrate was the c-Jun member of the AP-1 transcription factor complex, which provided the first link between JNK signaling and gene transcription (Kyriakis et al., 1994; Minden et al., 1994). Likewise, it has been shown that JNK phosphorylates JunB and JunD, other members of the AP-1 transcription complex (Davis, 2000).

The c-Jun substrate interaction with JNK occurs when JNK is activated by dual-phosphorylation by upstream MAPKKs (MKK7 and MKK4) which promotes JNK association, or docking, at the D-domain in the amino terminal of c-Jun. The c-Jun JNK docking site has been compared to other known JNK binding proteins in an attempt to elucidate conserved residues that form a consensus docking site. Although there is no clear overall consensus, general principles emerge. The D-domain contains an LxL ($\varphi X\varphi$) motif located 3-5 amino acids downstream from a region containing several basic residues. The D-domain is present not

only in c-Jun, but other JNK substrates like ATF2, JIPs, MKK4, MKK7, Elk-1, MEK1, MEK2 and MEK3 (Enslen and Davis, 2001; Ho et al., 2003; Kallunki et al., 1994; Mooney and Whitmarsh, 2004; Sharrocks et al., 2000; Tanoue et al., 2000). However, differences in the spacing and composition of these motifs are apparent for substrates that are recognized by different classes of MAP kinases. Similarly studies on ERK targeting to the ETS-domain transcription factor LIN-1 have identified an additional motif (the FxF motif), located downstream from the phosphoacceptor residues, that is required for efficient phosphorylation in addition to the D-domain (Jacobs et al., 1998).

JNK phosphorylates the amino-terminal serines 63 and 73 of c-Jun, leading to gene expression mediated by the AP-1 transcriptional complex. JNK also phosphorylates another member of the AP-1 complex, ATF-2, as well as NFAT, Myc and members of the Ets family (e.g. ELK-1) which are differentially regulated by phosphorylation.

The kinase cascade that transduces signals from the cell surface to these nuclear transcription factors eventually modulate gene transcription. JNK phosphorylation of transcription factors regulates gene expression both directly and indirectly, which provides a mechanism of gene expression regulation in response to an appropriate biological signal. One method of direct gene regulation involves JNK phosphorylation on specific Ser/Thr residues present in their activation domains. Gene expression is indirectly regulated by transcription factor stability and subcellular localization. JNK phosphorylation can increase

the half-life of certain transcription factors by inhibiting their ubiquitin-mediated degradation, and thus increasing its accumulation within the cell (Fuchs et al., 1998c; Gao et al., 2004; Musti et al., 1997; Nateri et al., 2004; Wertz et al., 2004). JNK mediated NFAT4 phosphorylation induces nuclear exclusion which inhibits its transcriptional activity (Chow et al., 1997).

As previously mentioned, JNK substrates are not limited to transcription factors, but include components of the apoptotic systems. It has been proposed that p53 tumor suppressor expression levels are controlled by JNK phosphorylation at both the transcriptional and protein expression levels by regulating p53 ubiquitin mediated degradation (Fuchs et al., 1998c; Schreiber et al., 1999). Other JNK phosphorylation substrates include the anti-apoptotic proteins Mcl-2 and Bcl2. Both proteins are substrates *in vitro* (Maundrell et al., 1997; Yamamoto et al., 1999), but the relevance of this interaction *in vivo* is still controversial. JNK phosphorylation of Mcl-1 is thought to inactivate its anti-apoptotic function (Inoshita et al., 2002). The biological effect JNK mediated Bcl2 phophorylation is unclear. Some reports have demonstrated that phosphorylation of the same residues in Bcl2 can modulate opposing apoptotic responses (Breitschopf et al., 2000; Ito et al., 1997). Other proteins implicated in JNK mediated apoptosis include Bax (Lei et al., 2002; Tsuruta et al., 2004), Bad (Danial and Korsmeyer, 2004), FOXO (Essers et al., 2004) and the 14-3-3 family of proteins (Sunayama et al., 2005). The pro-survival protein Akt phosphorylates 14-3-3 which assembles the pro-apoptotic proteins Bad and FOXO3a,

sequestering them to the cytoplasm. JNK phosphorylation of 14-3-3 has a pro-apoptotic function by releasing Bad and FOXO3a from Akt mediated inactivation (Sunayama et al., 2005).

The Dual Roles of JNK in Life and Death

There is strong evidence that JNK has a dual role in mediating both apoptosis and cell survival. These opposing cell functions can be reasoned when one considers the JNK signal transduction pathway is activated by stress conditions which might force a damaged cell to decide between life and death. While JNK has a clear dual, pivotal role in this cellular decision, it is also important for other cell contexts such as development and differentiation.

Programmed cell death (apoptosis) is a timely, efficient and appropriate process that is essential to eliminate damaged cells, mediate proper embryology and to maintain cellular homeostasis for optimal cellular proliferation. The process of apoptosis involves a tightly regulated signaling cascade that has been highly conserved throughout evolution. Strict regulation of this process is critical because the pathological consequences of uncontrolled apoptosis include neurodegenerative and neuromuscular diseases from excess apoptosis and limb development abnormalities.

The apoptosis process is characterized by several distinct and identifiable events, and these events are distinct from less specific methods of cell death such as necrosis. There is a caspase mediated change to cell morphology that includes cell shrinkage, plasma membrane blebbing, DNA condensation and

fragmentation, mitochondrial membrane depolarization as well as the release of cytochrome-c from the mitochondria (Delhalle et al., 2003). Likewise, JNK has been implicated in roles with caspase-independent cell death (Eby et al., 2000; MacFarlane et al., 2000; Toyoshima et al., 1997; Ventura et al., 2004) and in response to disruption of microtubule dynamics (Wang et al., 1999).

Apoptosis mechanisms can be separated into two systems. The "intrinsic pathway" which is mediated by members of the Bcl-2 family of proteins and the "extrinsic pathway" which is mediated by death receptors, like those of the TNF receptor superfamily. JNKs role in apoptosis is controversial as it has dual roles promoting cell survival and apoptosis. This appears to be dependent on cell type, the activating stimuli and the duration of activation as well as the participation of other signaling pathways.

JNK activation is essential for mediating the "intrinsic pathway" of apoptosis in response to certain types of stress stimuli. Early experiments with neurons indicated a pro-apoptotic role for JNK. Nerve cells can undergo apoptosis upon nerve growth factor (NGF) withdrawal. Conversely, NGF withdrawal induced apoptosis is blocked by the expression of dominant negative c-Jun or injection of c-Jun neutralizing antibodies (Ham et al., 1995). Consistant with this, the expression of dominant negative mutants of the JNK signaling pathway inhibit NGF withdrawal induced apoptosis while over expression of a constituitively active MEKK1 induces apoptosis (Xia et al., 1995). A possible transcriptional target of JNK induced neuronal cell death is the pro-apoptotic

protein Fas-ligand (FasL). FasL is upregulated in neurons upon NGF withdrawal in a JNK dependent fashion (Faris et al., 1998; Kasibhatla et al., 1998; Le-Niculescu et al., 1999). The involvement of JNK in neuronal cell death has been confirmed in studies with *Jnk3*$^{-/-}$ animals. These mice are defective in kainate-induced neuronal apoptosis suggesting a JNK role in brain response to stress by excitotoxins (Yang et al., 1997b). Also, neurons isolated from these JNK3 deficient mice are resistant to NGF withdrawal induced apoptosis (Bruckner et al., 2001).

The pro-apoptotic role of JNK is also observed in non-neuronal cells. Biochemical analysis of *Jnk1*$^{-/-}$/*Jnk2*$^{-/-}$ mouse embryonic fibroblasts have demonstrated they are defective for apoptosis in response to UV and anisomycin (Tournier et al., 2000). Further studies demonstrated that UV irradiated *Jnk1*$^{-/-}$ /*Jnk2*$^{-/-}$ mouse embryo fibroblasts fail to induce mitochondrial membrane depolarization and cytochrome-c release, which indicates a role of JNK in the regulation of the mitochondrial response to stress. However, it is still controversial if JNK only induces, or also promotes apoptosis.

Although JNK has an established role in apoptosis, there is also evidence that JNK can contribute to cell survival as well. Analysis of *Jnk1*$^{-/-}$/*Jnk2*$^{-/-}$ embryos has demonstrated a dysregulation of apoptosis that results in brain defects. There was an increase in apoptosis in the fore and hindbrain regions of *Jnk1*$^{-/-}$ /*Jnk2*$^{-/-}$ E10.5 embryos, which suggests that JNK conveys a survival signal during brain development (Kuan et al., 1999; Sabapathy et al., 1999). There is also

evidence for a JNK survival signaling role from the characterization of the TNFα response in *Jnk1*$^{-/-}$/*Jnk2*$^{-/-}$ MEFs. These JNK null cells are more sensitive to TNFα induced apoptosis than normal cells (Lamb et al., 2003).

Cellular context is important regarding JNK mediated survival signaling. Several antisense studies in tumor cells demonstrated that if JNK2 activity was inhibited with specific antisense oligonucleotides, the growth of certain tumor cells possessing p53 mutations were repressed (Bost et al., 1999; Potapova et al., 2000a; Potapova et al., 2000b). These studies suggest a pro-survival role for the JNK signaling pathway. Also, it has been shown that JNK1 mediates a survival signal in transformed B lymphoblasts and the lack of JNK1 activity promotes apoptosis (Hess et al., 2002). Further evidence is presented by studying gene disruptions of MKK4, an upstream activating kinase of JNK. Immature thymocytes and peripheral mature T-cells from *Mkk4*$^{-/-}$ mice are susceptible to Fas induced apoptosis (Nishina et al., 1997). Together, these experiments provide strong evidence that the JNK signaling pathway is capable of transducing anti-apoptotic, pro-survival signals.

An important question that arises from these studies is how does JNK mediate opposite biological signals such as apoptosis and cell survival? This biological dichotomy can possibly be explained by examining cellular context and the duration and extent of JNK activation. The combined effects of JNK activation and suppression of the ERK signaling pathway in NGF withdrawal induced apoptosis (Xia et al., 1995). Likewise, the integration of JNK and NF-κB

pathways in TNFα induced survival signaling (Lamb et al., 2003). In addition, cell status may be important as well for the interpretation of a specific signal. The p53 status in a cell may change the biological outcome from a JNK mediated signaling event (Potapova et al., 2000b). Similarly, the correlation of the time course of JNK activation may mediate different biological responses. Sustained activation of JNK, and not the transient acivation, has been associated with apoptosis (Chen et al., 1996). This is consistant with the observation that TNFα induces only a transient activation of JNK and this corresponds with cell survival.

The Microtubule Cytoskeleton

Microtubules are subcellular structures found in most eukarotic organisms that are a critical part of the cytoskeletal structural matrix. In mammals, microtubules consist of polarized assemblies of α and β-tubulin subunit monomers which polymerize in a GTP and temperature dependent mechanism. Microtubules are polarized structures, consisting of a "positive" and "negative" end that form macromolecular protein polymer arrays which nucleate at the centrosome. Microtubules are dynamic structures which continually polymerize and depolymerize throughout the cell cycle. Microtubules generally polymerize from their positive ends, but a lower rate of polymerization is also observed at the minus ends. Depolymerization occurs with a rapid "catastrophe" from the positive end which corresponds to a decrease in tubulin-bound GDP/GTP ratios. Microtubule polymerization and catastrophe are sensitive to temperature, with

catastrophe rates increasing with lower temperatures. Similary, the rates of polymerization and catastrophe vary throughout the cell cycle.

The centrosome is usually a centrally located organelle in mammalian cells about 1-2μm in diameter which consists of two barrel-shaped centrioles arranged perpendicular to each other. The centrioles are surrounded by a complex network of proteins called the pericentriolar material (PCM). One protein in the PCM is γ-tubulin, which forms ring complexes (γTuRCs) that nucleate the minus end of microtubules, although other proteins are believed to be involved with this complex (Hannak et al., 2002).

Microtubules serve various necessary functions within the cell. As part of the cytoskeleton, they have roles in cell morphology, motility and cell division. However, they also serve as a trafficking and scaffolding network within cells. Microtubule motor proteins function to transport molecular "cargos" throughout the cell. This function is believed to be necessary for spatial regulation of other cell signaling functions, as well as maintaining cellular homeostasis. There are several well characterized microtubule motor proteins, including dynein and kinesin. The JIP group of JNK interacting proteins are known to associate with the kinesin light chain, part of the kinesin complex of microtubule motor proteins (Bowman et al., 2000; Verhey et al., 2001; Whitmarsh et al., 2001). This association is known to be required for JIP colocalization at the growth cones of developing neurites.

Similarly, the centrosome and microtubule network serve as a scaffolding device for discrete cell signaling modules. The centrosome itself is believed to serve as a multiplatform scaffold complex containing hundreds of scaffolding proteins that serve as docking sites for a multitude of regulatory, cell cycle control and signaling networks (Andersen et al., 2003). The microtubule associated protein 2 (MAP2) family of proteins is an abundant group of cytoskeletal components that are predominately expressed in neurons. These proteins participate in the stability of microtubules and the regulation of organelle transport within axons and dendrites, as well as the anchoring of signaling proteins (Sanchez et al., 2000). MAP2 was the first protein shown to directly interact with the regulatory subunit of PKA (Theurkauf and Vallee, 1982). The A-Kinase Anchoring Proteins (AKAPs) serve as scaffolding proteins for the cAMP-dependent protein kinase (PKA). AKAP350 and Pericentrin, both PCM proteins, has been demonstrated to function as AKAPs at the centrosome (Diviani et al., 2000; Takahashi et al., 1999). The Smad proteins are intracellular signaling effectors of the TGFβ superfamily. Microtubules are believed to serve as a cytoplasmic sequestration network for Smads in quiescent cells (Dong et al., 2000a). Both microtubule destabilization with chemical inhibitory agents (MIAs) and TGFβ induced signaling promote the disassociation of Smads from the microtubules, leading to a transcriptional response (Dong et al., 2000a).

Microtubules and Cell Division

Microtubules serve a critical role in cell cycle regulation and cell division. In order to initiate and complete cell division, the cell generates a spindle assembly from centrosomes which serve to nucleate the microtubule network. Various complex processes are involved with spindle assembly. Amongst these are changes in microtubule dynamics, bipolar attachment of chromosomes to the spindle, assembly of a spindle lattice with sufficient rigidity to move chromosomes, movement and segregation of the chromosomes, and coupling of chromosome attachment to the spindle with cell cycle progression (Compton, 2000).

As cells progress through the cell cycle, two changes in microtubule organization and behavior are critical for spindle assembly. First, a shift from a single microtubule organizing center (MTOC) to two discrete MTOCs. During the G1 phase of the cell cycle, each cell contains a single centrosome which acts as a MTOC. Centrosomes duplicate along with genomic DNA during S phase so that cells enter the G2 phase, and subsequently M phase with two functional centrosomes. Each of these centrosomes function as a MTOC and segregate during late G2/early M phase. Thus two prominent mitotic asters are observable during cell division (Fig. 1-2).

There are dramatic changes in microtubule dynamics during metaphase. During interphase, microtubules form an extended array throughout the cytoplasm with a stable turnover half life exceeding 10 mins. During metaphase,

the rate of microtubule catastrophe increases 7- to 10-fold which results in a population of microtubules that are relatively short and unstable having a turnover half life of less than 60 seconds (Cassimeris, 1999; Inoue and Salmon, 1995; McNally, 1996). One protein implicated in regulating microtubule dynamics during mitosis is the severing protein katanin, which may act to promote microtubule turnover within the spindle since it is localized to the spindle poles (McNally and Thomas, 1998).

The breakdown of the nuclear envelope at prometaphase permits microtubule access to the chromatin. The positive ends of microtubules attach to the chromosomes at sister kinetochores to form bipolar attachments from each spindle pole, and once attached, the kinetochore stabilizes it against catastrophe (Cassimeris et al., 1990; Mitchison et al., 1986). The bipolar kinetochore attachment can be a lengthy process, as each must achieve attachment to the two spindle poles, but a spindle checkpoint ensures that the cell cycle will not progress into anaphase until these bipolar attachments are complete (Hardwick, 1998; Li and Murray, 1991).

The microtubule minus end at the spindle poles undergoes significant changes during mitosis. The centrosomes are responsible for microtubule nucleation and critical for spindle assembly (Compton, 1998; Maniotis and Schliwa, 1991; Zhang and Nicklas, 1995). However, later in mitosis when the bipolar mitotic spindles are well developed, the centrosomes are dispensable for spindle organization and function. Micromanipulation experiments where the

centrosomes are removed from the mitotic spindle late enough in M phase have demonstrated that the spindles remain intact and functional for chromosome separation (Nicklas et al., 1989). The spindle poles remain organized by the recruitment of non-centrosomal proteins which are involved in focusing the microtubule minus ends. The minus end-directed microtubule motor protein dynein and the Kin C family of kinesin-related proteins are involved with this process at the spindle poles (Gaglio et al., 1997; Gaglio et al., 1996; Mountain et al., 1999). These microtubule motor proteins rely on cross-linking and sliding of one microtubule relative to the other in order to achieve cytokinesis (Fig. 1-3). For dynein, cross-linking relies on its association with dynactin and NuMA. Dynactin is a complex activator of cytoplasmic dynein (Gill et al., 1991; Schroer et al., 1996) and NuMA is a nuclear protein that associates with the mitotic apparatus (Compton and Cleveland, 1994).

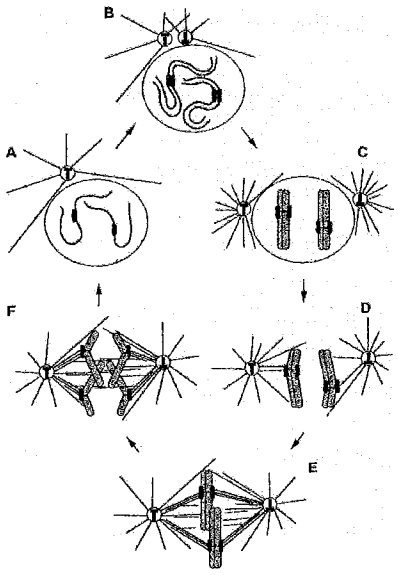

Figure 1-3 Diagram of the spindle assembly during mitosis. Chromosomes, centrosomes and microtubules are highlighted in G1 (A), G2 (B), prophase (C), prometaphase (D), metaphase (E), and anaphase (F) (Compton, 2000).

The primary function for the mitotic spindles are equal segregation of the sister chromatids during cytokinesis. The principal microtubule motors involved with poleward flux are still poorly understood, but the methods for chromatin positioning and separation are generally attributed to three distinct mechanisms. Although a direct link has not been established, one method of chromatin separation is believed to be due to the "treadmilling" of microtubules within the spindles (Mitchison, 1989). Treadmilling is achieved by the continuous addition of tubulin monomers to the positive end of microtubules at the kinetochores and their removal at the spindle pole minus ends. There is no net change in overall microtubule length from treadmilling, resulting in a poleward microtubule flux. Mild taxol treatment can suppress the addition of tubulin monomers to the positive end of microtubules while leaving the spindle pole minus ends unaffected, resulting in a net chromatin separation equivalent to the rates of microtubule treadmilling (Waters et al., 1996). Similarly the rates of poleward flux and anaphase chromatid separation in frog egg extracts are equivalent, suggesting that chromain separation is primarily due to poleward flux (Desai et al., 1998).

Polar ejection forces are a second mechanism involved in chromatin arrangement (Rieder and Salmon, 1994). These microtubule forces arise from the mitotic spindles and are critical for the congression of chromosomes on the metaphase plate. Evidence for this movement come from micromanipulation experiments where the arms of chromosomes were severed from the centromeric

regions. The chromosomal arms move rapidly away from the nearest mitotic spindle and take a position midway between the two spindles (Ault et al., 1991; Rieder et al., 1986).

The forces exerted on the kinetochore provide the dominant mechanism of poleward movement. This mechanism involves the microtubule attachment at the kinetochore involving structural proteins CENP-A, B and C, cytoplasmic dynein and CENP-E, a variety of structural proteins (CLIP170, CENP-F and ZW10), passenger proteins (INCENPs) and cell cycle checkpoint signaling proteins (Mad2, Bub1, PP2A and ERK) (Minshull et al., 1996; Minshull et al., 1994; Rieder and Salmon, 1998; Taylor and McKeon, 1997; Yen and Schaar, 1996). These proteins perform critical kinetochore associated functions that modulate microtubule dynamics as the chromosomes separate.

During anaphase, the kinetochores power poleward motion at equivalent rates and pull the chromatids to opposite poles. The Kin I kinesin-related proteins are likely involved in mediating microtubule depolymerization during anaphase chromatin separation, but the motors involved with kinetochore associated poleward movement are not known (Maney et al., 1998).

MAPK Signal Transduction: The Cell Cycle and Microtubule Dynamics

MAPKs are activated during meiotic maturation of *Xenopus* oocytes and have an essential role in both the transition from G2 to M phase of meiosis and metaphase arrest of mature oocytes (Ferrell et al., 1991; Gotoh et al., 1995; Gotoh et al., 1991; Haccard et al., 1995; Haccard et al., 1993; Kosako et al.,

1994a; Kosako et al., 1994b; Posada et al., 1991). The p38 kinase is essential for the spindle assembly checkpoint in *Xenopus* egg extracts and is activated by disruption of the spindle in mammalian cells (Takenaka et al., 1998). ERK (p42/p44) is also essential for the spindle assembly checkpoint in *Xenopus* egg extracts, but may play a different role than p38 in mammalian cells (Minshull et al., 1994; Takenaka et al., 1997). ERK localizes to the kinetochore and spindle microtubules during somatic cell mitosis (Shapiro et al., 1998; Zecevic et al., 1998). ERK also interacts with and phosphorylates the kinesin-like motor protein CENP-E, which functions in prometaphase and anaphase chromosome movement (Zecevic et al., 1998).

JNK signal transduction also has a role in cell cycle control. JNK contributes to, but is not sufficient for the transcription of cyclin D1 (Lee et al., 1999b). In addition, JNK has been reported to interact with and is inhibited by the cyclin dependent kinase (CDK) inhibitor, $p21^{Waf1/Cip1}$ (Patel et al., 1998; Shim et al., 1996). JNK activation is known to result in the disruption of p53/JNK interactions that results in the stabilization of p53 protein (Fuchs et al., 1998a; Fuchs et al., 1998b). Similarly, p53 is known to upregulate the expression of $p21^{Waf1/Cip1}$ in response to DNA damage and inhibition of Cdk2/cyclin complexes by $p21^{Waf1/Cip1}$ arrests the cell cycle at G1 (Tarapore et al., 2001). Recently, it has been demonstrated that treating HeLa cells with a specific small molecule inhibitor of MLK disrupted the mitotic spindle and arrested the cells in

prometaphase. Similarly, this arrest could be partially reversed by overexpression of exogenous MLK3 (Cha et al., 2005).

Eukaryotic cells treated with microtubule-inhibitory agents (MIAs) such as vinblastine, nocodazole and paclitaxel undergo cell cycle arrest at the G2/M transition (Jordan et al., 1998; Sorger et al., 1997). Cell cycle arrest at the G2/M transition after treatment with these drugs is initiated by the G2/M checkpoint in response to the disruption of the mitotic spindle apparatus (Burke, 2000; Clarke and Gimenez-Abian, 2000). At high concentrations, vinblastine and nocodazole disrupt the microtubule network and mitotic spindle assembly by binding to tubulin monomers and preventing microtubule polymerization. Paclitaxel binds to microtubules and stabilizes them, preventing the dynamic instability required for normal functioning at the mitotic spindle apparatus (Downing, 2000; Jordan et al., 1998).

Treatment of eukaryotic cells with MIAs cause an intracellular stress condition which, in addition to cell cycle arrest, can also cause apoptosis. This pro-apoptotic consequence of drug treatment has made these drugs powerful candidates as chemotherapeutic agents (Boldt et al., 2002). Both the p38 and JNK signal transduction pathways are activated in response to MIAs in a variety of cell lines (Amato et al., 1998; Stone and Chambers, 2000; Wang et al., 1999; Wang et al., 1998; Yujiri et al., 1999). Although a direct association between SAPK activation and apoptosis in response to MIA treatment has not been conclusively demonstrated, there is evidence for it. Overexpression of dominant-

negative MEKK1 in HL-60 cells prevented paclitaxel-induced JNK activation, Bcl-2 phosphorylation and apoptosis (Shiah et al., 2001). Similarly, the disruption of *Mekk1* in the chicken bursal B-cell line DT40 demonstrated that it was essential for vinblastine-mediated JNK activation and apoptosis (Kwan et al., 2001). The examination of *Mekk1*$^{-/-}$ embryonic stem cells revealed that MEKK1 was required for JNK activation in response to nocodazole treatment, but MEKK1 also partially protected these cells against nocodazole-induced apoptosis (Yujiri et al., 1998). Studies in *Mekk1*$^{-/-}$ MEFs demonstrated that it was required for JNK, but not NF-KB activation in response to microtubule disruption (Yujiri et al., 2000).

Although there is growing evidence that links the disruption of microtubule dynamics with JNK mediated apoptosis, there is a need for further study in elucidating these signal transduction pathways and their roles in pro-survival and apoptotic signaling.

CHAPTER II

CLONING OF JIP1: A JNK SCAFFOLD PROTEIN

Abstract

The c-Jun amino-terminal kinase (JNK) is a member of the stress-activated group of mitogen-activated protein (MAP) kinases that are implicated in the control of cell growth. A yeast Two-Hybrid screen was employed to identify novel JNK interacting proteins. From this screen, several cDNAs were identified that expressed proteins specifically capable of binding JNK. One of these, a cytoplasmic protein [the JNK interacting protein -1 (JIP1)] was characterized and cloned. Overexpressed JIP1 is a cytoplasmic protein that can bind JNK and can retain JNK in the cytoplasm.

Introduction

The JNK signal transduction pathway is activated in response to environmental stress and by the engagement of several classes of cell surface receptors, including cytokine, serpentine and tyrosine kinase receptors (Whitmarsh and Davis, 1996). Genetic studies in *Drosophila* have demonstrated that JNK is required for early embryonic development (Sluss et al., 1996). In mammalian cells, JNK has been implicated in the immune response (Su et al., 1994), oncogenic transformation (Raitano et al., 1995; Xu et al., 1996), and apoptosis (Chen et al., 1996; Verheij et al., 1996; Xia et al., 1995; Zanke et al., 1996). These effects of JNK may be mediated by an increase in gene expression. Targets of the JNK signal transduction pathway include the transcription factors c-Jun, activating transcription factor -2 (ATF2), and Elk-1 (Whitmarsh and Davis, 1996).

Although JNK is located in both the cytoplasm and nucleus of quiescent cells, activation of JNK is associated with an increase of phospho-JNK in the nucleus, with some cytoplasmic phospho-JNK translocating to the nucleus (Cavigelli et al., 1995). Interaction with anchor proteins, also known as scaffold proteins, is one mechanism that that may account for the retention of JNK in specific regions of the cell. Anchor proteins participate in the regulation of multiple signal transduction pathways, including nuclear factor kappa B inhibitor IκB, the A-kinase anchor protein (AKAP) group of proteins that bind type II cyclic adenosine 3',5'- monophosphate-dependent protein kinase, and the p190 protein

that binds Ca^{2+} - calmodulin-dependent protein kinase II (Faux and Scott, 1996b; McNeill and Colbran, 1995; Verma et al., 1995). These anchor proteins localize their tethered partner to specific subcellular compartments or serve to target enzymes to specific substrates (Coghlan et al., 1995; Cohen, 1989; Inglese et al., 1993; Mochly-Rosen, 1995; Shibasaki et al., 1996). Anchor proteins may also create multienzyme signalling complexes, such as the Ste5p MAP kinase scaffold complex and the AKAP79 kinase-phosphatase scaffold complex (Choi et al., 1994; Faux and Scott, 1996a).

The yeast Two-Hybrid screen is a powerful, high-throughput genetic technique for detecting novel *in vivo* protein interactions to an experimental "bait" protein of interest. Using JNK1 as our "bait", we screened a murine embryo cDNA expression library to identify novel JNK interacting proteins. Of the novel clones we analyzed, NFAT4 (nuclear factor of activated T cells – 4) was identified as not only a JNK binding protein, but a JNK substrate resulting from this screen (Chow et al., 1997). Another protein, discussed in Chapter III of this dissertation, is JMP1 (JNK interacting, Microtubule associated Protein – 1) which represents a novel class of JNK interacting proteins. The focus of this chapter is to introduce the cloning and JNK interaction analysis of the first member of the JNK scaffold proteins, JIP1 (JNK Interacting Protein – 1), which was also identified through this Two-Hybrid screen.

Experimental Procedures

Yeast Two-Hybrid Screen - Cloning of JIP1

A JIP1 cDNA fragment was isolated by a yeast Two-Hybrid screen of a mouse embryo cDNA library in the yeast strain L40 (MATa his3Δ200 trp1-901 leu2-3,112 ade2 LYS2::$(lexAop)_4$-HIS3 URA3::$(lexAop)_8$-lacZ) (Galcheva-Gargova et al., 1996). The mouse embryo cDNA library was generated by random-primed synthesis of 9.5/10.5 d.p.c. CD1 mouse embryo $polyA^+$ RNA. Following second-strand synthesis, the cDNA was repaired with T4 DNA Polymerase and linkered with top strand (5'-ATCCTCTTAGACTGCGGCCGCTCA-3') and bottom strand (5'-TGAGCGGCCGCAGTCTAAGAG-3') oligonucleotides which generates a double-stranded DNA linker with a top-strand 5'-ATCC-3' overhang. Fragments of 350-700nts were selected by agarose gel electrophoresis, pooled and amplified by PCR using a sense primer in the linker sequence. After amplification to near saturation, the reaction was diluted ten-fold and repeated one additional cycle. The pVP16 cDNA library vector carries the LEU2 gene and contains a NLS-VP16-linker unit driven by the ADH promoter. The amplified library cDNA was digested overnight with Not1 and inserted into the Not1 site of pVP16. The lexA fusion vector pBTM116 carries the TRP1 gene and has a polylinker downstream of the lexA coding sequence. LexA contains no nuclear localization sequence (NLS), thus non-interacting proteins will be predominantly localized to the

cytoplasm, therefore reducing the background signal; only NLS-tagged VP16 fusion partners will transport the lexA fusion into the nucleus. The bait plasmid (pLexA-JNK1) was constructed by insertion of full length JNK1 in the polylinker of pBTM116. pLexA-JNK1 was transformed into L40 yeast using a standard lithium acetate/PEG and DMSO/heat-shock method, and plated on TRP^- selective media. The pLexA-JNK1 transformed yeast were then transformed with the pVP16-cDNA library DNA and plated on TRP^- and LEU^- selective media at a density approximately $5x10^4$ colonies per 25cm plate. Colonies were transferred by replica overlay on nitrocellulose filters. The replica filters were placed in a pool with 50μL 25mg/mL X-Gal in Z Buffer (60mM Na_2HPO_4, 40mM NaH_2PO_4, 10mM KCl, 1mM $MgSO_4$, pH 7.0) and observed for color development. Plasmids from positive clones were shuttled to *E. coli* for further analysis (Ward, 1990). For JIP1, seven independent clones overlapping a common 300bp cDNA sequence were identified. The Two-Hybrid JIP1 fragment was used to screen a mouse brain λZAPII cDNA library (Stratagene) to clone the full length, 2.8kB JIP1 cDNA. DNA sequencing was performed with an 373A machine (Applied Biosystems).

Plasmids

GST (Glutathione-S-Tranferase) fusion proteins with JIP1 were cloned in pGEX-3X (Pharmacia). Deletion constructs of the JIP1 cDNA were done by PCR and subcloned into pGEX-3X to create pGST-JIP1 127-281, pGST-JIP1 127-202, pGST-JIP1 203-281 and pGST-JIP1 164-240. Small end deletions of the JIP1

yeast Two-Hybrid fragment were done by PCR and ligation of the product into pGEX-3X to create a GST fusion expression vector.

The FLAG-JIP1 expression plasmid was created by inserting the FLAG epitope (DYKDDDDK) between codons #1 and #2 of the 2.8kb JIP1 open reading frame. pHA-JNK1 has been previously described (Gupta et al., 1996).

Northern Blots

Northern blots with 2μg poly A^+ mRNA per lane isolated from eight different adult murine tissues were probed with a ^{32}P-labled random-primed 460bp JIP1 cDNA fragment isolated from the yeast Two-Hybrid screen. This cDNA fragment encodes JIP1 amino acid residues #127-281. The blot was exposed for 24 hours, then stripped and reprobed with a ^{32}P-labled random-primed β-actin probe (Clontech) and exposed for 24 hours to Kodak X-AR autoradiography film.

Co-immunoprecipitation Assays

COS-1 cells were transfected with either an empty pcDNA3 vector, HA-JNK1, FLAG-JIP1 or co-transfected with both JNK1 and JIP1 expression vectors using LipofectAMINE reagent (Life Technologies) and expressed for 24 hours. Some cells were exposed to UV-C light (40J/m^2) and recovered for 1 hour before being lysed in Triton lysis buffer with un-irradiated control cells (TLB; 20mM Tris-Cl pH 7.4, 137mM NaCL, 2mM EDTA, 1% Triton X-100, 25mM β-glycerophophate, 1mM Na-orthovanadate, 2mM sodium pyrophosphate, 10%

glycerol, 5μg leupeptin per mL, 5μg aprotinin per mL, 1mM phenylmethylsulfonyl fluoride). Lysates were clarified by centrifugation at 15,000 x *g* (15mins. at 4°). Total soluble, supernatant proteins were quantitated by the Bradford method (Bio-Rad). In a total volume of 0.5mL TLB, 50μg of total cell lysate was immunoprecipitated with 1μg of either anti-hemagglutinin (HA) rabbit polyclonal antibody or anti-FLAG M2 (Sigma) monoclonal antibodies bound to 20μL Protein-G Sepharose beads. The immunoprecipitates were washed four times, boiled with 10μL Laemmli sample buffer and separated by SDS-PAGE. The blots were then examined by immunoblot analysis with either the M2 monoclonal antibody to detect JNK co-immunoprecipitates, or a polyclonal JNK1 to detect JIP1 co-immunoprecipitates. To detect for expression of both JNK1 and JIP1, total lysates from the cells were immunoblotted with a mixture of M2 and HA monoclonal antibodies.

GST-JIP1 Fusion Proteins

Glutathione-S-transferase (GST) fusions were made to various JIP1 cDNA deletions within the Two-Hybrid recovered JIP1 fragment. GST-JIP1 fusion proteins expressing JIP1 amino acid residues 127-281, 127-143, 127-153, 127-163, 127-202, 135-202, 144-202, 154-202, 164-240 and 203-281 were created by PCR.

Binding Assays

In vitro translated JNK1 and JNK2 from rabbit reticulocyte lysate (was used to study the JNK binding region on JIP1 (Gupta et al., 1996). GST-JIP1 fusion proteins were bound to Glutathione Sepharose 4B beads (Amersham-Pharmacia) and incubated for two hours at 4°C with 5μg of *in vitro* translated JNK1 or JNK2 labeled with ^{35}S-Methionine. Beads were washed and separated on SDS-PAGE. The blots were incubated with a polyclonal anti-JNK antibody to detect JNK co-precipitation with the GST-JIP1 fusions. For positive controls, c-Jun (1-79) and ATF2 (1-109) GST fusions were included in the pull-down assay.

Peptide Competition Assays

COS-1 cells were transfected with FLAG epitope tagged JNK1 and incubated for 24 hours. Lysates were prepared from these cells using TLB buffer. GST and GST-JIP1 (residues 127 to 281) were bound to glutathione-Sepharose beads and washed. 50μg of COS-1 cell lysate expressing FLAG epitope tagged JNK1 were incubated with either GST or GST-JIP1 (127-281) bound to Sepharose beads for one hour at 4°C. A series of synthetic peptides corresponding to JIP1 residues 148 to 174 or a peptide with a scrambled sequence as a control were synthesized. Increasing concentrations of the JIP1 or scrambled peptide (0, 4, 8, 16, 32 and 64 μg/mL) were added to the GST bound Sepharose beads with the COS-1 lysate. GST bound proteins were then washed and examined by SDS-PAGE immunoblot with the M2 monoclonal antibody.

Synthetic peptides were synthesized with point mutations corresponding to JIP1 (residues 148 to 174), JIP1 (residues 159-162 replaced with Gly), JIP1 (T159G), JIP1 (L160G), JIP1 (L162G) and JIP1 (K155G) as well as a peptide with scrambled sequence as a control. COS-1 lysate expressing FLAG epitope tagged JNK1 was incubated to glutathione-Sepharose bound GST or GST-JIP1 (residues 127 to 281). Peptides were added to these incubations at a concentration of 64μg/mL for one hour at 4°C. Sepharose-bound proteins were washed, separated by SDS-PAGE and examined by immunoblot to the M2 monoclonal antibody.

Immunofluorescence Analysis

COS-1 cells were plated on acid washed 22mm x 22mm glass No. 1 coverslips (Corning) and allowed to grow to 70% confluence. The COS-1 cells were then transfected with HA-JNK1, FLAG-JIP1 or both using Lipofectamine reagent and expressed for 24 hours. The cells were exposed to UV-C light ($40J/m^2$) and allowed to recover for 1 hour prior to fixation. The cells were fixed in fresh 4% paraformaldehyde (pH 7.2) and permeabilized (5 mins.) with 0.2% Triton X-100 in PBS. Coverslips were blocked (30 mins.) with 5% normal donkey serum (Jackson ImmunoResearch, Inc.) in PBS.

The coverslips were incubated for 1 hour with either anti-FLAG M2 monoclonal antibody (1:500) or polyclonal anti-HA serum (1:2000) in PBS with 5% normal donkey serum. Immune complexes were detected (30 mins.) with Texas Red conjugated anti-mouse Ig antibodies and fluorescein-isothiocyanate

(FITC) conjugated anti-rabbit Ig antibodies (1:200; Jackson ImmunoResearch Inc.) in PBS with 5% normal donkey serum. The coverslips were mounted onto slides with Gel-Mount (Biomeda Corp) for digital imaging microscopy analysis. All procedures were performed at room temperature in a dark, humidified environment.

Digital Imaging Microscopy and Image Restoration

Digital images of the fluorescence distribution in single cells were obtained using a Nikon 60x Planapo objective (numerical aperture = 1.4) on a Zeiss IM-35 microscope equipped for epifluorescence as described previously (Carrington et al., 1995; Fay et al., 1989). Images of various focal planes were obtained with a computer controlled focus mechanism and a thermoelectrically cooled charged-coupled device camera (Model 220; Photometrics Ltd.). The exposure of the sample to the excitation source was determined by a computer-controlled shutter and a wavelength selector system (MVI). The charged-coupled device camera and microscope functions were controlled by a microcomputer, and the data acquired from the camera were transferred to a Silicon Graphics model 4D/GTX workstation (Silicon Graphics) for image processing. Images were corrected for non-uniformities in sensitivity and for the dark current of the charge-coupled device detector. The calibration of the microscopy blurring was determined by measuring the instrument's point spread function as a series of optical sections at 0.125μm intervals of a 0.3μm diameter fluorescently labled latex bead (Molecular Probes Inc.). The image restoration algorithm used is based upon the

theory of ill-posed problems and obtains quantitative dye density values within the cell that are substantially more accurate than those in an unprocessed image (Carrington et al., 1995; Fay et al., 1989). After image processing, individual optical sections of cells were inspected and analyzed using computer graphics software on a Silicon Graphics workstation. Single optical sections were also imported and processed with Photoshop software (Adobe Inc.).

Results

JIP1 was originally identified by a screen of a murine embryo cDNA library using a yeast Two-Hybrid assay looking for new JNK1 substrates. A cDNA library was constructed from a size-selected pool of 300-750nts of random-primed cDNA sequences generated from polyA$^+$ mRNA obtained from CD1 whole E9.5-10.5 murine embryos. The cDNA library sequences were fused to a VP16 activator (pVP16). The "bait" protein was full length JNK1 fused downstream of a LexA (pLexA-JNK1). Yeast strain L40 was transformed with both plasmids and screened by auxotrophic selection. Positive interacting clones were selected by β-galactosidase color detection. We screened approximately 10^6 yeast colonies and identified seventeen clones passing secondary screening. The seventeen clones were isolated and analyzed by *in vitro* JNK binding assays. Fifteen of these novel "positive" clones from various overlapping sequences were found to directly bind JNK1 when analyzed by *in vitro* binding assays. JIP1 was identified from seven overlapping cDNA clones corresponding to a 300bp fragment. JIP1 was selected for further study since its 300bp fragment strongly bound JNK1 in an *in vitro* binding assay when compared to the well characterized JNK1 binding δ-domain in cJun (1-79). The yeast Two-Hybrid fragment was used to screen a murine λZAPII cDNA library and the full length JIP1 cDNA was obtained. The full length 2.8kb JIP1 cDNA has an open reading frame coding for a 660 amino acid protein. It also contains an NH_2-terminal JNK binding domain (JBD) and a

putative SRC homology 3 (SH3) domain in the COOH-terminus. The putative SH3 domain is most closely related to domains in the tyrosine kinase c-Fyn and the p85 subunit of phophoinositide-3 kinase. JIP1 is widely expressed in murine tissues (Fig. 2-1).

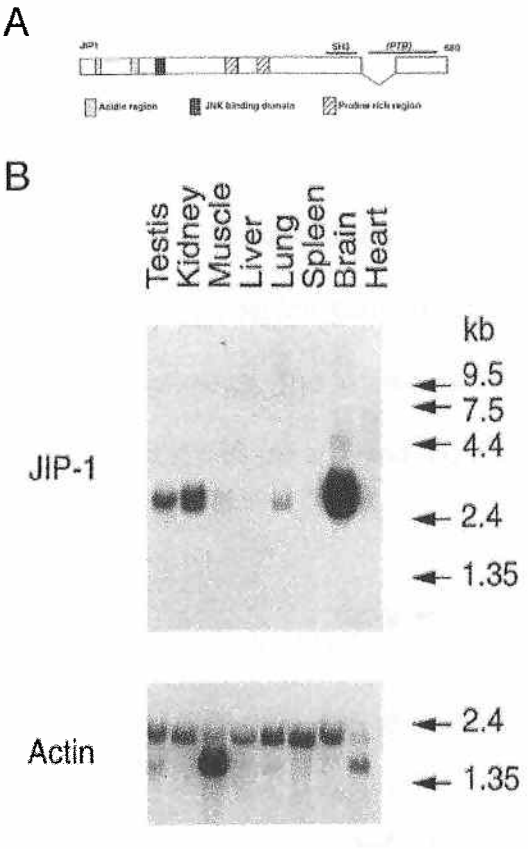

Figure 2-1 JIP1 is a 2.8kB cDNA with a 660 amino acid open reading frame and expressed in a wide variety of murine tissues. (A) JIP1 has an amino-terminal JNK Binding domain and carboxyl-terminal SH3 domains. JIP1β has a PTB domain. (B) 2μg of poly A^+ mRNA isolated from various murine tissues were hybridized with a 460bp JIP1 cDNA probe isolated from the yeast Two-Hybrid screen. The blot was exposed for 24 hours. The integrity of the mRNA was determined by hybridization to a b-actin probe (bottom panel). RNA size standards are indicated to the right of the blots in kilobases.

JIP1 is a JNK binding protein

The yeast Two-Hybrid screen we employed to identify novel JNK binding proteins yielded a fragment of JIP1 coding for residues 127-281. Therefore, we assumed a JNK binding site was present within this NH_2-terminal fragment, but wished to determine if JIP1 was capable of *in vivo* JNK binding in an *in vitro*

system. Finally, we wished to determine the JNK binding domain (JBD) by *in vitro* binding of JNK to subdeletions in the yeast Two-Hybrid JIP1 fragment.

We examined the interaction of JIP1 and JNK1 by co-immunoprecipitation analysis of lysates from COS-1 cells that were transfected with vectors encoding JIP1 and JNK1. JIP1 was detected in JNK1 immunoprecipitates by protein immunoblot analysis. Conversely, JNK1 was detected in JIP1 immunoprecipitates (Fig. 2-2). Coimmunoprecipitation of transfected JIP1 with endogenous JNK1 and JNK2 was also observed (*data not shown*). Exposure of cells to UV-C radiation caused no change in the amount of JNK-JIP1 complex that was detected. The related MAP kinases extra-cellular signal-related kinase-2 (ERK2) and p38 did not coimmunoprecipitate with JIP1 (*data not shown*).

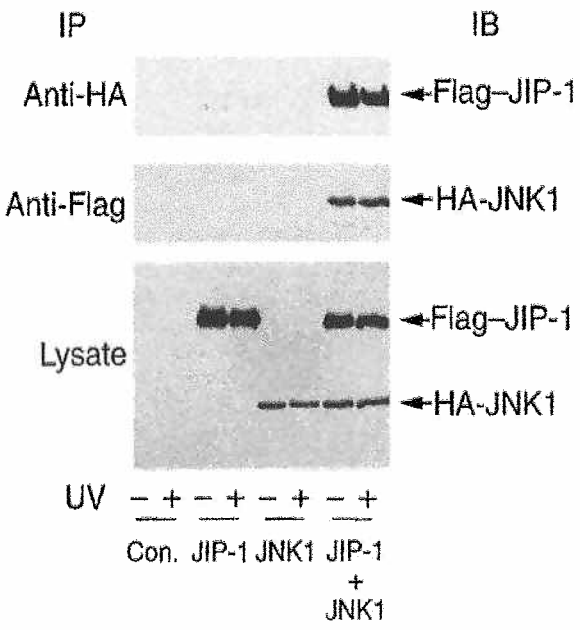

Figure 2-2 JNK-JIP1 complex formation *in vivo*. COS-1 cells were mock-transfected [control (Con.)] or transfected with FLAG-JIP1 and HA-JNK1. The cells were irradiated without (-) or with (+) UV-C light ($40J/m^2$) and incubated for 1 hour. Lysates prepared from the cells were examined by protein immunoblot (IB) analysis with a mixture of antibodies to FLAG and HA (bottom panel). FLAG immunoprecipitates (IP) were probed with a polyclonal antibody to JNK1 (middle panel), and HA immunprecipitates were probed with an antibody to FLAG (top panel). *Experiment done in collaboration with Martin Dickens.*

To test whether JIP1 interacts directly with JNK, we performed *in vitro* binding assays. The putative JNK binding domain (JBD; residues 127-281) was expressed as a glutathione-S-transferase (GST) fusion protein. Recombinant JNK prepared by *in vitro* translation (Gupta et al., 1996) was incubated with GST-JIP1 that was immobilized on glutathione-agarose. JNK binds to transcription factors c-Jun and ATF2 in an isoform-dependent manner (Dai et al., 1995; Derijard et al., 1994; Gupta et al., 1996; Kallunki et al., 1994; Sluss et al., 1994). Thus, a larger amount of JNK2 than JNK1 bound to c-Jun and ATF2. In contrast, the amount of JIP1 that bound both JNK1 and JNK2 was similar (Fig. 2-3). Control experiments demonstrated that JIP1 did not bind to p38 MAP kinase (*data not shown*).

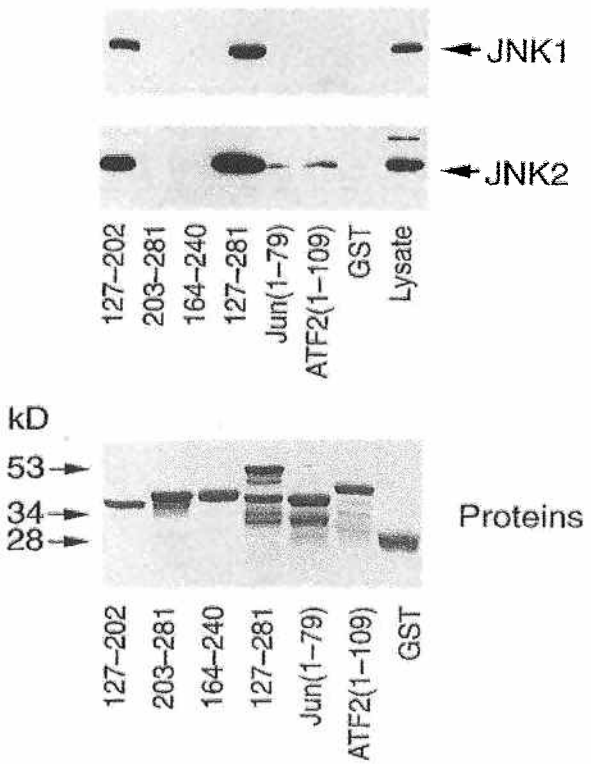

Figure 2-3 *in vitro* binding of JIP1 deletion constructs. The GST fusion proteins (Coomassie-stained gel) and the results of the binding assay (immunoblot) are shown. The binding of JNK1 and JNK2 to GST and GST fusion proteins corresponding to residues 127 to 202, 203 to 281, 164 to 240, and 127 to 291 of JIP1; residues 1 to 79 of c-Jun; and residues 1 to 109 of ATF2 is also shown. The mobility of of molecular size standards is indicated to the left in kilodaltons. *Experiment done in collaboration with Martin Dickens.*

The JIP1 fragment isolated from the Two-Hybrid screen (residues 127 to 281) contains the JBD. This region is capable of binding both JNK1 and JNK2. No JNK binding with the central region of the JBD (residues 164 to 240) or the COOH-terminal region (resdues 203 to 281) was detected. However, JNK binding activity was observed in experiments that used the NH_2-terminal region (residues 127 to 202) of the JBD. The effect of progressive deletions within the JBD indicated that JIP1 residues 144-163 are important for the interaction of JIP1 with JNK (Fig. 2-4).

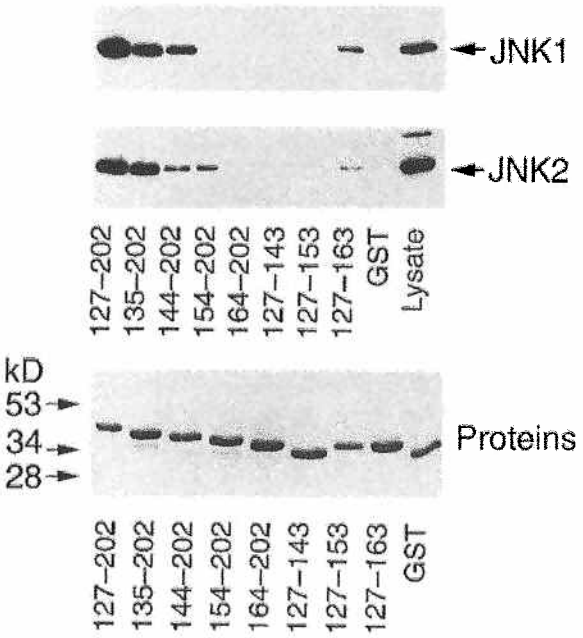

Figure 2-4 Binding of JNK1 and JNK2 to GST and GST fusion proteins corresponding to JIP1 with small deletions between residues 127-202. Glutathione-Sepharose immobilized GST-JIP1 fusion proteins were incubated with *in vitro* translated JNK1 and JNK2. The immobilized GST-fusion proteins were washed and immunoblotted for JNK1 and JNK2 to detect co-association. The GST-JIP1 fusion proteins added to the reactions are indicated in a Coomassie-stained gel (bottom panel). The mobility of molecular size standards is indicated on the left in kilodaltons. *Experiment done in collaboration with Martin Dickens.*

We prepared a series of synthetic peptides corresponding to the JBD region. Competition studies demonstrated that a peptide representing the wild-type JIP1 sequence caused a dose-dependent inhibition of JNK binding to JIP1

(Fig 2-5A). In contrast, a peptide with a scrambled sequence caused no change in JNK binding. This region of JIP1 contains three amino acids (Lys^{155}, Thr^{159}, and Leu^{160}) that are conserved in the JBD of c-Jun, though ATF2 has a conservative Met^{160}. A hydrophobic amino acid (Leu) at residue 162 is also found in c-Jun (Leu) and ATF2 (Leu). Individual replacement of each of these residues with Gly caused a reduction in the peptide competition of JNK binding to JIP1 (Fig. 2-5B). Together, these data are consistent with a role for Lys^{155}, Thr^{159}, Leu^{160} and Leu^{162} in the function of the JNK binding domain of JIP1.

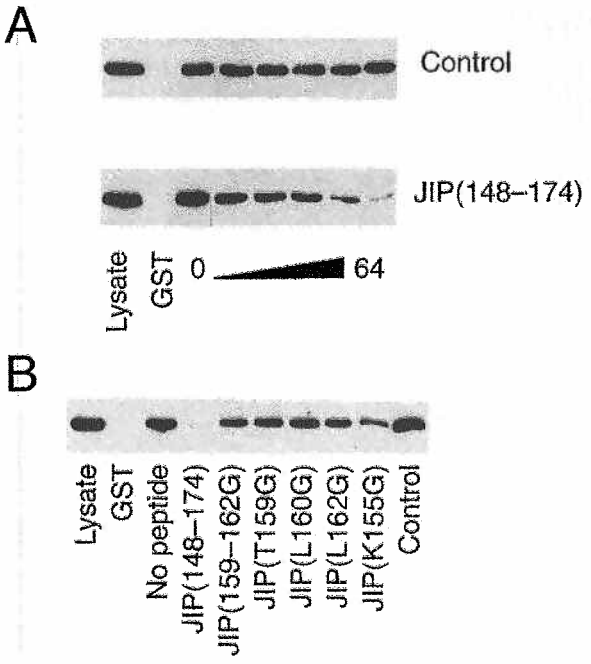

Figure 2-5 A small NH_2-terminal region of JIP1 is sufficient for interaction with JNK. (A) Cell lysates containing FLAG epitope tagged JNK1 were incubated with GST and GST-JIP1 (residues 127 to 281) bound to glutathione-Sepharose, and bound proteins were detected by protein immunoblot analysis with the M2 monoclonal antibody. The effect of increasing concentrations (0, 4, 8, 16, 32 and 64mg/mL) of synthetic peptide corresponding to JIP1 residues 148 to 174 or to a peptide with a scrambled sequence (control) was examined. (B) Binding of JNK1 to GST and GST-JIP1 (resdiues 127 to 281) was examined in the absence and presence of synthetic peptides (64mg/mL). The effect of the wild-type peptide (JIP1 residues 148 to 174), peptides with point mutations (substitution with Gly) [Thr^{159}→ Gly^{159} (T159G)], and a peptide with a scrambled sequence (control) was examined. The mutant JIP1 (159-162G) was constructed by replacement of JIP1 residues 159 to 162 with Gly. *Experiment done in collaboration with Martin Dickens.*

Over-expressed JIP1 causes cytoplasmic retention of JNK1

Epitope tagged full length JIP1 was detected primarily in the cytoplasm of control (*data not shown*) and UV-C irradiated COS-1 cells (Fig 2-6). However,

transfected epitope tagged JNK1 was detected in both cytoplasmic and nuclear compartments of cells of UV-C irradiated COS-1 cells. Interestingly, in cells co-transfected with both JNK1 and JIP1, there was a marked reduction of JNK1 nuclear localization in UV-C irradiated cells (Fig. 2-6).

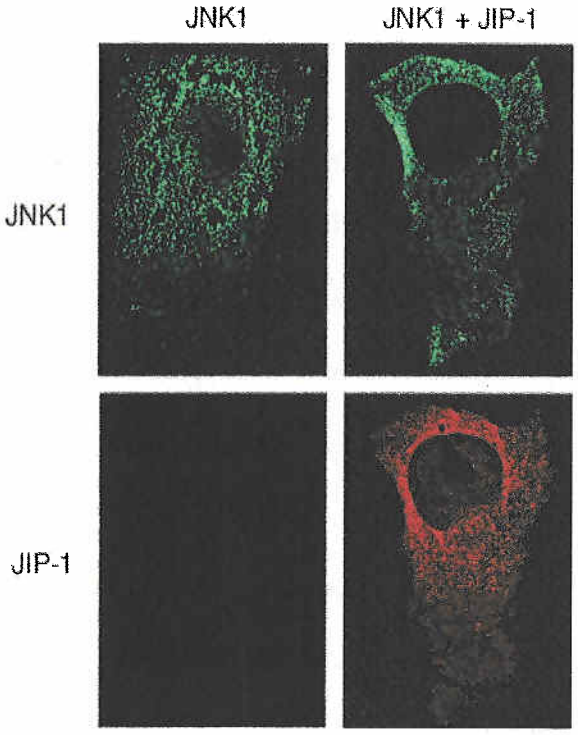

Figure 2-6 Indirect immunofluorescence analysis of the subcellular distribution of transfected JNK1 and JIP1. The cells were exposed to UV-C ($40J/m^2$) for 1 hour prior to fixation. FLAG-JIP1 was detected with the M2 monoclonal antibody and a Texas Red-conjugated secondary antibody (red). HA-JNK1 was detected with a polyclonal antibody to HA and fluorescein-isothiocyanate (FITC) labled secondary antibody (green). Three-dimensional images were collected by digital imaging microscopy (Raingeaud et al., 1995). Single optical sections of the images are presented.

In contrast, JIP1 caused no change in the subcellular distribution of p38 MAP kinase (*data not shown*) which was also located in both nuclear and cytoplasmic compartments of cultured cells (Raingeaud et al., 1995). Thus, overexpression of JIP1 causes cytoplasmic retention of JNK.

Discussion

The organization of components within a signaling pathway is critical for the integrity of efficient signal transduction. JIP1 repesents the first member of a new class of proteins within the JNK signal transduction pathway, the JNK scaffold proteins, that have a role in regulating JNK signal transduction. Scaffold proteins appear to function by providing component organization and creating an optimal local concentration of kinase cascade components. Since these data were originally presented (Dickens et al., 1997), the JIP group of JNK binding proteins have become the best characterized group of JNK scaffold proteins. There have been four JIP genes (JIP1-4) identified. JIP1 (also known as IB1), the subject of this chapter, and the closely related JIP2 (also known as IB2) (Bonny et al., 1998; Negri et al., 2000; Yasuda et al., 1999) are capable of forming signaling complexes with MKK7 and MLK3 that enhances JNK signalling (Whitmarsh et al., 1998; Yasuda et al., 1999). However, it has also been proposed that JIP2 might have a cross-activity with the p38 MAPK signalling pathway (Buchsbaum et al., 2002; Schoorlemmer and Goldfarb, 2001). JIP3 is structurally unrelated to JIP1 and JIP2, but also forms interactions with MLK, MKK7 and JNK (Ito et al., 1999; Kelkar et al., 2000). JIP4 is structurally related to JIP3, but its function is apparently different from other JIP members as it does not activate JNK. In contrast, JIP4 seems to activate the p38 MAP kinase pathway (Kelkar et al., 2005).

In this chapter, I have presented how JIP1 was cloned and the original analysis of its interaction with JNK. I have also demonstrated that over-expressed JIP1 is capable of retaining JNK in the cytoplasm of cultured cells.

JIP1 is a JNK binding protein

The yeast Two-Hybrid screening method used in this study to identify novel JNK binding proteins resulted in the recovery of several potential cDNA clones. A fragment corresponding to JIP1 residues 127-281, corresponding to the NH_2-terminus of JIP1, was obtained from this screen. The full length JIP1 transcript is 2.8kb with a 660 amino acid open reading frame. GST fusions of JIP1 sub-deletions within the 127-281 fragment were used to determine the JNK binding domain (JBD) in an *in vitro* protein binding assay with both JNK1 and JNK2. The JBD appears to require residues 144-163. Similarly, full length JIP1 and JNK1 associate *in vivo* and this can be demonstrated by co-immunoprecipitation from transfected COS-1 cells. Immunoprecipitated JIP1 pulls down JNK1 and vice versa. This association was not altered in UV-C irradiated cells, which activates the JNK signal transduction pathway.

The analysis of the JBD of JIP1 demonstrated an amino acid sequence consensus within the JBD as compared with other JNK binding proteins (Fig. 2-7). The JNK binding domain of both JIP1 and JIP2 are similar to the JBDs of the transcription factors c-Jun and ATF2. The consensus docking site, called the D-domain, are found in transcription factors and other MAPK substrates (Enslen and Davis, 2001; Sharrocks et al., 2000).

	φxφ
c-Jun	KILKQS-MTLNL
ATF2	KH-KHE---MTL
JIP1	RP-KRPT-TLNL
JIP2	EPHKRPT-TLRL
Consensus	K TL L M

Figure 2-7 The JNK Binding Domains (JBD) of JIP1 and JIP2 compared to the JBDs of other JNK binding proteins showing consensus residues. The JBDs of JNK binding proteins often have a LxL motif as well as a stretch of basic residues just amino-terminal of this region.

The scaffold function of JIP1 requires a JNK docking domain. Comparisions of JNK binding to JIP1 demonstrate that the two proteins associate *in vivo*, but originally it was believed JIP1 was a JNK signal transduction inhibitor, rather than an activator. Transfection and over-expression of JIP1 in CHO cells selectively blocked the activation of JNK and not p38 or ERK in response to interleukin-1 (IL-1) cell treatment and suppressed the effects of JNK on apoptosis and malignant transformation (Dickens et al., 1997). However, subsequent studies on JIP1 demonstrated this was an effect of over-expression of JIP1. This effect is presumably caused by disrupting the normal signaling component stoichiometry and sequestration of JNK from critical upstream kinases. Subsequent transfection analysis with additional upstream cascade components revealed rapid and specific JNK activation facilitated by JIP1 from activation by MLK3 (Whitmarsh et al., 1998; Yasuda et al., 1999). The physiological importance of JIP1 as an activator of the JNK signaling pathway has been demonstrated in *Jip1*$^{-/-}$ mice. There was a complete abrogation of JNK activation in these JIP1-deficient animals in response to excitotoxic and anoxic stress (Whitmarsh et al., 2001). Thus, the normal function of JIP1 appears to be the

facilitation of the JNK signal transduction pathway by acting as a scaffold protein for JNK and upstream kinase cascade components.

Over-expressed JIP1 sequesters JNK1 to the cytoplasm

Transfecting epitope tagged JIP1 into COS-1 cells demonstrates that it is a cytoplasmic protein by immunofluorescence analysis. Irradiating cells with UV-C light, which activates the JNK signaling pathway, had no effect on JIP1 localization. JNK is normally present in the cytoplasmic compartment in quiescent cells, while UV-C irradiation causes a nuclear translocation event so JNK localizes in both nuclear and cytoplasmic compartments. Co-transfecting JIP-1 and JNK demonstrated that JIP-1 was capable of retaining JNK in the cytoplasm in UV-C irradiated COS-1 cells as determined by immunofluorescence.

In order to have a better understanding of this cytoplasmic retention, we decided to use a relatively new form of epifluorescent microscopy that was capable of producing digital microscopic images with a higher resolution than normal epifluorescent microscopy. With the assistance of the UMASS Biomedical Imaging Facility directed by Dr. Fred S. Fay, we examined the immunofluorescence of co-transfected JIP1 and JNK1 COS-1 cells. The digital imaging microscopy and image restoration uses a process called "Exhaustive Photon Reassignment" (EPR) to take a series of single images of a cell at different focal lengths and "reassign" emitted fluorescent wavelengths back to the point of origin within the sample (Carrington et al., 1995; Fay et al., 1989). The

imaging results demonstrated a remarkable retention of JNK1 in the cytoplasm in cells co-transfected and over-expressing JIP1. The retention of JNK in the cytoplasm by over-expressed JIP1 was further evidence of its inhibitory effect on JNK signal transduction by sequestering of limiting JNK pathway components into separate components from the nucleus. This cytoplasmic sequestration is also observed with MKK7, but not MKK4 (Whitmarsh et al., 1998).

The sub-cellular localization of both JIP1 and JIP2 were later confirmed by confocal immunofluorescence using JIP monoclonal antibodies. However, in examining endogenous JIP1 and JIP2 in Rin5F insulinoma cells, JIP1 accumulated in peripheral cytoplasmic projections that extend from the cell surface. JIP2 also localized to these projections, but also accumulated in a cytoplasmic compartment that did not include JIP1 (Yasuda et al., 1999). Also, JIP3 localization in differentiated PC12 cells accumulate in the growth cones of the developing neurites (Kelkar et al., 2000). Over-expressed JIP1 in CHO cells inhibits the JNK signal transduction in CHO cells *in vivo*. Similarly, this over-expression inhibited pre-B cell transformation by *Bcr-Abl* and blocked apoptosis of PC12 cells (Dickens et al., 1997).

Over-expressed JIP1 mediated cytoplasmic retention of JNK, inhibits JNK activity and blocked JNK signal transduction *in vivo*. This differs from the function of endogenous JIP1, which functions to promote JNK signal transduction. However, inhibiting JNK signal transduction by ectopic introduction of the JBD of JIP1 has a demonstrated utility as a new therapeutic agent for

cerebral ischemia and diabetes. The HIV Tat transporter sequence was linked to a protease-resistant *all-D-retroinverso* form of the JIP1 JBD on a synthetic peptide. The JIP1-JBD peptide was capable of crossing the blood-brain barrier and was permeable to cells. Direct systemic delivery of this peptide reduced the lesions from excitotoxicity and cerebral ischemia in mice. This protection was correlated with a prevention of c-Jun activation resulting from an inhibition of the JNK signal transduction pathway (Borsello et al., 2003; Hirt et al., 2004). In another study, peritoneal introduction of a JIP1 JBD peptide led to its transduction to various tissues *in vivo* and it markedly improved insulin resistance and amerliorated glucose tolerance in diabetic mice (Kaneto et al., 2004). These studies demonstrate not only a critical role the JNK pathway has in diabetes and cerebral ischemia, but the promise of a powerful therapeutic agent against these diseases by inhibition of the JNK signaling pathway.

Conclusions

The yeast Two-Hybrid screen for novel JNK binding proteins yielded the first member of the JIP group of JNK scaffold proteins. This chapter focuses on the cloning and the initial JNK binding analysis of JIP1 and how JIP1 over-expression can act as a inhibitor of the JNK signaling pathway, rather than as protein scaffold that enhances it. JIP1 binds JNK both *in vitro* and *in vivo* and the JNK Binding Domain (JBD) of this protein is similar to the JBDs of other known JNK binding proteins. Furthermore, over-expression of JIP1 is capable of inhibiting JNK signal transduction *in vivo* and retaining JNK to the cytoplasm in stressed cells.

CHAPTER III

JMP1: A NOVEL JNK BINDING, MICROTUBULE LOCALIZED PROTEIN

Abstract

The c-Jun N-terminal Kinases (JNKs) are members of the mammalian MAPK family that are activated by environmental stress and pro-inflammatory cytokines. JNK is involved in the activation of c-Jun, a component of AP-1, by binding and phosphorylating the N-terminal serines 63 and 73, resulting in enhanced transcription from promoters under the regulation of AP-1. JNK is required for several biological processes including differentiation and apoptosis. Reorganization of the microtubule cytoskeleton occurs in response to various cellular events such as migration, proliferation, interaction with the extracellular matrix, immune cell infiltration, mitosis and meiosis. Microtubule interfering agents (MIAs), such as paclitaxel and nocodazole, are drugs that disrupt normal microtubule dynamics in cells by interfering with microtubule assembly. There is evidence the structural reorganization of the microtubule network has a regulatory effect on JNK signal transduction. MIAs have been shown to activate JNK by the MEKK1 signal transduction pathway, because *Mekk1* gene disruption abrogates JNK activation. Here we report the cloning and analysis of JMP1 (c-Jun N-terminal kinase binding Microtubule Localized Protein – 1), a microtubule associated protein that binds JNK and is expressed in murine spermatocytes.

JMP1 represents a novel microtubule colocalized protein that is linked with the JNK signal transduction pathways and shows stage-specific, restricted tissue expression.

Introduction

Cells respond to a broad variety of extracellular stimuli in their environment with evolutionarily conserved signal transduction mechanisms involving protein kinase cascades that regulate migration, proliferation, differentiation and death. The mitogen-activated protein kinase (MAPK) signal transduction pathways play a critical regulatory role with these mechanisms. The extracellular signal-regulated protein kinases (ERK), the c-Jun NH_2-terminal kinases (JNK) and the p38 MAPKs are the three major groups of MAPKs pathways described in mammals (Schaeffer and Weber, 1999). Each of these groups are activated by dual phosphorylation on Thr and Tyr by a MAPK kinase (MAPKK) which are, in turn, activated by a MAPKK kinase (MAPKKK) in a protein kinase cascade.

Three mammalian genes encode the JNK protein kinases. *Jnk1* and *Jnk2* are ubiquitously expressed, but *Jnk3* is primarily expressed in the brain, heart and testis (Derijard et al., 1994; Gupta et al., 1996; Kallunki et al., 1994; Kyriakis et al., 1994; Rincon et al., 1998).The JNK group of MAPKs are activated by exposure of cells to inflammatory cytokines (e.g. IL-1 and TNFα) and various types of environmental stress (e.g. osmotic and redox stress, ultraviolet radiation) (Davis, 2000). JNK protein kinases are required for several biological processes including T-cell differentiation and apoptosis (Dong et al., 1998; Rincon et al., 1998; Sabapathy et al., 1999; Yang et al., 1998) and neuronal apoptosis during early brain development (Kuan et al., 1999; Yang et al., 1997a). JNK is activated by dual phosphorylation on Thr and Tyr by the MAPK Kinases MKK4 and MKK7.

These are activated by phosphorylation by MAPKKKs including ASK1, TPL2, TAK1 and members of the mixed-lineage protein kinase (MLK) and MEKK kinase families (Davis, 2000).

Reorganization of the microtubule cytoskeleton occurs in response to various cellular events such as migration, proliferation, interaction with the extracellular matrix, immune cell infiltration and mitosis. The structural reorganization of the microtubule network stimulates signal transduction pathways, and several studies demonstrate that microtubules play a critical regulatory role. Evidence of the regulatory effects of microtubules on JNK signal transduction have been demonstrated in studies using microtubule interfering agents (MIA). MIAs, such as paclitaxel and nocodazole, are drugs that disrupt normal microtubule dynamics in cells by interfering with microtubule assembly (Wilson and Jordan, 1994). MIAs are known to arrest cells at the G2/M phase of the cell cycle, but also activate JNK by MEKK1 (Yujiri et al., 1998). *Mekk1* gene disruption demonstrate defects in cell migration, altered apoptosis and it is required for JNK activation in response to MIAs (Yujiri et al., 1999; Yujiri et al., 1998).

Microtubules clearly have a regulatory role in JNK signal transduction, but to date, there is little demonstrated evidence of interactions between microtubules and members of the JNK signal transduction pathway. Studies with MLK2 have shown a link between microtubule dynamics and the JNK signal transduction pathways. MLK2 is a potent activator of the JNK kinases MKK4 and

MKK7 (Cuenda and Dorow, 1998; Hirai et al., 1998) and has been shown to bind β-tubulin monomers (Rasmussen et al., 1998). It has also been demonstrated to localize along microtubules in Swiss 3T3 cells, and associate with the kinesin superfamily motor KIF3 (Nagata et al., 1998). MLK2 is expressed in brain and skeletal muscle (Dorow et al., 1995), and also has a restricted expression in post-mitotic, late pachytene spermatocytes and round haploid spermatids (Phelan et al., 1999).

Here we report the cloning and analysis of JMP1 (c-Jun N-terminal Kinase binding Microtubule associated Protein 1), a microtubule associated protein which binds JNK and is expressed in post-mitotic murine spermatocytes. JMP1 represents a novel member of microtubule associated proteins that are linked with the JNK signal transduction pathway, and show stage specific, restricted tissue expression.

Experimental Procedures

Cloning of JMP1

A JMP1 cDNA was isolated by a two-hybrid screen of a mouse embryo cDNA library in the yeast strain L40 using a bait-plasmid that expresses a LexA-JNK1 fusion protein as outlined in Chapter 2 of this thesis (Dickens et al., 1997). Four positive clones were isolated overlapping a common 315bp cDNA fragment. This cDNA was radiolabled with [^{32}P]-dATP (Amersham) using the Prime-It II DNA radiolabeling kit (Stratagene) and employed to screen a mouse testis cDNA λUni-ZAP XR library (Stratagene). A 1.8kb clone corresponding to a 3' fragment of the JMP1 cDNA was isolated. The 5' region of the full length JMP1 cDNA was isolated by RACE (Marathon cDNA Amplification Kit, Clontech) from reverse transcribed murine testis mRNA using the JMP1 specific primer 5'-GAGGAGCTGAGCTGTGGGCGGCGGCAAAGC-3'. Standard methods were used to construct the 4.6kb full length JMP1 cDNA from the overlapping fragments to create pBS-JMP1. DNA sequencing was performed with a 373A machine (Applied Biosystems).

Plasmids

GST (Glutathione S-Transferase) fusion proteins with JMP1 were expressed in the vector pGEX-5X-1 (Pharmacia). FLAG epitope tagged JNK1 has been previously described (Gupta et al., 1996). Fragments of the JMP1 cDNA were generated by PCR and subcloned in the BamH1 and EcoR1

polylinker sites to create pGST-JMP1 (residues 1187-1291), pGST-JMP1 (residues 1187-1235), pGST-JMP1 (residues 1187-1270), pGST-JMP1 (residues 1214-1291) and pGST-JMP1 (residues 1236-1291). JMP1 base-pairs (3313-4573) were amplified by PCR and subcloned into the BamH1 and Xho1 polylinker sites of pGEX-5X-1 to create pGST-JMP1 (residues 1083-1502).

The JMP1 cDNA (4.6kb) was subcloned in the Not1 and Xho1 sites of pcDNA3 (Invitrogen) to create the pJMP1 expression vector. The FLAG epitope (DYKDDDDK) was inserted between codons 1 and 2 of the JMP1 cDNA by insertional overlapping PCR (Ho et al., 1989) to generate pFLAG-JMP1. pFLAG-JMP-NT was created by subcloning the 2340 base-pair Not1 and Bgl2 cDNA fragment, coding for JMP1 residues #1-757, from pFLAG-JMP1 into pcDNA3. pFLAG-JMP-CT, coding for JMP1 residues #1025-1502, was generated by PCR amplification and subcloning of JMP1 base-pairs (#3141-4570) into pcDNA3 and fusing the FLAG epitope 3' of JMP1 methionine residue #1025. The sequence of the clones were verified by DNA sequencing.

Cell Lines

3T9 cells have been previously described (Harvey et al., 1993; Kennedy et al., 2003; Tournier et al., 2000). HeLa, TM3, TM4 and GC-2spd^{ts} cells were obtained from the American Type Culture Collection (ATCC) (American type Culture Collection). The TM3 and TM4 cell lines are derived from murine Leydig and Sertoli cells respectively (Mather, 1980). GC-2spd^{ts} cells are derived from murine spermatocytes and possess a temperature senstive mutation that has

been reported to allow cells to differentiate into round haploid spermatids *in vivo* (Hofmann et al., 1994).

Protein Purification

JNK1 and JNK2 proteins were FLAG epitope tagged and expressed using the *Pichia pastoris* overexpression system (Invitrogen) as described by the manufacturer's protocol. Glutathione-S-Transferase (GST) JMP1 fusion proteins were obtained from BL21 (DE3) bacterial lysates expressing GST-JMP1 (residues 1187-1291), GST-JMP1 (residues 1187-1235), GST-JMP1 (residues 1187-1270), GST-JMP1 (residues 1214-1291) or GST-JMP1 (residues 1236-1291). Cells were induced for fusion protein expression for 2 hours with 1mM IPTG and then harvested in Buffer X (20mM Tris-Cl pH 7.4, 1M NaCl, 0.2mM EDTA, 0.2mM EGTA). Fusion proteins were purified by glutathione affinity chromatography (Smith and Johnson, 1988).

Western Blots

Proteins were separated by SDS-PAGE and transferred to an Immobilon-P membrane (Millipore) by semi-dry electrotransfer. Blots were blocked (1 hour) in TBST (25mM Tris-Cl, 100mM NaCl, 0.1% Triton-X100) with 5% non-fat dry milk then incubated (1 hour) with either M2 monoclonal antibody (1:1000; Sigma) or JNK monoclonal antibody (1:200; Pharmingen). Blots were washed four times in TBST, then incubated (30 mins) with horseradish peroxidase (HRP) conjugated goat anti-mouse Ig secondary antibody (Amersham). Blots were washed and

labled proteins were detected with the Rennaissance chemiluminescence kit. (NEN).

Antibodies

JMP1 antiserum was produced in rabbits following a standard immunization protocol utilizing GST-JMP1 (residues 1083-1502) fusion protein as antigen (Panigen Inc.). The antiserum was clarified by centrifugation and anti-GST reactive antibodies were removed by diluting antiserum (1:10) in 0.1M HEPES pH 8.0 and passing it four times through a Glutathione-Sepharose column with immobilized GST in 0.1M HEPES pH 8.0 at 4°C. GST-JMP1-(residues 1083-1502) fusion protein was immobilized on a 5mL Affi-Gel-15 matrix following manufacturer's protocols. (BioRad Inc.) The antiserum was incubated (3 hours) with the immobilized antigen at 4°C. The matrix was loaded into a column and subsequent washes and elutions were performed at 4°C. The column was washed twice with 0.1M HEPES pH 8.0, once with HT-1 buffer (0.1M HEPES, 0.1% Triton X-100), once with HT-2 buffer (0.1M HEPES, 0.5% Triton X-100) and once with 0.1M HEPES pH 8.0. Bound antibodies were eluted with Antibody Elution Buffer (0.2M Glycine-HCl pH 2.5) and collected in 0.1mL fractions. The pH of the eluted fractions were equilibrated to 7.4 with 0.5M HEPES (pH 7.4) and antibody containing fractions were pooled and concentrated using Centricon-30 microconcentrators (Amicon Inc.). An anti-pericentrin antibody was a gift from Dr. Stephen Doxsey. A rabbit polyclonal antibody to γ-Tubulin (IgG fraction of antiserum) was obtained from Sigma Corp. JNK1

monoclonal antibody G151-333 was obtained from Pharmingen Inc. and JNK1 polyclonal antibody sc-571 (FL) was obtained from Santa Cruz Biotechnology Inc.

Tissue culture and transfection assays

COS-1 and HeLa cells were cultured at 37°C in Dulbecco's modified Eagle's medium (DMEM) supplemented with 10% heat-inactivated fetal bovine serum (Life Technologies, Inc.), 2mM glutamine, 100U penicillin per ml, and 100U streptomycin per ml in a humidified environment with 5% CO_2. Transient transfections were performed with the LipofectAMINE reagent (Life Technologies) according to the manufacturer's recommendations. After 20 hours, some cells were treated with UV-C (60 J/m^2) and then recovered in DMEM with 10% fetal bovine serum 30 mins. prior to cell lysis. Cell extracts were prepared in Triton lysis buffer (TLB; 20mM Tris-Cl pH 7.4, 137mM NaCl, 2mM EDTA, 1% Triton X-100, 25mM β-glycerophosphate, 1mM Na orthovanadate, 2mM sodium pyrophosphate, 10% glycerol, 5μg of leupeptin per ml, 5μg of aprotinin per ml, 1mM phenylmethylsulfonyl fluoride) and centrifuged at 15,000 x *g* (15min at 4°C). The concentration of total soluble protein in the supernatants were quantitated by the Bradford method (Bio-Rad).

JNK Binding Assays

GST-JMP1 fusion proteins (5μg) were bound to 10μl of washed Glutathione Sepharose 4B beads (Amersham-Pharmacia) in 0.5mL volume of

phosphate buffered saline with 0.5% Triton X-100 (PBS-T) for 30 minutes at 4°C, washed three times, then 5μg of *Pichia* lysate expressing FLAG-JNK1 or FLAG-JNK2 were added in 0.5mL PBS-T and incubated for 2 hours at 4°C. Pellets were washed four times in PBS-T and boiled with 10μl Laemmli sample buffer. The samples were separated with SDS-PAGE and examined by immunoblot analysis with the M2 monoclonal antibody.

Co-immunoprecipitation

FLAG epitope tagged JMP1, JMP1-NT and JMP1-CT were transfected into COS-1 cells and lysates harvested in TLB. Total lysate (50μg) was incubated with 1μg of M2 monoclonal antibody for 3 hours at 4°C. Protein G-Sepharose (10μL) (Amersham-Pharmacia) was washed and incubated (30 mins.) at 4°C. Beads were pelleted, washed four times with ice cold lysis buffer, and boiled for 5 mins. in 10μL Laemmli buffer. Samples were separated on SDS-PAGE and examined by immunoblot analysis with a JNK1 monoclonal antibody (1:200; Pharmingen). As a loading control, total cell lysate (10μg) was examined by immunoblot analysis with the JNK1 monoclonal antibody.

Northern Blots

Northern blots with 2μg poly A^+ mRNA per lane isolated from eight different adult murine tissues and 2μg total RNA isolated from murine embryos at four different embryonic stages (Clontech) were probed with a ^{32}P-labeled random-primed 313bp JMP1 cDNA probe (nucleotides #3627-3940). The blots

were exposed for 24 and 96 hours. The blots were stripped and reprobed with a ^{32}P-labeled random-primed β-Actin probe (Clontech) and exposed for 24 hours to Kodak X-AR autoradiography film.

Immunocytochemistry

Slides with paraformaldehyde-fixed, paraffin-embedded 7μm sections of whole mouse testis (Novagen) were washed three times (5 mins) with mixed xylenes (Sigma) and rehydrated in graded ethanol baths. The slides were washed twice in PBS (5 mins) and blocked (30 mins) in PBS with 2% normal goat serum (Jackson ImmunoResearch, Inc.) in a humidified atmosphere. The slides were incubated (30 mins) with affinity purified rabbit anti-JMP1 antibody (diluted 1:50 in PBS) in PBS with 2% normal goat serum using probe clips to isolate the incubated samples (Grace BioLabs). The slides were washed twice (5 mins) in PBS and incubated (30 mins) with biotinylated goat anti-rabbit IgG (1:200; Vector Labs) in PBS with 2% normal goat serum. The sections were washed twice (5 mins) and incubated (30 mins) with ABC Vectastain horseradish-peroxidase labeling reagent (Vector Labs). The slides were washed again and peroxidase staining was detected with the Vector VIP system according to the manufacturer's recommended protocol (Vector Labs). Color development was arrested by washing in water. Sections were counter-stained with methyl green, post-fixed with 0.05% acetic acid in acetone (1 min) and dehydrated with graded ethanol baths. Sections were permanently mounted with Vecta-Mount (Vector Labs). Photographs were taken with a Zeiss Axiovert 35 microscope. Control

slides incubated with no anti-JMP1 antibody or no secondary antibody were done to verify antibody specificity and minimal cross reactivity.

Immunofluorescence microscopy

COS-1 and HeLa cells were seeded onto glass 22mm x 22mm No. 1 coverslips (Corning) and allowed to grow for 48 hours. The cells were fixed (15 mins) with 4% paraformaldehyde in PBS and permeabilized (5 mins) with 0.2% Triton X-100 in PBS. Some cells were pre-permeabilized prior to fixation. Pre-permeabilization was performed by incubating cells (5 mins.) with 0.5% Triton X-100 and Paclitaxel (10μM) (Sigma) in PEM buffer (100mM PIPES-HCl pH 6.9, 6mM $MgCl_2$, 0.5mM EGTA). These cells were fixed (15 mins) in 4% paraformaldehyde in PEM. Coverslips were blocked (20 mins.) with 5% normal donkey serum (Jackson ImmunoResearch, Inc.) in PBS. Paclitaxel binds and inhibits the disassembly of microtubules (Scialli et al., 1994).

Coverslips with COS-1 cells were incubated for 1 hour with the M2 monoclonal antibody (1:500) in PBS with 5% normal donkey serum, washed three times in PBS then incubated with rabbit anti-α-tubulin polyclonal serum (1:1000; gift from Dr. C. Bulinsky, Columbia University College of Physicians & Surgeons) in PBS with 5% normal donkey serum. Immune complexes were detected (30 mins.) with Texas red-conjugated anti-mouse immunoglobulin (Ig) and fluorescein-conjugated anti-rabbit Ig antibodies (1:200; Jackson ImmunoResearch, Inc.) in PBS with 5% normal donkey serum.

Coverslips with HeLa cells were incubated with affinity-purified rabbit anti-JMP1 antibody (1:500) and monoclonal anti-α-Tubulin (1:500, Clone DM1α; Sigma) in PBS supplemented with 5% normal donkey serum for 1 hour. Immune complexes were detected with fluorescein-conjugated anti-mouse Ig and Texas red-conjugated anti-rabbit Ig antibodies (1:200; Jackson ImmunoResearch, Inc.) in PBS with 5% normal donkey serum. All coverslips were stained with 4',6-diamidino-2-phenylindole (DAPI; 0.2μg per ml in PBS; 1 min), and mounted with Vectashield (Vector Laboratories, Inc.) All procedures were performed at room temperature. Fluorescence microscopy was performed with a Zeiss Axioplan microscope and digital images were post-processed with Photoshop software (Adobe Inc.).

Cell Cycle Synchronization

HeLa cells were seeded into 12-well tissue culture plates. Individual plates, done in duplicate, were labled "unsynchronized", "2° thymidine", "release + 6hrs" or "NOC + 6hrs". The cells were grown until a 50% cell density was achieved. All plates except the "unsynchronized" plates were washed and overlayed with 2mM thymidine supplemented DMEM media + 10% fetal bovine serum (Sigma Co.) and further incubated for 16 hours. Thymidine supplemented media was then aspirated, the cells washed three times with fresh media, then incubated in medium supplemented with 24μM 2'-deoxycytidine (Sigma Co.) for 4 hours. The media was then aspirated, the cells washed as above, and a second 2mM thymidine block was again applied for 16 hours. The rest of these plates

were again washed and overlayed with 2'-deoxycytidine supplmented media and allowed to incubate another 6 hrs. The "NOC + 6hrs" plates were then washed and overlayed with 0.1μM nocodazole supplemented media and allowed to incubate for 4 more hours.

RNA Purification & RT-PCR

Total RNA from the cell cycle synchronized HeLa cells was harvested using the RNEasy total RNA extraction kit (Qiagen Corp.). RNA was harvested from the "2° Thymidine block" plates after the second thymidine block. RNA was harvested from the "release + 6hrs." plates after being incubated for 6 hours in 2'-deoxycytidine supplemented media. RNA was harvested from both the "NOC + 6hrs." and "unsynhronized" plates after the 4 hour nocodazole incubation.

Relative levels of JMP1 mRNA were determined using the One-Step RT-PCR kit (Qiagen Corp.). JMP1 primers "JMP-2638" (5'-CTACCAGCCACATGGCCGTTGGGC-3') and "JMP-2998" (5'-GTCGCCTTGCTGGTCTTCAGGTCC-3') were used in this coupled reverse transcription PCR reaction, which amplify a JMP1-specific 360bp fragment. 10ng of each total RNA was amplified according to the manufacturer's protocol.

siRNA Analysis

Candidate JMP1 siRNA sequences for expression silencing were designed using standard siRNA guidelines (Meister 2004) and the double stranded RNA siRNA design algorithm selection program web-tool designed by

the Bioinformatics and Research Computing group at the Whitehead Institute. (http://jura.wi.mit.edu/siRNAext/) Of the possible candidates retrieved, three were selected based on their strong selection patterns for RNA silencing. JMP1-597 (5'-AACATGACATGGTCCTCAATGTT-3'), JMP1-2504 (5'-AAAACACCATCCAAAGACAGCTT-3') and JMP1-4409 (5'-AACTGTATGGCTGCAGCTAACTT-3'). These siRNA candidate sequences are located within the N-terminal, the central and the C-terminal domains of JMP1 respectively. For a non-silencing negative control, a "scrambled" sequence (JMP1-NC; 5'-CAGTCGATGCAAGTCAGTACGC-3') was selected with no known sequence database matches. The Ambion "Silencer" siRNA Construction Kit (Ambion Inc.) was used to generate JMP1 specific, kit-supplied GAPDH positive control and the "scrambled" double-stranded siRNA negative control according to the manufacturer's protocol.

3T9 cells were plated into 6-well tissue culture dishes and allowed to reach 75% confluence. The siRNA complexes were transfected using Oligofectamine reagent (Invitrogen Corp.) and allowed to grow for either 24 or 48 hours. Total RNA was then harvested using the RNEasy kit (Qiagen Corp.) and quantitated. RNA silencing was quantitated by the One-Step RT-PCR kit (Qiagen Corp.) JMP1-specific primers JMP-4110 (5'-TCCAACTTCTAGAGACCAGGTCTA-3') and JMP-4417 (5'-CATACAGTTGCTGGCTTCTAGC-3'), GAPDH specific primers GAP-F (5'-CAAGCATTGGACTGTAGGCTG-3') and GAP-R (5'-

AGACTCCACGACATACTCAGCACC-3') were used in this coupled reverse transcription PCR reaction. The JMP1 primers amplify a 309bp fragment and the GAPDH primers amplify a 204bp fragment. Either 5ng or 50ng total RNA were used in the RT-PCR reactions.

Results

Molecular Cloning of JMP1

In order to identify novel JNK interacting proteins, we screened a mouse embryo fibroblast expression library with JNK1 in a yeast Two-Hybrid assay (Dickens et al., 1997). We obtained four overlapping positive clones with a 315bp common cDNA sequence with no alignment similarity to known database sequences at the time (Altschul et al., 1990) and no apparent sequence motifs. We decided to examine this clone further since the expresssed cDNA strongly bound JNK1 in an *in vitro* binding assay and the Northern expression pattern was localized to testis tissues. The 315bp cDNA fragment was used to screen a mouse testis cDNA library. Six overlapping clones were recovered, the longest being 1.8kb with a contiguous open reading frame of 535 amino acids that includes the probe's open reading frame and a 3' stop codon. Since there were no 5' stop codons in this reading frame, we postulated that additional 5' coding sequence was not recovered in the testis cDNA library screen. We therefore used rapid amplification of cDNA ends (RACE) with mouse whole testis cDNA as a template to obtain the remaining 5' upstream sequence. A cDNA (4,602 nucleotides) with a single, 1,502 amino acid open reading frame (nucleotides 68 to 4576) was obtained. The first ATG matches a Kozak consensus ribosome binding site (Kozak, 1984) and the upstream sequence contains two in-frame stop codons with additional stop codons in alternative reading frames, suggesting that the entire coding sequence was isolated. We named this new protein JMP1.

The JMP1 (JNK binding Microtubule localized Protein-1) cDNA encodes a protein of 1502 amino acids with a calculated mass of 163kDa and a pI of 5.0. The C-terminus of JMP1 contains the JNK binding domain, which includes the 105 amino acid fragment isolated from the yeast Two-Hybrid screen. The N-terminal 50 amino acids contains a basic region (pI = 12.4) and a PFAM database search (Bateman et al., 2000) identified twelve potential WD40 repeats within amino acids 105-743 (Fig. 3-1A). The twelve WD40 repeats match a motif consensus within the four beta-sheet strands of the structure. Although several of the JMP1 WD40 repeats only partially match the consensus sequence, this is observed in other WD-repeat proteins with known function (Fig. 3-1B) (Neer et al., 1994).

A

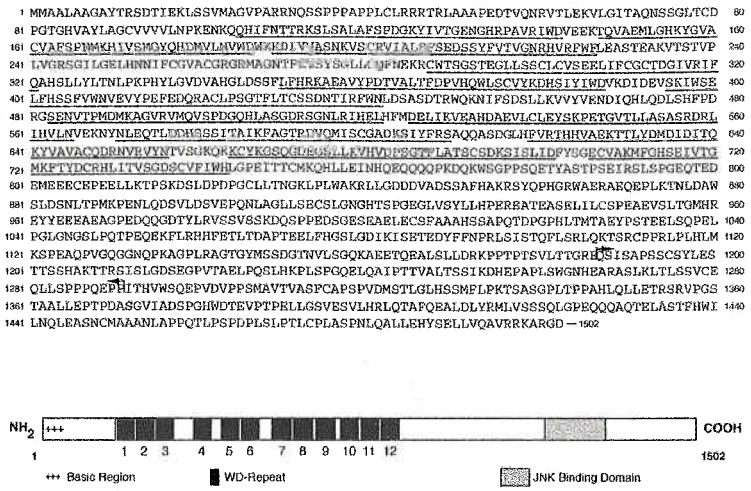

B

WD-Repeat	Strand d		Strand a		Strand b	Strand c
	xxxxxxx[1 ?]GHxxxV	xxVxFxx[0-?]PDG[0-3]	xLASGSxDx	TIKVWD
	A I	L W I L C I V	SNS DSP	IVTAG VL SA FI C	SVRLFN L IY A
105-142	QHIFNTT	RKSLSALAFSPD	GKYI	VTGENGHRPAVRIWD
149-186	TQVAEML	GHKYGVACVAFS	PNMKHI	VSMGYGHDMVLNVWL
189-226	KDIVVAS	NKVSCRVIALSF	SEDS	SYFVTVGNRHVRFWH
287-321	EKRCWTS	GSTEGLLSSCLC	VSEE	LIFCGCTDGIVRIFQ
350-387	LFHRKAE	AVYPDTVALTFD	PVHQ	WLSCVYKDHSIYIWD
404-441	SKIWSEL	FHSSFVWNVEVY	PEFEDQRACLPSG	TFLTCSSDNTIRFWN
484-521	SENVTEM	DMKAGVRVMQVS	PDGQ	HLASGDRSGNLRIHE
527-565	DELIKVE	AHDAEVLCLEYS	KPETGVT	LLASASRDRLIHVLN
573-609	NLEQTLD	DHSSSITAIKFA	GTRDV	QMISCGADKSIYFRS
619-656	FVRTHHV	AEKTTLYDMDID	ITQK	YVAVAQQDRNVRVYN
664-701	KCYKGSQ	GDEGSLLKVHVD	PSGT	FLATSCSDKSISLID
706-743	ECVAKMF	GHSEIVTGMKFT	YDCR	HLITVSGDSCVFIWH

Figure 3-1 Primary structure and sequence of murine JMP1. (A) The amino terminal region has a calculated basic (pI=12.4) domain and twelve WD40 repeats. The carboxyl terminal has a calculated acidic (pI=5.2) domain and contains a JNK binding domain. The murine JMP1 cDNA encodes a 1502 amino acid protein. The twelve WD40 repeats are underlined. The arrows define the JNK binding region isolated from a yeast Two-Hybrid library. (B) The JMP1 WD40 repeats compared with a consensus sequence. The four beta-sheet strands of the WD40 motif are indicated. "x" defines any amino acid residue while residues matching the consensus sequence are in bold. Bracketed numbers indicate the number of residues allowed within the consensus region.

JMP1 is expressed as a single 4.6kb mRNA transcript at high abundance in murine testis. A low level of JMP1 mRNA is detected in other adult tissues (Fig. 3-2A). The JMP1 mRNA is also detected in murine embryos, but at much lower levels than in testis. Murine embryos express relatively similar levels of JMP1 from E4 through E14 (Fig. 3-2B).

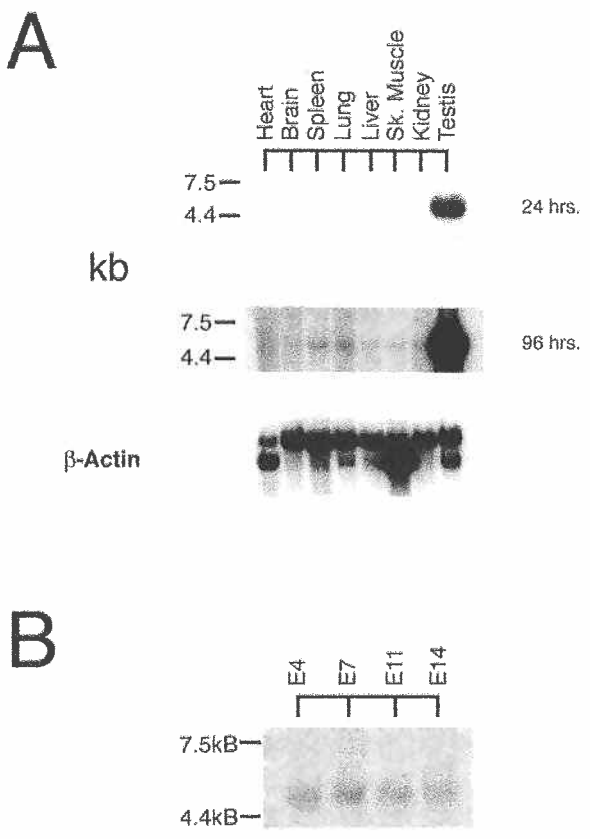

Figure 3-2 Tissue distribution of murine JMP1. (A) Northern blot analysis of JMP1 mRNA distribution in murine tissues. 2μg of poly A^+ mRNA isolated from various murine tissues were hybridized with a cDNA probe specific for carboxyl nucleotides 3624-3937 of JMP1. Two exposures (24 and 96 hours) of the blot are shown. The blot was reprobed with a β-Actin probe to confirm equal loading in each lane. (B) Northern blot analysis of JMP1 mRNA from whole murine embryos at E4, E7, E11 and E14. 2μg of poly A^+ mRNA was loaded in each lane and hybridized with the JMP1 probe. The blot was exposed for 48 hours.

JMP1 is Expressed in Murine Spermatocytes

Since JMP1 was highly expressed in the testis, we examined the expression of JMP1 using immunocytochemistry on sections of adult murine testis. The testis is a complex organ containing several cell types with varied function and morphological localization. Spermatocytes are derived from spermatogonia that have entered a committed spermatogenic differentiation pathway and reside along the periphery of the seminiferous tubule (Hecht, 1995). As the spermatocyte matures, it migrates towards the lumen of the tubule and undergoes two rounds of meiosis, and develops into a round-haploid spermatid.

Round-haploid spermatids further differentiate into immature spermatids which begin to morphologically resemble mature sperm cells, which are eventually released into the lumen.

The tissue sections were probed with an affinity-purified JMP1 polyclonal antibody generated from the C-terminal 419 amino acids. The specificity of the JMP1 antibody was verified using competition control incubations on testis sections with GST-JMP1-CT added to the antibody. No testis staining was observed when GST-JMP1-CT was included in the incubation media (*data not shown*). Horseradish-peroxidase staining indicates JMP1 expression limited to the lumenal compartment of the seminiferous tubule, the region where spermatocytes differentiate by two rounds of meiosis into round haploid spermatids. There appears to be no expression in the basal compartment surrounding and including the seminiferous tubule periphery. (Fig 3-3A). Higher magnification of cells expressing JMP1 show horseradish-peroxidase staining distinct from the nuclear methyl green stain, suggesting JMP1 localizes in the spermatocyte cytoplasm. In order to confirm cell type, we performed JMP1 Northern blot analysis on the TM3 and TM4 cell lines. A single 4.6kB transcript was detected in both cell lines, but its expression was comparable to the level seen in other murine somatic tissues (*data not shown*). However, Leydig cells are usually present in the peritubular regions outside the seminiferous tubule and Sertoli cells are often localized at the junction between luminal and basal compartments (Eddy, 2002). Since the morphology of the cells observed by

immunocytochemistry are indicative of spermatocytes (yellow box; Fig 3-3B) we believe JMP1 expression increases to high levels in spermatocytes.

Spermatogenesis occurs by "differentiation waves" through the seminiferous tubule and there was no change in JMP1 localization in any of the tubule cross sections observed. The intensity of JMP1 expression was consistant along the tubule cross-sections. JMP1 immunocytochemistry on murine spermatozoa isolated from the caudate epididymus (Syntin and Cornwall, 1999) showed no detectable JMP1 expression (*Data Not Shown*).

Since JMP1 was expressed in the meiotic spermatocytes within murine testis sections, we wanted to confirm JMP1 protein expression in the GC-2spd^{ts} cell line dervied from murine spermatocytes (Hofmann et al., 1994). A cell line that replicated spermatocyte differentiation *in vitro* would make a convenient model for the study of JMP1. The GC-2spd^{ts} cell line possess a temperature sensitive mutation that was believed to allow the cells to undergo both rounds of meiosis as spermatocytes *in vivo*. Surprisingly, we were not able to detect an increased JMP1 expression by immunocytochemistry in this cell line from cultures at either the permissive or non-permissive temperatures. However, we were also unable to determine if this cell line was differentiating. This suggested there was a critical difference between this cell line and normal spermatocytes, which indicated the GC-2spd^{ts} cell line would not be useful for our purposes. However, later observations made on this cell line called into question their ability to enter and complete both rounds of meiosis. It was observed the GC-2spd^{ts} cell

line could not generate haploid cells in culture (Wolkowicz et al., 1996). This makes it difficult to mark the point in spermatogenesis this cell line can accomplish in culture. Also, since JMP1 immunolocalization is only detected in the luminal compartments of the seminiferous tubule where committed spermatocytes are actively undergoing or have completed meiotic differentiation, the lack of increased JMP1 protein expression in GC-2spd^{ts} cells indicates they may not accurately reflect a post-meiotic phenotype.

Our data supports the observation that JMP1 expression occurs within spermatocytes during the meiotic phases of spermatogenesis *in vivo*.

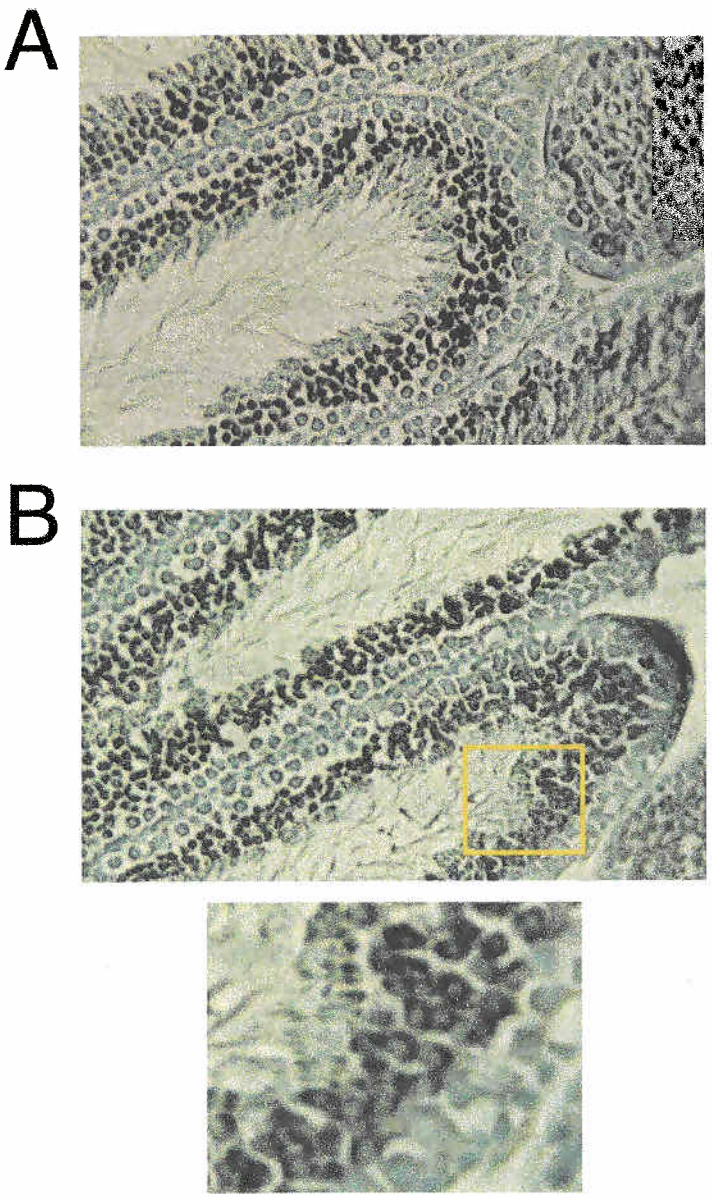

Figure 3-3 JMP1 is expressed in the post-mitotic spermatocytes of murine testes. Paraformaldehyde fixed, paraffin embedded 7μm thick murine testis tissue sections were incubated with affinity-purified anti-JMP1 antibody, washed, then incubated with a horseradish peroxidase (HRP) conjugated anti-rabbit secondary antibody. Sections were processed with Vector VIP peroxidase developing kit (Vector Laboratories) and counterstained with methyl green. (A) JMP1 localizes to the lumenal seminiferous spermatocytes corresponding to an area with post-mitotic germ cells. No staining was evident along the periphery of the seminiferous tubules indicating JMP1 was not expressed in mitotically active spermatogonia. (B) A another testis section photograph with a region of higher magnification showing JMP1 spermatocyte localization. There is a notable absence of JMP1 within the methyl green counterstained spermatocyte nucleii.

JMP1 is a JNK Binding Protein

Since JNK was used as the bait in the Two-Hybrid screen, the recovered JMP1 fragment was likely to contain an active JNK binding region. The JNK pathway is activated by a kinase signal transduction cascade in response to

various cellular stresses including UV-C light (Davis, 2000). We used JNK1 co-immunoprecipitation assays to examine if full length JMP1 was capable of binding JNK *in vivo*. We generated three FLAG epitope tagged constructs from the full length FLAG epitope tagged JMP1 cDNA (Fig. 3-4A). The full length JMP1 and C-terminus constructs, but not the N-terminal construct, co-immunoprecipitated endogenous p46 JNK from COS-1 lysates. Both full length and the C-terminal end of JMP1 demonstrated a marked increase in JNK co-immunoprecipitated from lysates irradiated with UV-C light (Fig. 3-4B). We were unable to determine if p55 JNK co-immunoprecipitation occured since the M2 monoclonal antibody Ig heavy chain co-migrates with the p55 band in SDS-PAGE. The arrows indicate a slower migrating p46 JNK band. In the full length JMP1 immunoprecipitates, this gel-shifted JNK band appears to be the predominate species that co-immunprecipitates with JMP1 in UV-C treated lysates. No JNK co-immunoprecipitation was detected with the JMP1 N-terminus construct. Binding associations were not detected with p38α, ERK1, ERK2, MKK7, or MKK4 (*data not shown*).

We attempted to co-immunoprecipitate endogenous JNK and JMP1 from 3T9, HeLa and COS1 cells using the affinity purified anti-JMP1 antibody and commercially available anti-JNK antibodies. We were unable to detect endogenous co-immunoprecipitation with either protein (*data not shown*).

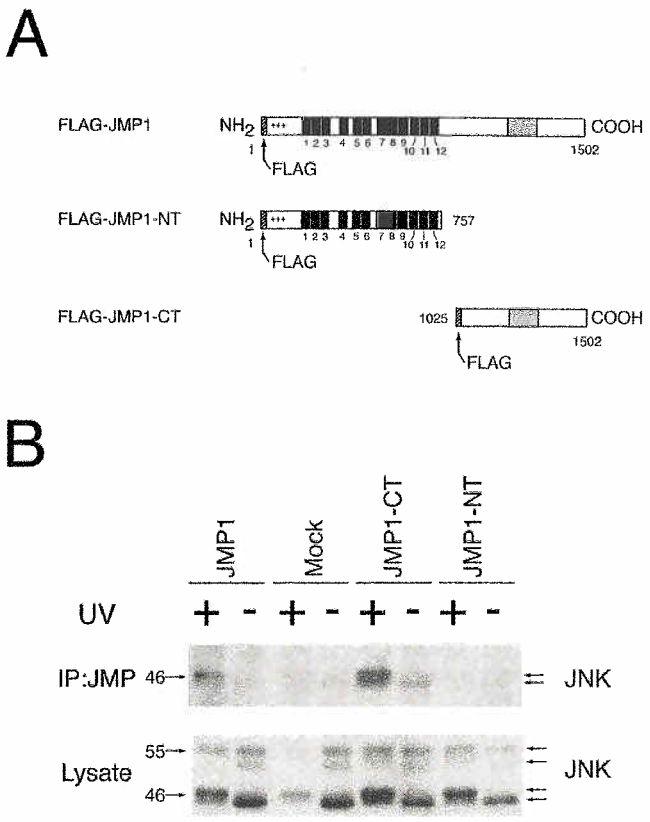

Figure 3-4 JMP1 binds JNK1 *in vivo* from COS1 cell lysates. (A) FLAG epitope tagged full length JMP1 (amino acids #1-1502), JMP1-CT (amino acids #1025-1502) and JMP1-NT (amino acids #1-757) were used in co-immunoprecipitation assays. (B) JMP1 preferentially immunoprecipitates UV activated endogenous JNK from COS1 cells. Transfected COS1 cells expressing JMP1 were treated with 60J/m^2 UV-C light. Lysates were prepared and incubated with Sepharose-Protein G immobilized M2 monoclonal antibody and washed. The immunoprecipitated proteins were separated on SDS-PAGE and transferred to Immobilon-PVDF. Membranes were probed with monoclonal JNK1 antibody. The lower panel shows COS1 lysates probed with the monoclonal JNK antibody.

To define the JNK binding site on JMP1, we performed *in vitro* binding assays with GST fused JMP1 constructs (Fig 3-5A) and FLAG epitope tagged recombinant JNK1 and JNK2. Both JNK isoforms bound a 55 amino acid sequence of JMP1 (amino acids 1236-1291), but another construct (amino acids 1187-1270) that partially overlaps this region does not bind. This suggests the JNK binding domain resides on the C-terminus within amino acids 1270-1291 (Fig. 3-5B).

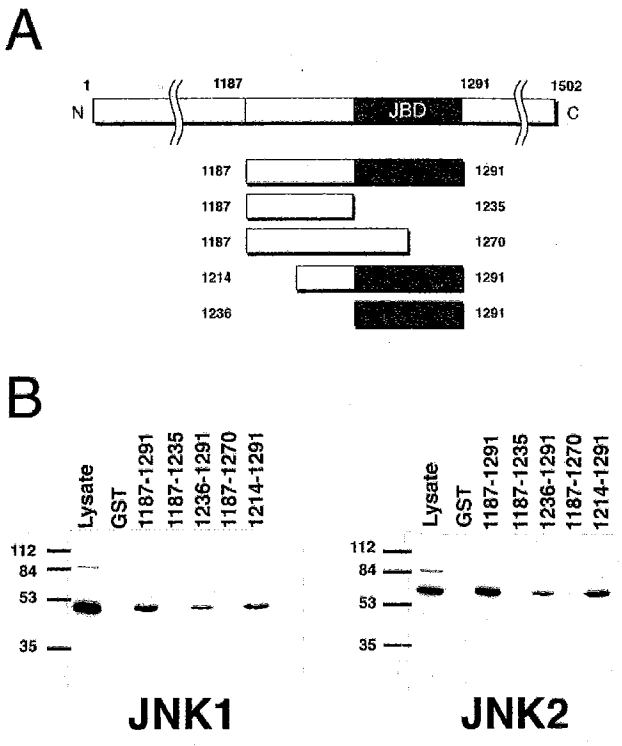

Figure 3-5 A 50 amino acid subregion of the JMP1 carboxyl terminus binds JNK1 and JNK2 *in vitro*. (A) The 105 amino acid sequence of JMP1 (1187-1291) recovered from the yeast Two-Hybrid screen was inserted into a glutathione-S-transferase fusion expression vector. Subfusions of the 105 amino acid JMP1 fragment were also generated and expressed in a bacterial expression system. (B) FLAG epitope tagged JNK1 and JNK2 were expressed in a *Pichia pastoris* overexpression system (Invitrogen Inc.). 5μg of clarified lysate was incubated with 5μg GST-JMP1 fusion protein immobilized on glutathione-sepharose beads. The beads were washed and bound proteins separated on SDS-PAGE, transferred to PVDF membranes and probed with M2 monoclonal antibody to the FLAG epitope.

A closer examination of this 50 amino acid region revealed amino acids JMP1 amino acids 1266 to 1275 contains a D-domain matching the consensus of other JNK binding protein D-domains (Fig. 3-6). The JMP1 amino acids Leu[1273] and Leu[1275] forming the conserved LxL motif seen in other D-domains.

	φxφ
JMP1	HEARASLK-LTL
c-Jun	KILKQS-MTLNL
ATF2	KH-KHE---MTL
JIP1	RP-KRPT-TLNL
JIP2	EPHKRPT-TLRL
Consensus	K L L
	R M

Figure 3-6 The JNK Binding Domain (JBD) of JMP1 compared to the JNK binding domain of other JNK binding proteins. The JBD, or D-domain consensus consists of an LxL motif and stretch of basic amino acids 3-5 amino acids upstream. The JMP1 amino acids Leu[1273] and Leu[1275] compose its D-domain LxL motif.

JMP1 Co-localizes at the Mitotic Spindles

The accurate segregation of chromosomes and cellular division during meiosis is a critical phase of spermatogenesis. The expression of JMP1 in meiotic spermatocytes suggests that JMP1 might have a functional role during meiosis. Since meiosis and mitosis share similarity in some functional mechanisms and there are no *in vitro* models to study meiosis during spermatogenesis (Hofmann et al., 1994), we decided to examine the sub-cellular distribution of JMP1 in HeLa cells using immunofluorescence. HeLa cells are a good cell model for studying subcellular JMP1 localiztion since they are easy to synchronize at various points in the cell cycle.

HeLa cells were plated and probed with an affinity-purified JMP1 antibody, and an antibody to α-tubulin to label microtubules. JMP1 appears to be a cytosolic protein in interphase cells. However, JMP1 clusters at the mitotic spindles in mitotic cells. The JMP1 immunolocalization at different phases in mitosis was then examined. The chromatin DAPI staining pattern indicates the mitotic phase of the cells. JMP1 begins to cluster at the mitotic spindles at pro-metaphase where the chromatin is just starting to condense and this localization appears to spread out along the minus-ends of the mitotic microtubule aster in metaphase. Interestingly, this association appears restricted to microtubules proximal the metaphase plate, and absent on other microtubules. This localization persists through anaphase and appears to decrease in telophase, diffusing back to a general cytosolic localization as observed in interphase cells.

To better resolve the mitotic spindle localization, cells were pre-permeabilized by detergent extraction prior to fixation and immunofluorescence. Soluble proteins not associated with the cytoskeletal matrix or otherwise anchored to structures within the cell are washed out. There is no JMP1 in detergent extracted interphase cells, indicating the protein remains soluble during this cell cycle phase. However, the mitotic spindles localization in mitotic cells persist as well as in telophase cells. (Fig. 3-7). The mitotic spindle structures were verified by co-localization immunofluorescence with an antibody to pericentrin, a protein which associates at mammalian centrosomes (*data not shown*).

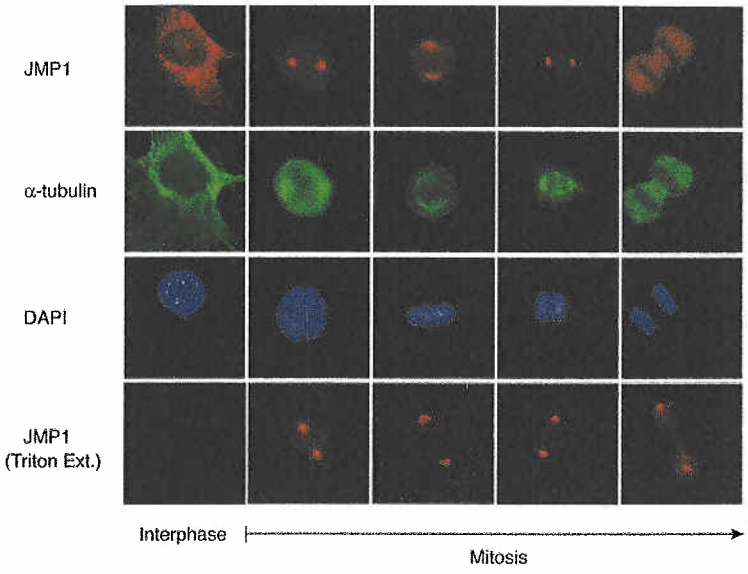

Figure 3-7 JMP1 co-localizes to the mitotic spindles. HeLa cells were plated on glass coverslips and allowed to grow for 48 hours. Affinity-purified rabbit anti-JMP1 antibody (green) and DM1α anti-α-tubulin monoclonal antibody (red) were incubated with fixed cells and processed for immunofluorescence. DAPI was used to stain chromatin in both interphase and mitotic cells. The cells were photographed in various phases of mitosis showing JMP1 localization at the mitotic spindles. Cells in the "Triton Ext." row were pre-permeabilized with Triton X-100 and Paclitaxel prior to fixation as described in Materials and Methods.

JMP1 Expression is Constant Through the Cell Cycle

Since JMP1 clusters at the mitotic spindles, we investigated whether this could be partially explained by varying JMP1 expression levels throughout the cell cycle. HeLa cells are very responsive to cell cycle synchronization techniques and a double-thymidine block with nocodazole arrest has been often used to obtain synchronized cell populations.. A double-thymidine block will cause cell cycle arrest at the G1/S phase boundary. When the drug is washed out, the cells will re-enter the cell cycle and progress through S-phase and enter G2 phase. Nocodazole, which depolymerizes the microtubule network, causes cell cycle arrest along the G2/M phase boundary. When nocodazole is washed out, the cells again re-enter the cell cycle and enter mitosis. Using this technique, synchronized populations of cells at the G1/S phase boundary, the G2/M phase boundary and in M phase were achieved. Using RT-PCR since it is a highly sensitive, semi-quantitative assay for mRNA expression, we were unable to detect any varying mRNA levels in synchronized cells when compared to the unsynchronized populations (Fig 3-8). While JMP1 mRNA does not significantly change throughout the cell cycle, JMP1 protein expression does not appear to alter as well. In mitotic HeLa cells, the JMP1 cytoplasmic localization appears to reduce concurrent with its increase in association at the mitotic spindles (Fig. 3-7).

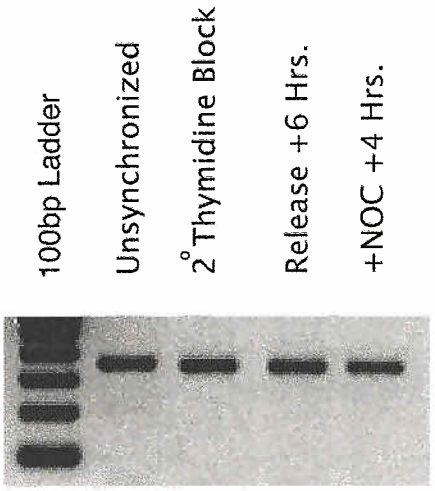

Figure 3-8 JMP1 mRNA expression levels do not change throughout the cell cycle. HeLa cells were synchronized by double-thymidine block and nocodazole arrest. Cells were collected after a double-thymidine block, or 6 hrs. after release from thymidine or after 4 hours treated with nocodazole. RNA was harvested and JMP1 specific primers were used to amplify a 360bp fragment by RT-PCR to compare relative JMP1 mRNA expression levels.

The N-terminus of JMP1 is Required for Microtubule Co-localization

In order to determine the region of JMP1 required for microtubule assocation, we performed immunofluorescence analysis of COS1 cells transfected with epitope tagged expression constructs of JMP1. Full length JMP1 remains in the cytosolic compartment of interphase cells, with no detectable nuclear expression. Like endogenous JMP1 in HeLa cells, recombinant JMP1 expressed in COS1 cells immunolocalizes to the mitotic spindles during mitosis and this localization remains after detergent pre-extraction (Fig. 3-9A).

Over-expressed full length JMP1 is soluble upon detergent pre-extraction in interphase cells, but remains insoluble in mitotic cells, suggesting it associates directly or indirectly with the microtubule network. We wanted to examine what region of JMP1 is responsible for microtubule co-localization. We examined the immunolocalization of the JMP1 amino terminal 757 amino acids (FLAG-JMP1-

NT) and the JMP1 carboxyl-terminal 477 amino acids (FLAG-JMP1-CT) in COS-1 cells. The JMP1 carboxyl fragment showed a cytoplasmic expression (Fig 3-9B*i*) similar to the full length protein, but the carboxyl fragment did not co-localize to the mitotic spindles in metaphase cells (Fig. 3-9B*ii*). However, the JMP1 amino-terminus construct yielded two populations of cells after transfection. The first population, which appear to be interphase cells, shows expression co-localizing with microtubules (Fig 3-9B*iii*). This localization persists after detergent pre-extraction. The second population of cells show an abnormal morphology. The microtubules radiate from a central point and are extremely short. The mitotic spindles apparently fail to migrate to opposite poles as determined by γ-tubulin immunofluorescence (*data not shown*). JMP1 localizes along these truncated microtubules (Fig 3-9B*iv*). We were unable to find any FLAG-JMP1-NT transfected cells displaying a normal mitotic morphology.

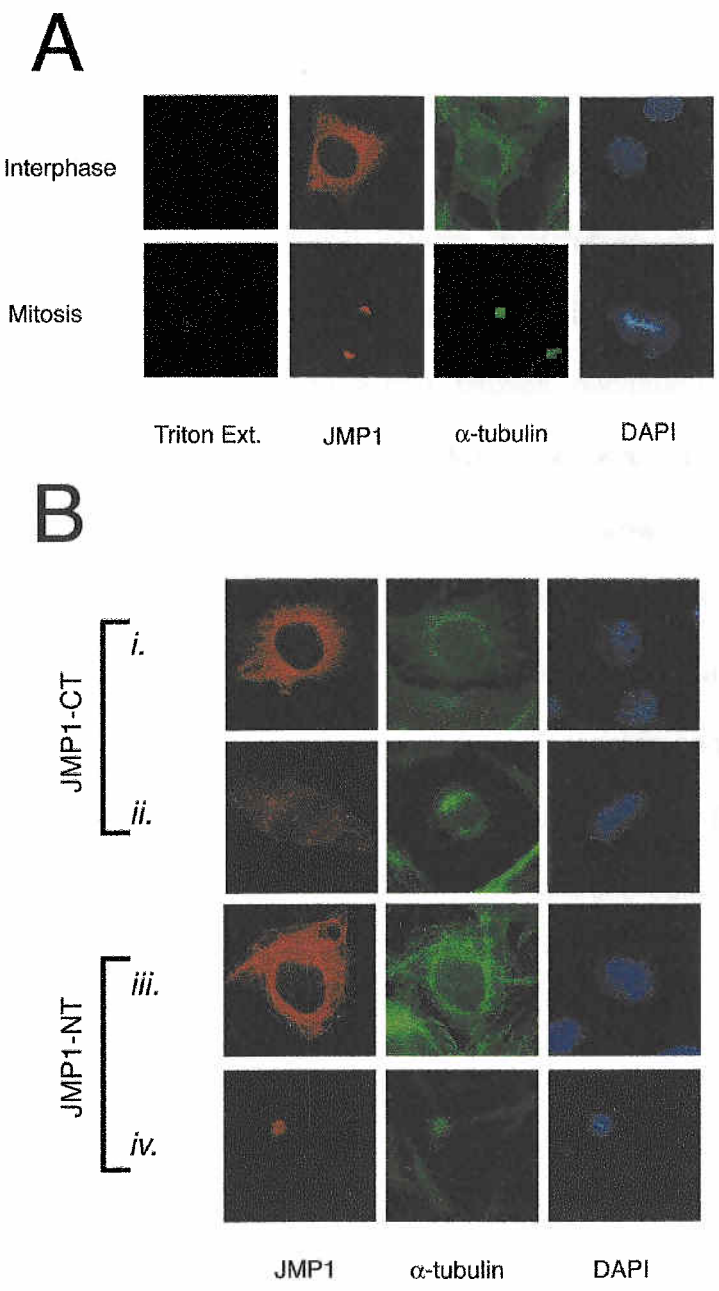

Figure 3-9 The N-terminal domain is required for JMP1 microtubule and mitotic spindle co-localization. (A) Recombinant JMP1 localizes to the mitotic spindles. FLAG epitope tagged full length JMP1 was transfected into COS1 cells, fixed and processed for immunofluorescence. Microtubules were co-labled (green) and nuclei were stained with DAPI. JMP1 is expressed as a general cytoplasmic protein in interphase cells, Transfected cells fixed in mitosis demonstrate JMP1 co-localizes to the mitotic spindle. Cells pre-permeabilized with Triton X-100 show JMP1 remains bound to the microtubules in mitotic cells, but the signal is washed away in interphase cells. (B) COS1 cells were transfected with either (*i, ii*) FLAG-JMP-CT (1025-1502) or (*iii, iv*) FLAG-JMP-NT (1-757). (*i*) The C-terminal recombinant JMP1 shows a cytoplasmic expression in interphase cells and a (*ii*) loss of mitotic spindle localization. The N-terminal recombinant JMP1 shows two different cell populations. One population (*iii*) of interphase cells shows JMP1-NT co-localizing with the microtubule network, another rarer population (*iv*) show an abnormal morphology with JMP1 clustering at the non-migrated spindle poles with a severly truncated microtubule network (green).

Mitotic Spindle Co-localization is Dependent on Intact Microtubules

Microtubules exhibit dynamic instability in mitotic cells, undergoing abrupt and rapid transitions between growing and shrinking. The localization of JMP1 at the mitotic spindles suggests there might be a regulated association with

microtubules that is dependent on the cell cycle phase. To determine if this localization is dependent on intact microtubules, we performed immunofluorescence on COS1 cells transfected with epitope tagged full length JMP1 and observed the effects microtubule disassembly have on its co-localization. JMP1 localization at the mitotic spindle is lost when cells are treated with nocodazole, a drug that causes microtubule disruption and prevents reassembly. (Fig 3-10, +NOC). When nocodazole is washed out and complete media is added back, the microtubules regrow from the mitotic spindles, and JMP1 relocalizes along the centrosomes . (Fig 3-10, 5 mins.) 30 minutes after drug removal, the cells have resumed a normal mitotic morphology with microtubules in a mitotic aster, the chromosomes congressing on the metaphase plate, and JMP1 relocalizing to the mitotic spindles. (Fig 3-10, 30 mins.). These data suggest JMP1 localization at the mitotic spindles is dependent on intact microtubules.

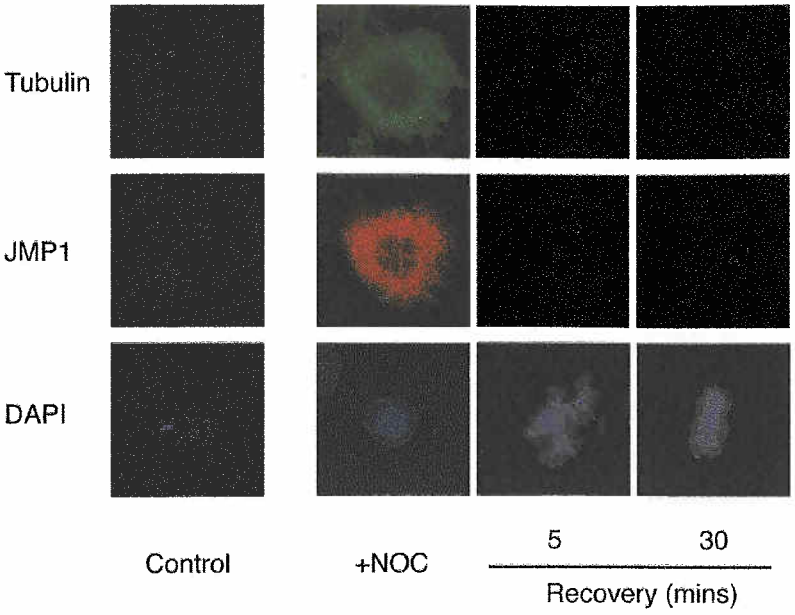

Figure 3-10 The localization of JMP1 at the mitotic spindles is dependent on intact microtubules. COS1 cells expressing FLAG epitope tagged, full length JMP1 were plated on glass coverslips. The cells were processed for immunofluorescence by labeling with the M2 monoclonal antibody to the FLAG epitope and rabbit anti-α-tubulin polyclonal serum to label microtubules. +NOC cells had nocodazole added at 10μg/mL for 1 hour then fixed. The recovery cells were treated as above, but then washed to remove nocodazole and allowed to recover in complete media for the timepoints indicated before fixation.

We also examined the ability of both full length JMP1 and JMP-NT to bind soluble β-tubulin and α-tubulin monomers by co-immunoprecipitation from nocodazole treated COS1 and NIH-3T3 cell lysates, but no association was detected by Western blot. Likewise, we were not able to demonstrate JMP1 association with dynein by similar methods (*data not shown*). We attempted an *in vitro* microtubule assembly assay using polymerized/depolymerized purified bovine brain microtubules to determine if FLAG epitope tagged exogenous JMP1 would precipitate by ultracentrifugation with polymerized microtubules. We were unable to detect JMP1 in the polymerized tubulin fraction (*data not shown*). This

result suggests that an unknown cellular co-factor required for JMP1 co-localization was absent from the assay or their stoichiometry was altered.

JMP1 Expression is not Suppressed by siRNA

Reducing the expression of a specific gene product and observing *in vivo* effects is a useful tool for investigating gene function and the downstream molecular events associated with it. Various protocols have previously been employed in order to study specific gene expression, such as temperature sensitive mutants and antibiotic sensitive promoters, but each had their own limits that would effect the interpretation and quality of the data generated from cellular and organismic models. Small inhibitory RNAs (siRNAs) are a relatively new and powerful method for selectively silencing gene expression. This technique allows the selective reduction or abolishment of a specific mRNA signal by causing *in situ* RNA targeting and degradation. Abrogating JMP1 expression in cells may give insight on the protein localization and downstream effects with JNK signal transduction.

Three JMP1 siRNA sequences were selected from the candidate pool. JMP-597 is located in the N-terminus near the beginning of the WD40 repeats, JMP-2504 is in the central region just C-terminal to the WD40 repeats and JMP-4409 is located in the C-terminal end. (Fig 3-11A). 3T9 cells, which are derived from primary murine fibroblasts, were selected for transfection since they not only express JMP1 at a low level (*data not shown*) but we had available 3T9 JNK1$^{-/-}$

/JNK2$^{-/-}$ cell lines which would be useful for studying the functional relationship between JMP1 and JNK.

Each JMP1 siRNA was co-transfected with a GAPDH positive control siRNA. The relative effect on JMP1 mRNA expression was determined by a coupled RT-PCR reaction that amplified a 309bp JMP1 or 204bp GAPDH bands. While the GAPDH signal was greatly reduced, evident by the lack of PCR amplification of its 204bp band, there seemed to be no silencing of JMP1 with either of the three JMP siRNAs when compared to the "scrambled" negative control lanes (Fig 3-11B).

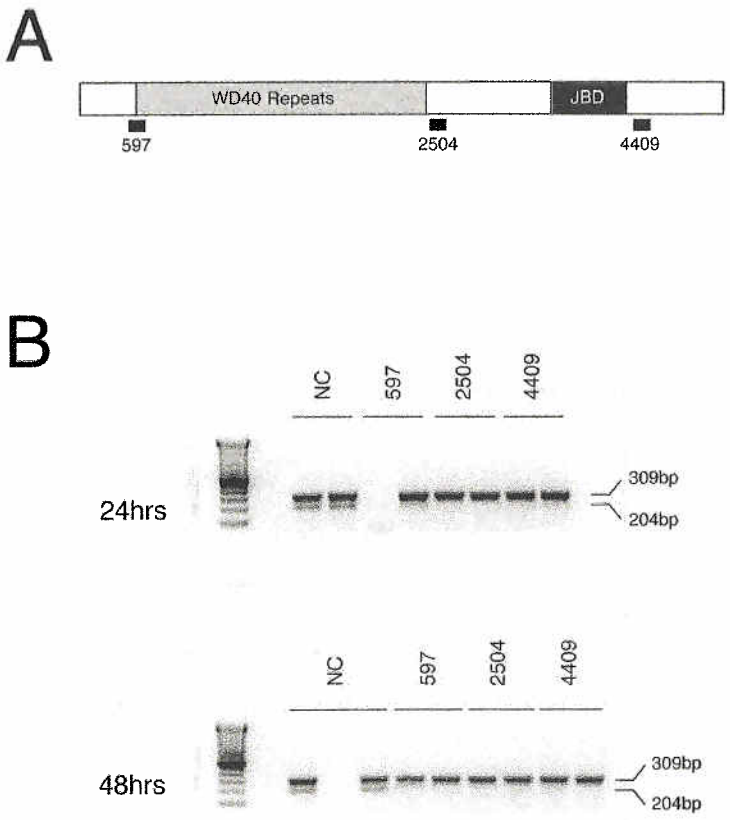

Figure 3-11 JMP1 expression was not suppressed by siRNA. (A) Three JMP1 siRNA candidates were selected based on standard siRNA selection protocols. JMP-597 in the N-terminus, JMP-2504 in the central region and JMP-4409 in the C-terminus. (B) These siRNAs were co-transfected, in duplicate, into 3T9 cells with a GAPDH positive control siRNA and expressed for either 24 or 48 hours. Total RNA from the cells were harvested with the RNEasy kit (Qiagen). 50ng total RNA was amplified with JMP1 and GAPDH specific primers with the One-Step RT-PCR kit (Qiagen). The JMP1 primers amplify a 309bp fragment, and the GAPDH a 204bp. The "NC" cells were transfected only with a non-specific "scrambled" siRNA control. None of the JMP1 siRNAs appeared to reduce JMP1 expression, as relative PCR signal is equal in all lanes.

In order to determine if the negative result reflected the choice of these three JMP1 siRNAs or protocol, the experiment was repeated using a different selection of siRNAs and silencing protocol. A SMARTPool siRNA reagent, which is a proprietory pool of four specific siRNA sequences, (Dharmacon Inc.) was used alongside manufacturer supplied Lamin A/C positive control siRNAs (Dharmacon Inc.) and the JMP1 "Scrambled" siRNA. The experiment was repeated and once again, JMP1 silencing was not observed (*Data Not Shown*).

Discussion

JMP1 represents a novel class of JNK binding protein which contain WD40 repeat domains and associate at spindle poles in mitotic cells. To date, it is the only WD-repeat protein that directly binds JNK and associates with microtubules. In this study, we have cloned and determined the primary structure of JMP1, examined its expression profile in murine testis and microtubule association at the mitotic spindle.

JMP1 is a JNK Binding Protein

The yeast Two-Hybrid system is an expression based system for identifiying cDNA clones that directly interact with a protein of interest. We employed this system to search for novel JNK substrates from a murine embryo cDNA library. As discussed in Chapter 2 of this thesis, the system identified fifteen "positive" JNK binding clones that demonstrated some degree of JNK binding. We selected a few of these clones for further analysis based on their degree of comparative JNK binding to the δ-domain from cJun (1-79). One of these yielded the first member of the JIP scaffold proteins, JIP1 (Dickens et al., 1997). From another clone, NFAT4 was identified as a JNK binding protein (Chow et al., 1997). The JMP1 fragment isolated from the yeast Two-Hybrid screen contained a JNK binding domain that demonstrated both *in vivo* binding and direct *in vitro* binding. The protein was also one of interest since Northern blots demonstrated a restricted expression to testis tissues. There appears to be

only one JNK binding domain in JMP1 residing within a 50 amino acid sequence in the C-terminal region. It is interesting to observe that JMP1 preferentially associates with UV light activated JNK. Examining this 50 amino acid region revealed JMP1 amino acids 1266 to 1275 contains a D-domain matching the consensus of other JNK binding protein D-domains (Fig. 3-6). The JMP1 amino acids Leu^{1273} and Leu^{1275} forming the conserved LxL motif seen in other D-domains, as well as a conserved basic residue Arg^{1268} (Enslen and Davis, 2001; Sharrocks et al., 2000). However, since JMP1 appears to preferentially bind activated, phosphorylated JNK, its is possible that JMP1 is binding an unidentified binding partner together with JNK, which might stoichiometrically increase the JMP1-phospho-JNK association. Such increased associations of JNK binding, and JNK activation are observed in the presence of the JIP family of scaffold proteins.

Although recombinantly expressed JMP1 could co-immunoprecipitate JNK in both *in vitro* and *in vivo* binding assays, it was disappointing to observe that endogenous JMP1 and JNK cannot co-immunoprecipitate from either COS1, HeLa or 3T9 cell lines. This might indicate that JNK and JMP1 have no true interaction when expressed at physiological concentrations. Although JNK and JMP1 interact when one or the other is overexpressed, it does not confirm a true physiological interaction exists between these proteins within the cell. This is one of the pitfalls of interpreting binding data using overexpression systems. However, the lack of data demonstrating endogenous protein interactions can

also be explained through experimental caveats. Immunofluorescence labeling of JMP1 with the affinity purified antibody demonstrated a very diffuse and low protein expression throughout the cytoplasm of COS1, HeLa and 3T9 cell lines. This suggests that JMP1 is expressed at low physiological levels that might be below the resolution of antibody detection. It is also possible that the anti-JMP1 antibody might disrupt JNK1 interaction since the antibody was generated to the C-terminus of JMP1 where the JNK binding domain is, thus detection of co-immunoprecipitated endogenous protein is not possible with this antibody. Alternative strategies to address these problems include the creation and use of a different JMP1 antibody generated to a different region of the protein, or to a specific epitope within it. Direct examination of protein interaction *in vivo* could also be approached using co-fractionation protein purification protocols.

The distinct protein motifs present in JMP1, and its microtubule localization at the mitotic spindles suggests that it is potentially a new class of JNK binding scaffold protein. Inhibition of microtubule dynamics have shown to have a regulatory effect on members of the JNK pathway (Osborn and Chambers, 1996; Shtil et al., 1999; Stone and Chambers, 2000; Wang et al., 1998; Yujiri et al., 1999). Likewise, members of the JNK pathway appear to have a role in cell cycle regulation in the divergent pathways of mitotic progression and apoptosis (MacCorkle-Chosnek et al., 2001; Wisdom et al., 1999). Although MKK4 and MKK7 were not found to associate with JMP1, it is distinctly possible the association is dependent on a dynamic *in vivo* system involving microtubules

and cell cycle phase contexts not replicated in the experimental condition, or there could be a still unidentified protein associating with JMP1 and facilitating a JNK complex within the scaffold.

When JMP1 was originally cloned, there were no similar sequences detected in the databases by the BLAST algorithms. However, in the proceeding time there was a protein reported, JNKBP1, that had similarities to JMP1 (Koyano et al., 1999). JNKBP1 was isolated from a murine brain cDNA library and has four WD40 repeats in its amino terminal end and a carboxyl terminal JNK binding site. Comparision of JMP1 with JNKBP1 lead us to conclude that they are different proteins. While the WD-repeat regions of both JNKBP1 and JMP1 exhibit significant identity, their JNK binding region and carboxyl ends are significantly dissimilar when compared with the MATCHER algorithm (Waterman and Eggert, 1987). Similarly, the putative JBD of JNKBP1 (amino acid residues 1063 to 1331) was compared to JMP1 by BESTFIT local alignment. The algorithm identified JMP1 amino acid residues 1051 to 1306 which includes the JMP1 JBD and its D-domain. However, the JBD sequences differ significantly and the JMP1 D-domain was not found in JNKBP1 (Fig. 3-12).

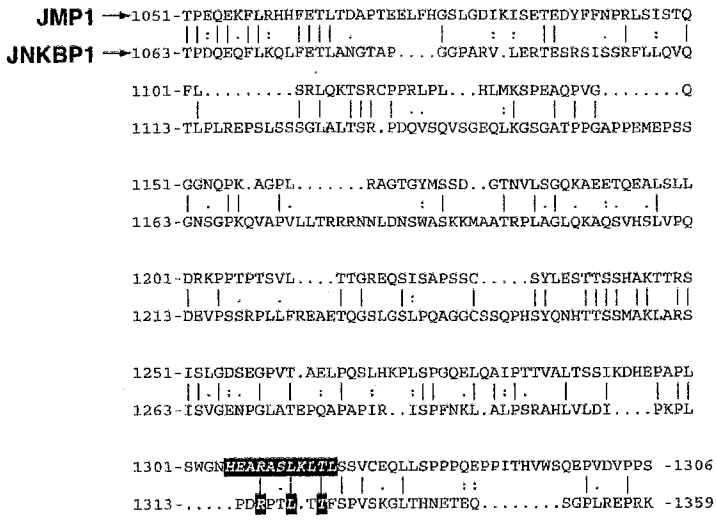

Figure 3-12 The JBD region of JNKBP aligned to JMP1 with the BESTFIT algorithm. This algorithm makes an optimal alignment of the best segment of similarity between two sequences. Optimal alignments are found by inserting gaps to maximize the number of matches using the *local homology* algorithm of Smith and Waterman. JMP1 is the top sequence, JNKBP1 is the bottom sequence. The JMP1 D-domain and matching residues in JNKBP1 are highlighted. This alignment demonstrates the dissimilarities of the JMP1 and JNKBP1 JNK binding domains.

The sequence similarities in the WD-repeats of both proteins demonstrates the WD-repeat consensus residues seen with this motif. A DOTMATCHER lineup of the two sequences demonstrates the similarities the two proteins share in their WD-repeat regions, but no similarity in their carboxyl regions (Fig. 3-13). The DOTMATCHER alignment demonstrates a significant similarity between JMP1 and JNKBP1 only in their WD-repeats. The large amino-terminal similarities observed with the DOTMATCHER graph suggests that JNKBP1 likely has more, unidentified WD-repeats than were originally identified. Similarly, JMP1 might have some WD-repeats that were not detected in the PFAM database search. This reflects the variable nature of the WD-repeat motif.

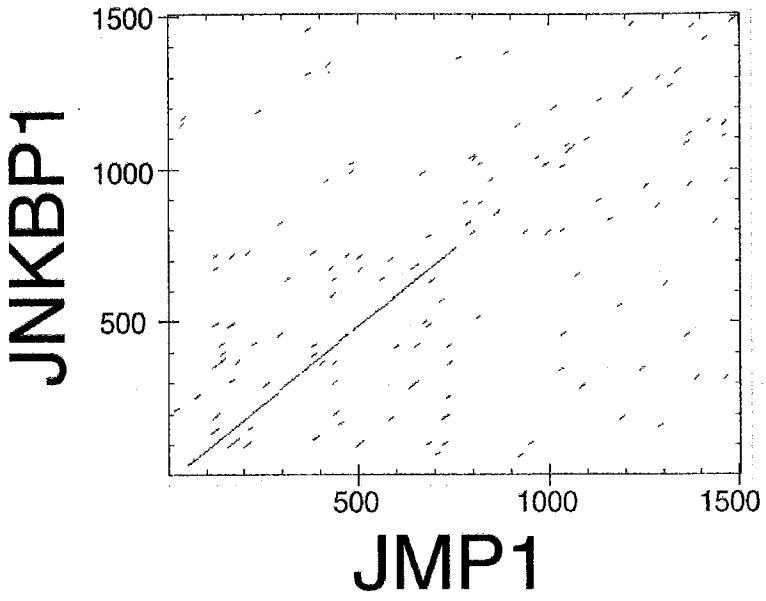

Fig 3-13 JMP1 and JNKBP1 lineup with the DOTMATCHER algorithm. This algorithm is a direct sequence to sequence comparision of two sequences. The two proteins are aligned on a grid and a "dot" is placed for amino acid matches with a similarity score over a certain threshold. DOTMATCHER is useful in demonstrating repeating stretches of similar sequences. JMP1 and JNKBP1 both demonstrate significant amino acid similarities with each other in their WD-repeat amino terminal ends (0~700aa) while having no significant similarities in the carboxyl ends (~700-1500) where both have JNK binding domains.

JMP1 is a WD40 Repeat Containing Protein

WD40 repeats, also known as β-transducin repeats, are a widespread sequence motif consisting of repeating ~40 amino acid stretches usually ending with a Trp-Asp (WD) dipeptide. The consensus sequence of the WD-repeat motif has diversity, but recently it has been discovered that some proteins have functional WD-repeats that do not match this consensus and many proteins may have functional WD-repeat regions so far undetected (Wilson et al., 2005). Originally discovered in the β-subunit of heterotrimeric GTP-binding proteins (G-beta), WD-repeat containing proteins have been found in a wide variety of proteins in all eukaryotes (Neer et al., 1994). The WD-repeat proteins usually consist of 4-16 WD40 motif units arrayed in tandem clusters. Each unit usually

assembles into a four-stranded, anti-parallel beta-sheet structure. The crystal structure of the G-beta subunit demonstrates that seven repeating units form a circular, propellar-like structure with seven blades each made up of the four beta sheets (Fig. 3-14) (Sondek et al., 1996; Wall et al., 1995).

Figure 3-14 Crystal structure of the β-subunit of heterotrimeric GTP-binding protein. The WD-repeat units each form a four-stranded, anti-parallel beta sheets. The G-beta protein consists of seven repeating units that form a circular, propellar-like structure resembling a toroid that is often called a "beta-barrel". Most WD-repeat proteins with known functions contain a similar structure with seven repeating WD-repeat units that are shown to function as a protein-protein interaction domain. (Wall et al. 1995; Sondek et al. 1996)

While the WD-repeat containing protein family demonstrates a wide variety of function, the purpose of the WD-repeats seem to modulate an association with other partner proteins involved in enzyme regulation, signal transduction and localization on the intracellular matrix. WD-repeats can have multiple roles in protein function. There are WD-repeat proteins involved in JNK signal transduction. One WD-repeat protein, TRAF7, specifically binds MEKK3 through its WD-repeats and regulate the signal transduction of AP1 and CHOP activation (Yang et al., 1997a).

The microtubule severing protein Katanin is a paradigm of how WD-repeats can have multiple function. Katanin is a heterodimeric protein consisting of p60 and p80 subunits originally isolated from sea urchin eggs (Hartman et al., 1998). The p80 subunit contains seven WD-repeats while the p60 subunit acts as a microtubule severing enzyme. The WD40 domain within p80 acts as a negative regulator of the p60 subunit's microtubule disassembly and is also required for the dimer's spindle pole localization. This localization is found to be dependent on intact microtubules (McNally et al., 2000). Katanin is believed to have an important role regulating microtubule dynamics in both mitosis and chromatin separation (McNally and Thomas, 1998; Quarmby, 2000). In *C. elegans*, the katanin homologs MEI-1 and MEI-2 are critical for meiotic spindle organization, with MEI-2 being necessary for spindle localization, but this function does not appear to be necessary in mitosis (Srayko et al., 2000). The WD-repeats in p80 katanin and MEI-2 are critical for regulating the heterodimer's microtubule severing function, as well as the microtubule and spindle pole localization, but the exact mechanism of this regulation by WD-repeats is still unknown.

JMP1 shares some structural similarity with katanin. JMP1 is a WD-repeat protein which colocalizes to the mitotic spindle and this is dependent on intact microtubules. However, JMP1 contains 12 WD-repeats, instead of the usual 7 found in katanin and other WD-repeat proteins. While the propeller shape of a seven-repeat WD40 domain is the known active structure in many

WD-proteins, the presence of more repeats might indicate they assemble into a different structure. Likewise, the presence of fewer than seven repeats, as seen with *C. elegans* Gad1p (Knight and Wood, 1998), suggests that other unlocated repeats might exist in the protein.

JMP1 colocalizes to the mitotic spindle during mitosis and this association requires the JMP1 amino terminal and intact microtubules. JMP1 does not contain a microtubule binding domain as seen in other Microtubule Associated Proteins (MAPs), but it does have structural similarities to the echinoderm EMAP-77 protein. Both are WD-repeat containing proteins and both have a highly basic amino terminus (Li and Suprenant, 1994). Microtubule binding of EMAP-77 was believed to occur by association of its basic amino terminus with the acidic carboxyl tail of β-tubulin, as was evident in the brain MAPs, MAP-2, MAP-4 and tau. However, subtilisin cleavage of the acidic carboxyl tail of β-tubulin did not abrogate EMAP-77 binding (Hamill et al., 1998), suggesting another mechanism was involved for microtubule association. Since the WD-repeats in katanin are required for its spindle pole localization and microtubule association, it appears that WD40 domains are capable of microtubule association and therefore are likely important for JMP1 microtubule and mitotic spindle association.

JMP1 Co-localizes with Microtubules at the Mitotic Spindle

JMP1 has a low level of protein expression in the cell lines we examined. This expression is detectable by immunofluorescent labeling, but is much more distinct in mitotic cells. In mitotic cells, JMP1 clusters at the mitotic spindles and

along microtubules radiating towards the condensed chromatin aligning on the metaphase plate. This distinct immunolabeling is likely due to the protein concentrating on the microtubules and mitotic spindles rather than a cell cycle dependent increase in JMP1 expression. This is supported by the observation that cell cycle synchronized HeLa cells show no significant increase in JMP1 mRNA in various stages of the cell cycle by RT-PCR analysis. However, it is possible that JMP1 mRNA levels remains constant, but translation is regulated in a cell cycle phase context by post-translational control mechanisms.

JMP1 microtubule association is likely regulated since it does not persist at the spindle poles throughout the cell cycle. JMP1 does not appear to remain bound to the microtubule network during interphase as evident by the loss of JMP1 from pre-permeabilized cells. The amino terminal of JMP1 is required for microtubule co-localization, but there is likely a regulatory region in the carboxyl end. COS1 cells transfected with JMP-NT, expressing only the amino-terminal 757 amino acids including the WD-repeat region, appear to localize solely along the microtubule network during interphase. This is in contrast with the localization of the full length construct. Moreover, there were some cells expressing JMP-NT with condensed chromatin and an abnormal microtubule network morphology. The spindle poles of these cells were unmigrated and JMP1 clustered at these structures along microtubules radiating away from them. It is likely the over-expression of JMP-NT is toxic to cells, acts as a dominant negative, or fatally alters the stoichiometric relationship or subcellular localization

of proteins involved with either JMP1 or other cell function. It is interesting to observe that this abnormal morphology occured in a small subset of transfected cells and we were unable to observe transfected cells displaying a normal mitotic morphology. Collectively, this strongly suggests there is a specific point in the cell cycle that causes these JMP-NT over-expressing cells to die by apoptosis.

JMP1 is Expressed in Spermatocytes

The mammalian testis is an organ that demonstrates a tightly regulated system of cell proliferation, differentiation and apoptosis. Spermatogenesis is a complex process of cell development that depends on extensive signal transduction networks and cell-cell interactions. Successful spermatogenesis requires a balance of proliferation, differentiation and apoptosis to form fully mature sperm cells (Print and Loveland, 2000; Rodriguez et al., 1997). Diploid spermatogonia undergo a differentiation pathway that commits the cell to a spermatogenic fate. Spermatocytes undergo two rounds of meiosis to become round haploid spermatids. During this differentiation, the cells transverse from the basal to the luminal compartments of the seminiferous tubule, behind the "blood-testis" barrier formed by junctional complexes between Sertoli cells (Eddy, 2002).

MAPK signal transduction is believed to play an important part in regulating spermatogenesis. The ERK family of MAPK kinases have been implicated in the control of G2/M phase transititions during spermatocyte meiosis (Inselman and Handel, 2004). The p38 family have been shown to have a role in

spermatocyte apoptosis (Kojima et al., 2001). Members of the JNK signal transduction pathway have roles in spermatocyte development and apoptosis (Shiraishi et al., 2002; Wong et al., 2005), and MLK2 demonstrates a tissue restricted expression in meiotic spermatocytes (Phelan et al., 1999). JNK1 and JNK2 appear to have a ubiqutious expression pattern in the testis when tissue sections are examined by immunocytochemistry. However, while JNK3 has a more restricted expression to the brain and testis, I was not able to detect satisfactory results from immunocytochemistry analysis to determine what testicular compartments JNK3 was expressed in.

There is a steady state, low level expression of JMP1 protein in several cell lines which reflects the low level transcription found in these cells as well as in several somatic tissues. We have demonstrated that JMP1 protein expression is restricted to spermatocytes within the luminal compartment of the seminiferous tubule. This localization appears to be behind the blood-testis barrier (BTB), thus in a region of the testis primarily composed of differentiating spermatocytes and Sertoli "nurse cells" coordinating their development. The expression of JMP1 protein in the spermatocytes also reflects the increased mRNA levels detected in the testis. There is little, if any JMP1 protein localized in the basal compartment of the seminiferous tubule, and none detected in the peritubular regions where myoid and Leydig cells are present.

JMP1 protein expression is likely restricted to meiotic spermatocytes as we were unable to detect similar protein expression in either Sertoli or Leydig

derived cell lines. Neither did we detect JMP1 immunolocalization in spermatozoa isolated from the caudate epididymus, which suggests JMP1 expression is reduced after the immature spermatids are released into the seminiferous tubule lumen. There were reduced amounts of JMP1 mRNA observed by Northern analysis on caudate epididymal sperm (*data not shown*). We also didn't detect increased JMP1 expression in the spermatocyte-derived GC-2spd(*ts*) cell line. The later observation that this cell line fails to undergo meiosis in culture indicates that may not accurately reflect *in vivo* conditions during spermatogenesis.

Since the testis is a difficult organ to study *in vivo*, future experiments to elucidate the physiological JMP1 role within the testis would be served by creating transgenic JMP1$^{-/-}$ mice. This approach has been used to successfully study the JNK signalling pathway roles in neurological pathologies and glucose metabolism in diabetes. Similarly transgenic JMP1 knock-out mice would allow for the study of the role of a potential JMP1 role within somatic cell mitosis and help determine a physiological role within the JNK signalling pathway.

Conclusions

In this study, we have presented a novel JNK binding protein expressed in spermatocytes which associates with the microtubule cytoskeleton and clusters at the mitotic spindle in dividing cells. JMP1 repesents a new class of JNK binding proteins with WD-repeats and a specific subcellular localization dependent on cell cycle context.

CHAPTER IV

ANALYSIS OF TESTIS FROM *Jnk3*$^{-/-}$ MICE

Abstract

The testis is a complex organ that has tightly regulated and concerted areas of cell survival and apoptosis that ensure successful spermatogenesis and the production of mature sperm cells. The JNK family of stress activated kinases have dual roles in both cell survival and apoptosis, thus the mammalian testis would be an interesting organ to study JNK signal transduction in the regulation of this cellular homeostasis. JNK3 has a restricted expression in the brain, heart and testis, and has a demonstrated phenotype in neuronal apoptosis, but any roles it might have in regulating testis cell survival and apoptosis is unknown. We observed that older *Jnk3*$^{-/-}$ male mice produce smaller numbers of pregnancies than age matched controls and younger *Jnk3*$^{-/-}$ mice, but the average litter size of these animals were unaffected. We examined the morphology of the testis and sperm from these animals and did not find any significant differences. Similarly, we did not detect any changes in apoptosis in the testis with adult animals, or defects in sperm motility. The observed breeding phenotype in aged *Jnk3*$^{-/-}$ males may therefore be due to a mating behavioral dysfunction.

Introduction

The mammalian testis is a complex organ that houses the process of spermatogenesis that creates haploid germ cells from diploid spermatogonia which then differentiate into spermatozoa. Spermatogenesis can be divided into three distinct intervals that include stem cell differentiation and renewal, meiosis and spermiogenesis (Hecht, 1987). Stem cells develop into spermatogonia, which are diploids cells that replicate and populate the periphery of the basal compartment of the seminiferous tubule. Upon hormonal signaling, spermatogonia commit to a process of differentiation into spermatocytes where they form syncytium with the sustenacular cells of the testis, the Sertoli cells, and migrate into the lumenal compartment of the seminiferous tubule. The lumenal compartment of the seminiferous tubule is an immune privileged site that is behind the blood-testis barrier and spermatocyte maturation and lumenal migration is dependent on specific proteolytic events (Wong et al., 2005). Spermatocytes undergo dual rounds of meiosis and further differentiatiate to become round haploid spermatids that populate the lumenal boundary, where they start developing nascent sperm tails and a pro-acrosomal vesicle in the sperm heads (Fig. 4-1). Spermatozoa are ultimately released into the seminiferous tubule lumen where they migrate and collect in the caudate epididymis as mature spermatozoa.

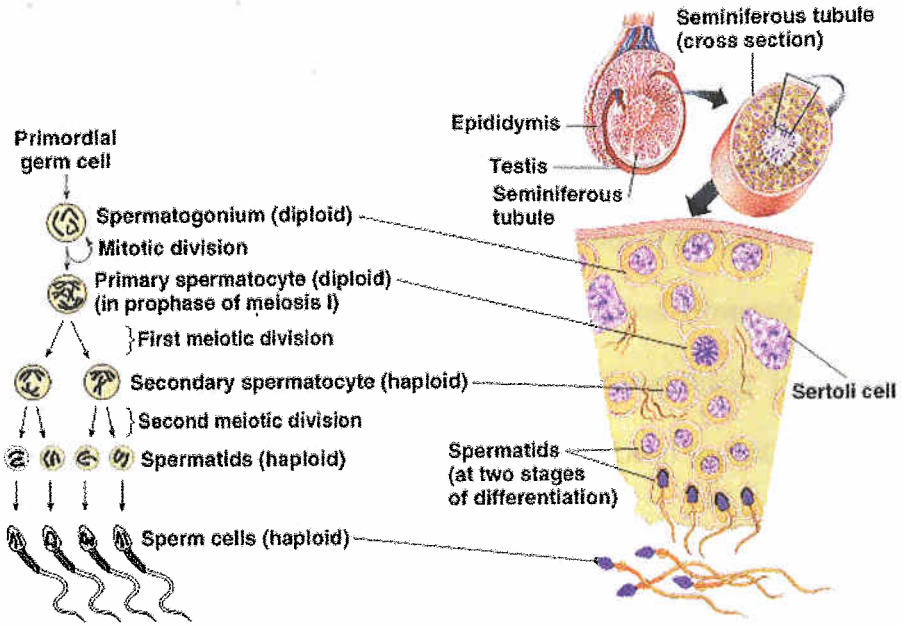

Figure 4-1 An overview of testis morphology and spermatogenesis.

The JNK signal transduction pathways, have dual roles involved with the regulation of both cellular survival and apoptosis (Davis, 2000). Because of the tightly regulated cellular proliferation, apoptosis and differentiation in the mammalian testis, it would be an attractive model to study the roles JNK and other stress-activated protein kinases have in spermatogenesis.

The SAPK signal transduction pathways have been implicated to have an important role in spermatogenesis. MLK2 expression rises in primary and secondary spermatocytes, as well as round haploid spermatids, but is absent in spermatogonia (Phelan et al., 1999). The p38 signal transduction pathway is activated in response to mild hyperthermia of the testis. Active p38 was detected in the spermatocytes of *Bcl6*$^{-/-}$ mice in the absence of hyperthermia, while hyperthermia increased the rate of apoptosis in the testis (Kojima et al., 2001).

Studies of vasectomized animals indicate that apoptosis has a key role in the deterioration of spermatogenesis after vasectomy (Lue et al., 1997; Shiraishi et al., 2001). At the early phase of the responses following vasectomy, when increased hydrostatic pressure has detrimental effects on germ cells, the number of apoptotic germ cells increases (Johnson and Howards, 1975). Experiments with rats demonstrated both p38 and JNK signaling pathways were rapidly activated (Shiraishi et al., 2002). α_2-Macroglobulin (α_2-MG) is a protease inhibitor that regulates tissue remodeling in the seminiferous tubules at the Blood-Testis Barrier (BTB) interface, specfically at the formation of Sertoli cell and spermatocyte Tight Junctions (TJ). The JNK signal transduction pathway is a regulatory mechanism for α_2-MG production, modulating homeostasis of spermatocyte migration to the seminiferous tubule lumen (Wong et al., 2005). However, research of the SAPK signal transduction pathway roles in the testis has been hampered by the inherent difficulties of replicating spermatogenesis *in vitro* (Nagano et al., 2001; Wolkowicz et al., 1996).

The availability of *Jnk*$^{-/-}$ transgenic mice has provided a powerful tool for the study of JNK signal transduction pathways and their roles in spermatogenesis (Kuan et al., 1999; Yang et al., 1997b). The cloning and analysis of JMP1 lead my focus into possible testis defects that might be associated with JNK deficiency (Chapter III of this thesis). The first indication of a potential testis dysfunction phenotype was observed during the colony maintainence of the *Jnk3*$^{-/-}$ mice. It was observed that older JNK3-deficient

males were not siring the same number of pups as younger *Jnk3*$^{-/-}$ or age matched *C57Bl/6* wild-type males. Here we describe the analysis of this potential breeding defect with older *Jnk3*$^{-/-}$ males and the examination of possible defects in the function and structure of the murine testis.

Experimental Procedures

Mice

C57Bl/6 and *BALB/c* mice were obtained from Jackson Laboratory (Bar Harbor, ME). The generation of *Jnk3*$^{-/-}$ mice has been previously described (Yang et al., 1997b). Briefly, the *C57Bl/6* wild-type mice were the parental strain for the *Jnk3*$^{-/-}$ mice. The *Jnk3*$^{-/-}$ mice were back-crossed ten times with the parental strain. The *C57Bl/6* mice are considered the wild-type animals in this study.

Histological Staining

Testis from 13 week old and 50 week old *C57Bl* wild type and *Jnk3*$^{-/-}$ mice were freshly dissected from animals sacrificed by cervical dislocation and fixed 24 hours in neutrally buffered 10% formalin solution. Testes were embedded in paraffin blocks and 7μm thin sections were mounted to glass slides by the UMASS Histology core facility. Sections were dewaxed by three 15 min. baths in 100% mixed xylenes then hydrated in graded ethanol baths. Two 2 min. baths in 100% ethanol, followed by sequential 2 min. baths in 95%, 70%, 50%, 30% ethanol. Residual ethanol was washed away with two 5 min. baths in tap water.

Sections were stained in Mayer's Hematoxylin (Sigma) for 15 mins. then washed under tap water for 20 mins. Slides were then dipped several times, then counterstained in aqueous 0.5%(w/v) Eosin Y solution for 1 min. (Sigma). Slides were then immediatey dehydrated twice in 95% then absolute ethanol for

2 mins. each and monitored under a microscope for optimal removal of excess counterstain. Slides were cleared with two baths in mixed xylenes for 2 mins. each then coverslips mounted to the sections using Permount (Fisher Biotech).

Sperm Motility Measurements

The caudate epididymus was freshly dissected from wild-type and *Jnk3*$^{-/-}$ mice age matched at 9, 19 and 73 weeks of age. The testes from three mice of each age and genotype were used. Sperm from the caudate epididymus was removed by gentle mechanical extraction using a blunt tipped dissecting probe into a M199 cell culture media (Gibco) supplemented with 1% bovine serum albumin, 1mM sodium pyruvate and 2mM sodium lactate at 32°C. The extracted sperm was resuspended using gentle pipetting then quantitated by counting sperm heads in a hemacytometer. The sperm cell concentration was equalized in the supplmented M199 media and processed for immediate motion analysis. 25μL of sperm suspension was spotted on a slide and covered with a coverslip which had its four corners lightly dabbed with petroleum jelly to support it slightly above the slide. This worked well to cover the sample and limit the microscopic depth of field, but not restrict sperm movement in the media.

We used a microscope-camera assembly intended for measuring *Chlamydomonas* phototaxis courtesy of the George Witman laboratory at UMASS Medical Center. Dark-field microscopy was done on a Zeiss Universal microscope with a turret condenser equipped with a 1.25NA cap and phase 3 annulus. An 8X projection ocular was used to project the image to the camera.

Images of cells were captured with a CCD camera (Nippon Electronics Corp. Model TI-22A), recorded using a high-resolution monochrome ¾ inch videocassette recorder (Sony Corp.) and displayed on a 12 inch monochrome monitor. The recordings of cells can be played back to the video processor for computer-assisted tracking and analysis of cell movements. A homemade control box is triggered by the electronic shutter driver and places on the videotape both visual and audio signals that precisely mark the onset and cessation of the time window. The motion analysis camera was set to take 30 second images at 30 frames per second, and sperm cells that cross into the microscopic camera field were counted once as a "track". Data analysis begins with the operation of the ExpertVision software/hardware package from Motion Analysis (Santa Rosa, CA). The package consists of a dedicated high-speed video processor (Motion Analysis VP100) and a software package which runs a PC/AT style x386-33Mhz computer. The direction of the cell motility track's vector and its relative bend in swimming direction were traced by the software. The auto-detection of sperm cell movement by the motion analysis software was coordinated by adjusting a threshold measurement which discounted immobile, floating debris and microscopic light aberrations from being included in the track measurements. The velocity of each track during the 30 second time frame was calculated and averaged. Five different field views from different areas of the sample were calculated this way. The sperm samples from five mice from each

age and genotype group were processed and sperm velocity was averaged amongst all five to give an average sperm velocity based on age and genotype.

Apoptosis in Wild-Type and Jnk3$^{-/-}$ Murine Testis

Testis from 13 week old and 50 week old wild-type and *Jnk3*$^{-/-}$ mice were freshly dissected from animals sacrificed by cervical dislocation and fixed 24 hours in neutrally buffered 10% formalin solution. Testes were embedded in paraffin blocks and 7μm thin sections were mounted to glass slides by the UMASS Histology core facility. The sections were dewaxed in three 10 min. mixed xylene baths then gently rehydrated in a series of graded ethanol baths. Two 5min. baths in 100% ethanol, then one 2 min. bath in 95%, 70%, 50%, 30% ethanol baths. Slides were equlibrated in water with two 5min. baths.

An *in situ* Cell Death Detection kit with alkaline phosphatase was selected to detect apoptotic events in the testis sections by TUNEL detection. (Roche Biomedical). Tissue section antigen unmasking was done by incubating the sections in Proteinase K (20μg/mL in 10mM Tris-CL pH 7.4) for 20 mins. at 20°C (Sigma), then washed in two 2min. baths with PBS. One positive control slide was created by treating a wild-type testis section with DNase I (100μg/mL in 50mM Tris-CL pH 7.4, 1mg/mL BSA) for 10 mins at 20°C then washed extensively with PBS. This was done in order to determine that the TUNEL labeling reaction was occuring. A negative control slide was also used by treating it with the buffers lacking enzyme. Unmasked experimental slides were processsed with the TUNEL labeling kit according to the manufacturer's protocol.

Slides were incubated with TUNEL enzyme reagent at 37°C for 1 hour in a humidified atmosphere.

After TUNEL labeling, slides were washed three times for 2 mins. in PBS then incubated with streptavidin-AP (alkaline phosphatase) converter solution reagent (Roche) for 30 mins. at 37°C in a humidified atmosphere. Slides were then washed three times for 1 min. each in PBS then overlayed with 0.2mL of Nitro-blue Tetrazolium, 5-bromo-4-chloro-3-indoyl phosphate (NBT/BCIP) solution for 10 mins. at 20°C. Alkaline phosphatase color development was quenched with water. Slides were counter-stained with 0.5% (w/v) aqueous Eosin-Y for 5 mins, quenched with water, then rapidly dehydrated in graded ethanol baths Slides were cleared with a 2 min. bath in mixed xylenes then coverslips mounted with Permount (Fisher Biotech).

Apoptotic events, as measured by TUNEL staining, were determined by light microscopy. In the microscopic field, the number of seminiferous tubule cross sections were counted and were scored based on the number of TUNEL labled cells within them. A total of 350 seminiferous tubule cross sections were counted for each age and genotype. Seminiferous tubules with two or greater TUNEL labled cells were counted together.

Breeding Assays

Five 13-week old and five 50-week old wild-type and age matched *Jnk3*$^{-/-}$ male mice were used in a breeding assay with 12-14 week old *BALB/c* female mice. One male was paired with two *BALB/c* female mice and kept together for

10 days. Gravid females were determined visually by the presence of a vaginal plug and transferred to single enclosures. The size of each litter and the total number of pups produced from each male was recorded. No evidence of mother cannibalism of pups was observed. The gender of each pup was determined by PCR amplification of the *Smcx* and *Smcy* genes from tail-tip genomic DNA. A single primer pair (SMCX-1; 5'-CCGCTGCCAAATTCTTTGG-3') and (SMC4-1; 5'-TGAAGCTTTTGGCTTTGAG-3') amplifies both the X-linked and the Y-linked genes but yields differentially sized products which were separated on agarose gels (Mroz et al., 1999).

A second breeding assay was conducted. The 13-week old male mice from the first assay were used when they reached 50-weeks of age. Fresh 13-week age matched wild-type and *Jnk3*$^{-/-}$ male mice were included. Fresh 12-14 week old *BALB/c* females were obtained. The enclosure setup and procedures of the first breeding assay were repeated for the second assay.

Results

Older Jnk3$^{-/-}$ Males Sire Fewer Pups

We first wanted determine if the male breeding dysfunction phenotype we observed with older *Jnk3*$^{-/-}$ males could be replicated under controlled conditions. We also did two breeding assays in order to have different breeding data sets. This allowed us to compare the data from younger males in the first breeding protocol with the data from the same males when they were older in the second breeding protocol (Fig. 4-2). We took 13-week old and 50-week old male mice from both wild-type and *Jnk3*$^{-/-}$strains and conducted a sequential breeding protocol with 12-14 week old *BALB/c* females. Initial pairings with *C57Bl/6* females resulted in attacks on the males, so we decided to use *BALB/c* females since this strain is generally less aggressive. Pairings with the *BALB/c* females resulted in no observable female aggression.

We selected five males of each age group and genotype, resulting in a total of 20 animals. We paired each male with two females and left them together for 10 days. This period of time assured that the females would enter estrus at some point during the pairings. Pregnant females were isolated to their own cages and watched carefully during the time they were expected to birth their litters. This was done in order to determine if the mothers were cannibalizing their pups, but we did not detect evidence of this behavior.

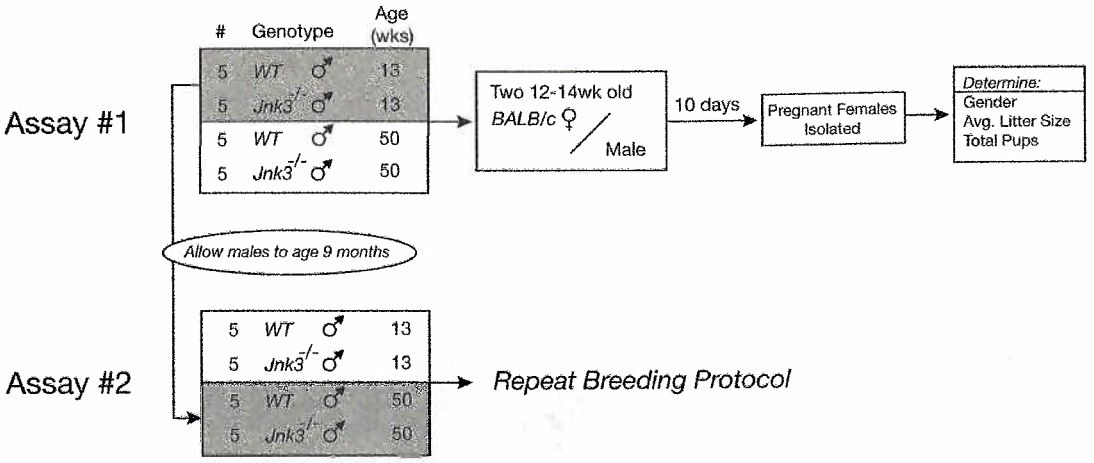

Figure 4-2 Breeding assay overview. Five wild-type (WT) and five *Jnk3*$^{-/-}$ male mice of 13 (young) and 50 (old) weeks of age were used in each assays. Each male was paired with two 12-14 week old *BALB/c* females and kept together for 10 days. Females displaying vaginal plugs were segregated to private cages and allowed to birth their litters. The total number of pups and average litter size was determined, as well as gender determination of each pup by PCR of the genes *Smcx* and *Smcy* from tail tip DNA. The 13 week old males used in the first breeding assay were allowed to age until they were 50 weeks old, whereupon they were used as the "old" males in an identical second breeding assay.

We first counted the number of litters each male had sired, then the size of each litter and the total number of pups sired for age and phenotype group. We then determined the gender ratios of the litters by PCR analysis.

The total number of pups sired by 13 week and 50 week old wild-type mice were relatively similar, while 13-week old *Jnk3*$^{-/-}$ males appeared to sire a slightly higher number of pups, though this difference was not significant. However, older 50-week old *Jnk3*$^{-/-}$ sired fewer pups in both breeding assays. The reduction in the total number of pups was compared to both the genotype matched younger *Jnk3*$^{-/-}$ and the wild-type young and older animals (Fig. 4-3).

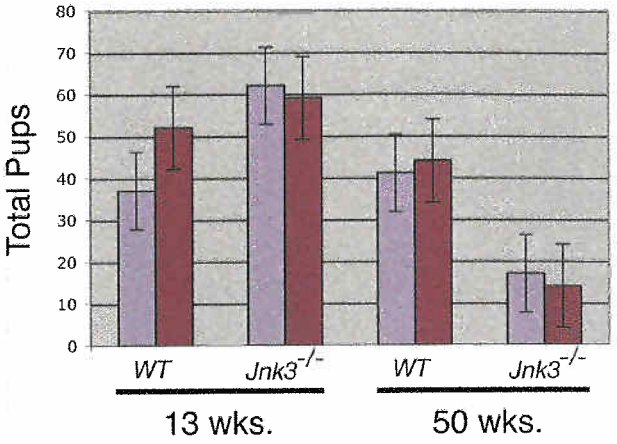

Figure 4-3 Older *Jnk3*$^{-/-}$ males sire fewer pups than younger, genotype matched males and both old and young wild-type males. The total numer of pups obtained from each genotype and age group of males were summed and represented graphically. The blue bars represent the data from the first mating assay, the red bars represent the second mating assay.

We tested whether there was a difference in litter sizes sired from these older *Jnk3*$^{-/-}$ males, and if the reduction in total number of pups was due to this. We reasoned that if there was a testis dysfunction with the older *Jnk3*$^{-/-}$ males, then they would sire smaller litter sizes compared to their age matched wild-type controls. Likewise, the reduction in the total number of pups by these older *Jnk3*$^{-/-}$ males would be reflected in smaller litter sizes. We calculated the average litter sizes of the age and genotype group males by dividing the total number of pups obtained from that group by the total number of litters obtained. We did not detect a statistically significant change in the average litter sizes by either age or genotype in either breeding assay (Fig 4-4).

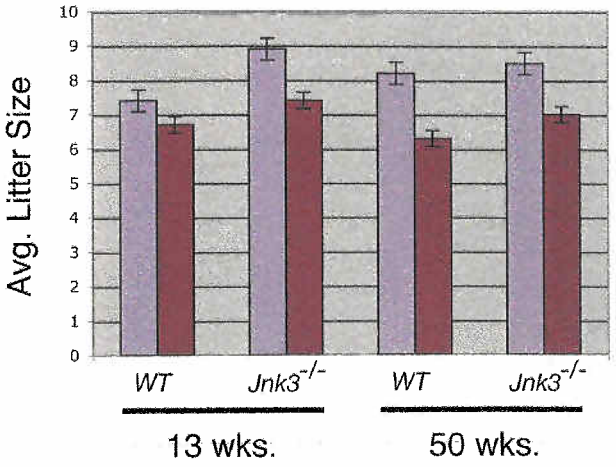

Figure 4-4 The average litter sizes of wild-type and *Jnk3*$^{-/-}$ males are unaffected by age. The total number of pups sired in each age and genotype group were divided by the total number of litters produced. The results from the first breeding assay are shown in blue, the results of the second breeding assay are shown in red.

Finally, we wished to determine if the pups sired in these breeding assays had any differences in their gender ratios. A shift in pup gender ratios with *Jnk3*$^{-/-}$ males would suggest a phenotype in sperm survival or integrity that might be sex linked. We determined the gender of each pup by PCR analysis from tail-tip DNA. We detected an upward shift in male ratios with the wild-type animals as they aged, and this replicated with the *Jnk3*$^{-/-}$ animals. We believe this shift in favoring male pups is strain specific, as this has been observed within our laboratory's other mouse colonies. However, the pup gender ratios do not appear to alter with respect to age of the male parent (Fig. 4-5).

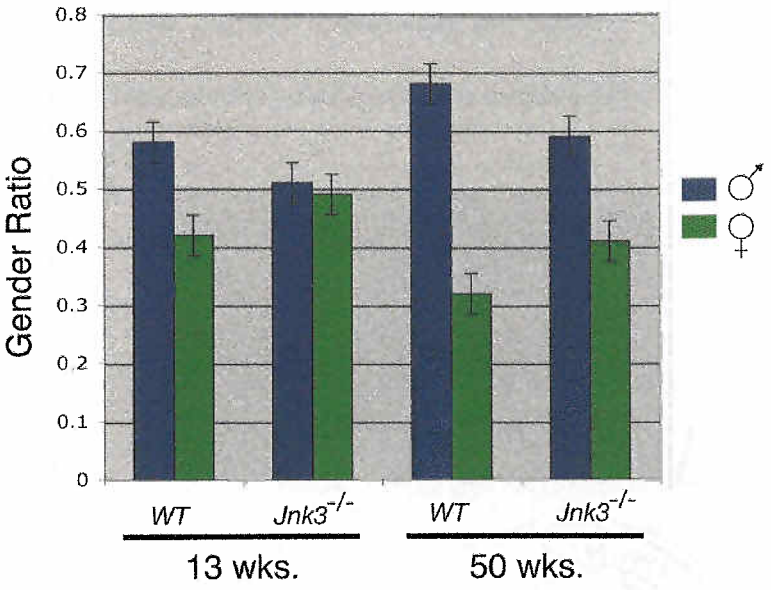

Figure 4-5 Pup gender ratios do not change with age. The gender of pups from both breeding assays were determined by PCR. The ratios from both breeding assays were combined in the results and displayed graphically. Male pup ratios are displayed with blue bars, the females by green bards.

Testis Morphology Appears Normal

The smaller number of pups sired from older *Jnk3*$^{-/-}$ males suggests that there might be a testis dysfunction in these animals. We examined the testis of these animals by hematoxylin-eosin staining of testis sections to detect gross morphological defects that might lead to clues for a *Jnk3*$^{-/-}$ phenotype in this organ. Thin sections from paraffin embedded testis prepared from 13-week and 50-week old wild-type and *Jnk3*$^{-/-}$ mice were stained with eosin and hematoxylin and examined by light microscopy. There were no apparent morphological differences between the testis of either 13-week (Fig. 4-6A) or 50-week old (Fig 4-6B) wild-type or *Jnk3*$^{-/-}$ mice. Both had distinct basal lamina separating the seminiferous tubules from the peritubular regions. Basal compartments of the seminiferous tubules had the distinctly large and round spermatogonia. The lumenal compartments displayed a normal spermatocyte syncytium and the

small, round haploid spermatids are present at the border with the lumenal space. Nascent spermatid tails are evident occupying the lumenal space as well.

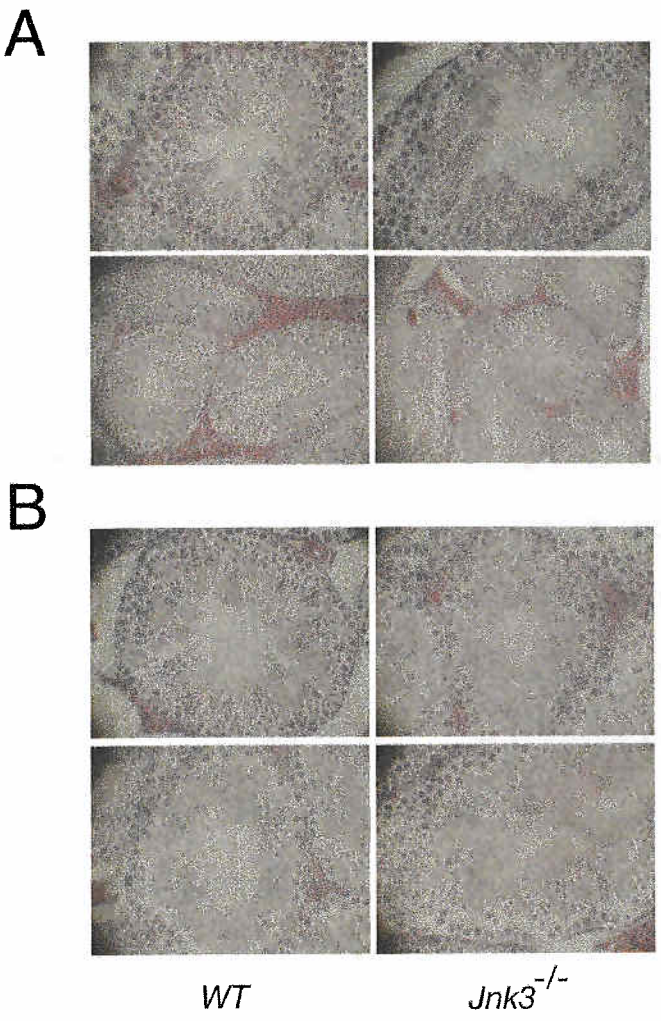

Figure 4-6 There are no gross morphological differences between wild-type and *Jnk3*$^{-/-}$ testis in either (A) 13 week old or (B) 50-week old animals. Testis from both genotypes and age groups were dissected, fixed in formalin and embedded in paraffin. 7μm sections were mounted to slides, dewaxed, rehydrated and stained with hematoxylin and eosin. Sections were then studied under light microscopy for morphological differences or abnormalities. The testis sections displayed are representative of three different animals examined for each age and genotype. Two different fields are presented for each age and genotype for comparision.

Sperm Motility Appears Unaffected by Age or Jnk3$^{-/-}$ *Genotype*

We reasoned that the reduction in the number of pups sired by these males might be due to a post-spermatogenic cellular defect. The process of spermiogenesis is the further differentiation of round haploid spermatocytes into immature, non-capacitated spermatids within the lumenal center of the

seminiferous tubule. It is possible that a phenotype defect in older *Jnk3*$^{-/-}$ males could be expresssed during this phase of sperm cell maturation. Since the testis of these animals didn't appear to have any gross morphological differences or any obvious structural abnormalities, we wanted to examine the motility and swimming behavior of sperm cells obtained from these animals.

We isolated fresh caudate epididymal sperm from five animals each of three different age groups of wild-type and *Jnk3*$^{-/-}$ mice by manual extraction. We first determined the yield of sperm isolated by counting sperm heads in a hematcytometer and determined yield averages amongst the age and phenotype groups. There were no significant differences in sperm yield by either age or phenotype (*data not shown*). We then observed the general swimming behavior of the isolated sperm under dark-field microscopy. We were concerned at first with the isolation buffer conditions and the lag times between observing samples under microscopy. However, we were able to determine an optimum buffer condition and temperature that did not show any appreciable loss of sperm motility until approximately 4-5 hours after dissection, whereupon all sperm samples kept in buffer after this time demonstrated a gradual loss of motility and live cells that did not appear to differ significantly from sample to sample (*data not shown*). Similarly, we did not detect changes in abnormal sperm swimming motility with respect to age or phenotype.

We examined sperm velocity with the live-motion capturing CCD camera. The computer "tracking" of sperm cell motility was set to discount cellular debris,

light aberrations and other non-scoring events within the tracking window. We compared the sperm velocities of the "young" (9 weeks of age), "mature" (19 weeks of age) and "old" (73 weeks of age) and were not able to detect significant differences with respect to phenotype or animal age (Fig. 4-7).

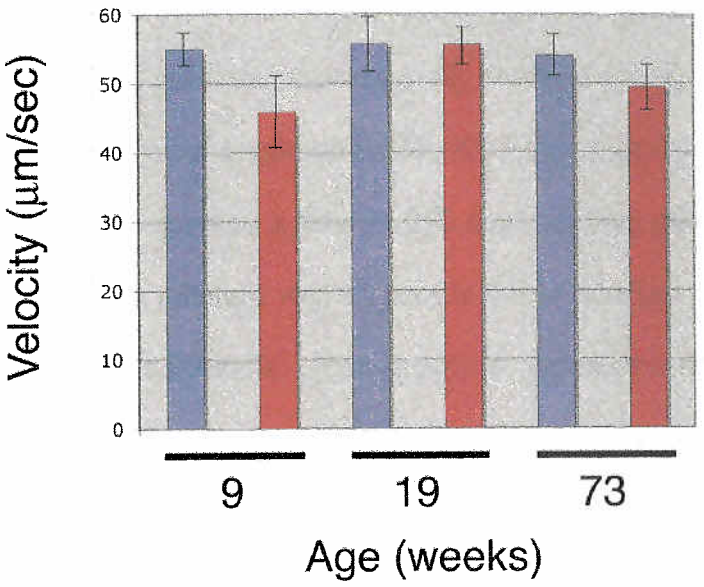

Figure 4-7 Sperm velocity is unaffected by age or genotype. Caudate epididymal sperm were isolated from wild-type and *Jnk3*$^{-/-}$ mice from three different age groups. The sperm were examined with a CCD camera-based motion detection and tracking software microscope. Velocity was averaged over five different measurements. Wild-type mice are represented by blue bars, *Jnk3*$^{-/-}$ are represented by red bars.

Apoptosis Rates are Unaffected

The testis is an active region of apoptosis throughout an animal's life. Apoptosis is a regulatory method to control both spermatogonial and spermatocyte replication to maintain a precise homeostasis between the Sertoli and germ cells within the lumenal compartments of the seminiferous tubule. However, when this homeostasis is imbalanced by genetic or cellular damage, or lesions in certain proteins critical for meiosis, increased rates of spermatocyte apoptosis is observed (Baker et al., 1996; Burgoyne and Baker, 1984; Dix et al.,

1996; Odorisio et al., 1998). Likewise, artificial lesions, such as physical and chemical vasectomy can increase the apoptosis within the testis (Johnson and Howards, 1975; Lue et al., 1997; Shiraishi et al., 2001). Since JNK may have a dual role in promoting cell survival and apoptosis, it was reasonable to think that the reduction in total pups sired by older *Jnk3*$^{-/-}$ might be due to an alteration in apoptosis within the testis, thus reducing the number of viable germ cells. Therefore, we used examined the testis of young and old wild-type and *Jnk3*$^{-/-}$ mice for altered apoptosis by TUNEL labeling of slide mounted testis sections.

We counted a total of 350 seminiferous tubule cross sections from each testis from different regions on the tissue section. As expected, the majority of seminiferous tubule cross sections demonstrated no apoptotic events, but positive sections were encountered and scored. Sections with two or more events were counted together. We compared the number of events with young, old and wild-type and JNK3-deficient testis, but we did not detect any significant differences in testicular apoptosis in these sections (Fig. 4-8).

A

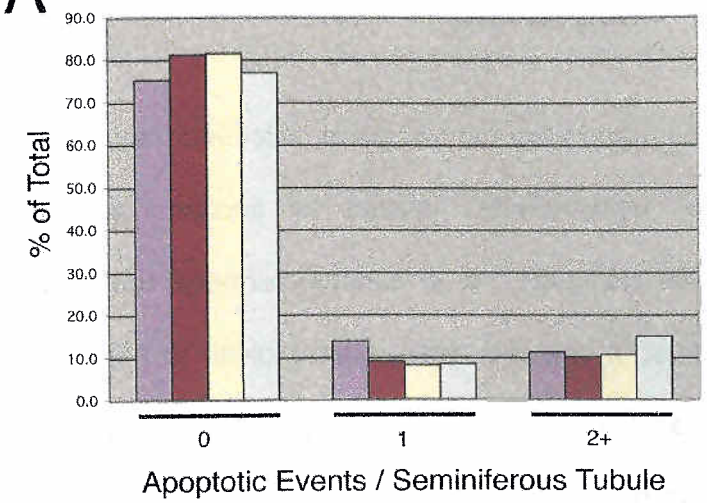

B

Age (weeks)	JNK3	Total	TUNEL positive cells / cross section 0	1	2+
13	+/+	350	263	48	39
	-/-	350	284	31	35
50	+/+	350	285	28	37
	-/-	350	269	29	52

Figure 4-8 Apoptosis in the testis of wild-type and *Jnk3*$^{-/-}$ animals is not altered by age. Tissue sections from paraffin embedded testis of wild-type (blue and yellow bars) and *Jnk3*$^{-/-}$ (red and green bars) were labled by TUNEL and then examined under a light microscope. A total of 350 cross sections of seminiferous tubules were counted at various regions throughout the testis section. Cells staining postive by TUNEL were scored as an "apoptotic event" and labled accordingly. (A) The results of the screen are displayed graphically, with 13-week old animals displayed in blue and red bars, and 50-week old animals displayed in yellow and green bars. (B) The numbers of counted apoptotic events are displayed.

Discussion

The mammalian testis is a complex organ consisting of distinct and tightly controlled regions of cellular differentiation, proliferation and apoptosis. Successful spermatogenesis is a committed differentiation pathway for the generation of haploid male germ cells and it depends on sequential rounds of apoptosis. Elimination of testicular germ cells serves as a mechanism to limit their clonal expansion to numbers that can be supported by the sustentacular cells of the testis, the Sertoli cells (Allan et al., 1992; Hikim et al., 1995; Lee et al., 1999a; Lee et al., 1997; Rodriguez et al., 1997). Although the presence of proliferation and apoptosis in spermatogenesis appears a likely region JNK signal transduction pathways would have a role, their precise roles in the physiological or pathophysiological signaling cascades of male germ cells have not been completely investigated.

During the routine handling and maintainence of our laboratory's $JNK^{-/-}$ knockout mice colonies, we made an empirical observation that older *Jnk3*$^{-/-}$male mice produced fewer pups when compared to the age matched, wild-type parental mouse strain. We wanted to test whether there was a breeding defect in a controlled assay, and determine if there was a cellular dysfunction in the testis that might be a new phenotype associated with the *Jnk3* gene.

Older Jnk3$^{-/-}$ Males Sire Fewer Pups than Age Matched Controls

Utilizing two sequential breeding assays with wild-type (*C57B/6*) and *Jnk3*$^{-/-}$ male mice of 13 and 50 weeks of age, we were able to replicate the empirical observation that older *Jnk3*$^{-/-}$males sired smaller numbers of pups compared to younger JNK3-deficient and either young or age-matched wild-type animals. We also determined that the average litter size from these animals was not significantly different than those of age-matched and wild-type controls. So, in short, the older *Jnk3*$^{-/-}$ males produced normal sized litters, but the number of litters they produced was significantly less. It is interesting to note that this reduction in sired pups was replicated in the second breeding assay with the same *Jnk3*$^{-/-}$ mice that had been used as the "young" animals in the first assay, and being used as the "old" animals in the second assay. It appears this is evidence of a *Jnk3*$^{-/-}$ phenotype.

There are a few observations that are important to note about these results. First, the average litter sizes were unaffected in older *Jnk3*$^{-/-}$ males, suggesting that when these animals did breed, they bred normally. Secondly, the older *Jnk3*$^{-/-}$ males demonstrated normal breeding behavior. The males took an obvious interest in the females and mounting behavior was observed, however we were unable to determine if the mounting resulted in successful matings comparable to wild-type animals. Third, the "young" JNK3-deficient animals used in the first breeding assay demonstrated this same phenotype as "old" animals in the second assay. These observations suggest that a behavioral dysfunction

might be a reason for the reduced number of pregnancies, but a cellular phenotype was not ruled out. We wanted to determine if there was a cellular defect within the testis or sperm of these older JNK3-deficient males. Therefore, we decided to do histological examinations of the testis and determine if these animals had a sperm cell defect or abnormality.

The Testis and Sperm of Older Jnk3$^{-/-}$ Mice Have No Apparent Defects

We took whole testis tissue sections of young and old wild-type and *Jnk3*$^{-/-}$ mice and examined their histology using nuclear and cytoplasmic counterstains under light microscopy. By observing the gross morphology of testis sections under microscopy, cellular abnormalities are often apparent in this tissue because there is a strict homeostasis that must be maintained for testis function. Structural defects can be observed due to the compartmentalization of the testis. Often if there is a reduction in the number of germ cells within seminiferous tubules, either due to increased apoptosis or a block to meiotic progression, the size of the seminiferous tubule would be decreased or the presence of nascent spermatid tails in the lumen would be absent. Likewise, a defect in the basal compartment of the testis would should changes in the presence and abundance of spermatogonia, which have a distinct cellular shape.

We were unable to detect gross morphological difference between either the young or old testis of wild-type or *Jnk3*$^{-/-}$ mice. The seminiferous tubule morphologies looked similar. The spermatogonia lining the periphery of the basal compartments had similar appearance with no multi-nucleated cells visible. The

basal-lumenal compartment boundary, formed by the Sertoli cells and cell syncytium with spermatocytes, displayed normal proportion and cell densities. The lumenal side of the seminiferous tubules showed no appreciable differences in round haploid spermatids or the emergence of immature spermatozoa into the lumenal space.

We then examined the sperm morphology and motility. Sperm isolated from the caudate epididymus are motile, structurally mature sperm cells. The manual extraction technique we used for extracting sperm minimizes the contamination from epididymal somatic cells and is efficient in extracting the majority of sperm from this organ. The sperm in the caudate epididymus are tightly packed and are extruded as a ribbon-like mass from both open ends of the dissected caudate epididymus. Gentle pipetting in the extraction buffer disassociated the sperm into individual, motile cells with minimal to undetectable damage to the cells. We first examined motile sperm cells and were unable to detect any morphological differences in their structure or the swimming motion of the tails. Sperm yield from the caudate epididymus was not appreciably different amongst the animals we examined, thus sperm yield from all animals were similar.

The motion-capturing microscope-camera tracking system and ExpertVision software functioned to detect and track motile sperm in the microscopic field. The software parameters were set to detect abnormal swimming tracks and score them differently than "normal" swimming tracks. It

also discounts cellular debris and aberrations in the light and extraction media. We were able to determine that the general sperm swimming patterns were similar in all animals we examined. Likewise, actual sperm velocities were unaffected. Thus, we conclude that the structure and motility of *Jnk3*$^{-/-}$ sperm in aged animals is not different from age matched wild-type controls. Since we only examined for morphological and motility defects in this assay, there might be a defect in the capability of sperm to fertilize and capacitate.

Testicular apoptosis is unaffected

The TUNEL method used for detecting cells undergoing apoptosis relies on detecting the fragmentation of DNA, which is a well characterized hallmark of programmed cell death. Although apoptosis in the testis doesn't necessarily reflect all the characteristic phenotypes of programmed cell death, DNA fragmentation appears to be a standard indication of apoptosis in this organ (Allan et al., 1992; Rodriguez et al., 1997). We did TUNEL labeling on whole testis tissue sections from 13 and 50 week old wild-type and *Jnk3*$^{-/-}$ mice. Although apoptotic events were rare, there was no difference detected in the number of apoptotic cells in young or old animals, nor any changes detected on genotype.

There appears to be two phases of testicular apoptosis in the life of an animal. There is an early wave of massive apoptosis, called the apoptotic wave, that occurs in pre-pubertal animals that is critical for establishing the optimum ratio of germ cells with sustenacular cells in the testis (Rodriguez et al., 1997).

This wave of apoptosis occurs in mice between 3-4 weeks of age. The second phase of apoptosis involves the maintenance of germ cells throughout the adult life of an animal. The breeding defect phenotype we observed occurs in older animals, therefore we focussed on adult germ cell apoptosis.

Conclusions

We made the observation that aged *Jnk3*$^{-/-}$ males have a reduced ability to sire pups compared to younger animals and age-matched wild type controls. However, the average litter sizes produced from these males was similar to wild type age matched animals. We examined the morphology of the testis and sperm from these older animals, as well as examined the rates of apoptosis within their testis. We were not able to detect any testis or sperm cellular defect with the older *Jnk3*$^{-/-}$ males that might account for their inability to sire normal levels of pups. Thus, it appears JNK3-deficiency in the testis does not affect the testis cellular homeostasis during spermatogenesis or sperm production.

CHAPTER V

CONCLUSIONS AND FUTURE DIRECTIONS

Our understanding of the JNK signal transduction pathway is constantly evolving as new members of the signaling pathway are discovered. My search for novel JNK substrates started with a yeast Two-Hybrid screen that yielded several new JNK interacting proteins. This thesis presented and analyzed two of these new JNK binding proteins, JIP1 and JMP1. The analysis of JMP1 lead me into the investigation of roles JNK may have in mammalian testis. We observed *Jnk3*$^{-/-}$ male mice had an age specific breeding dysfunction, then investigated the causes for this in the testis and sperm of these animals.

JIP1

The yeast Two-Hybrid screen for novel JNK binding proteins yielded the first member of the JIP group of JNK scaffold proteins. Chapter II focussed on the cloning and the initial JNK binding analysis of JIP1. It also examined how JIP1 over-expression can act as a inhibitor of the JNK signaling pathway, rather than as a protein scaffold that enhances it.

The JIP group of scaffolding proteins are a well characterized family of proteins. The complexity of the signalling pathways affected by these scaffold protein functions are just now starting to be appreciated as their biological mechanisms are starting to be elucidated. There is strong evidence that members of the JIP family might integrate both positive and negative regulators

of JNK as, in addition to binding protein kinases, JIP1 and JIP2 can associate with the JNK phosphatase MKP-7 leading to a reduction in JNK activity (Willoughby et al., 2003). The JIP proteins might also cross talk with the p38 MAPK signaling pathway (Buchsbaum et al., 2002; Kelkar et al., 2005; Schoorlemmer and Goldfarb, 2001; Schoorlemmer and Goldfarb, 2002).

An important goal for future studies will be to determine the physiological significance of the JIP protein and the cell context cross-talk they might have in different MAPK signal transduction pathways. Studies in JIP knockout mice will be a useful tool in elucidating these functions. There are already *Jip1*$^{-/-}$ (Whitmarsh et al., 2001) and *Jip3*$^{-/-}$ (Kelkar et al., 2003) mice constructed and their phenotype has been analyzed. Furthermore, *Jip4*$^{-/-}$ animals might help determine the JIP role in p38 signal transduction.

Similarly, further investigation of the JIP scaffold binding specificity will help elucidate the selective association of JIP with members of the SAPK signaling components. This will be important to determine cell context and cell localization function of these signaling pathways and determine their roles in different tissues.

Investigations into JIP biology are also being done using synthetic JIP-JBD peptides that have given insight into diseases involving the JNK signal transduction pathway, such as cerebral ischemia (Borsello et al., 2003; Hirt et al., 2004) and diabetes (Kaneto et al., 2004). The function of these drugs demonstrate a pharmacological utility that have applications in medicine.

JMP1

Another protein identified through the yeast Two-Hybrid screen for novel JNK interaction proteins was JMP1. Chapter III of this thesis discusses the cloning and analysis of this new JNK binding protein. JMP1 demonstrates a strong expression in testis and my examination revealed that JMP1 protein is expressed in meiotic spermatocytes. The structure of JMP1 suggests that it might be a new type of JNK binding scaffold proteins. WD-repeats are known to function as protein-protein interaction domains in a wide variety of proteins, so it is possible that the WD-repeats of JMP1 are recruiting other unidentified protein partners into a JNK scaffold complex as observed with the JIP scaffold proteins. JMP1 appears to preferentially bind activated phospho-JNK from cell lysates. This is evidence of a potential scaffold function. Unidentified proteins associating with the JMP1 "scaffold" might be enhancing the association of active JNK within it, or JNK might be made more accessible to upstream activating kinases. Elucidating other JMP1 binding proteins and determining the relationship within the JNK signalling pathway would help determine if JMP1 is indeed a new scaffold protein. The JMP1 phenotype in dividing cells hints that cell cycle dependent protein associations are a possibility, which requires further examination of binding partners within that cell environment context.

The JNK signal transduction pathway has been shown to be activated when normal microtubule dynamics are disrupted in a cell by microtubule inhibitory agents (MIAs) such as nocodazole, taxol and colchicine (Amato et al., 1998; Wang et al., 1999; Wang et al., 1998; Yang et al., 1998). JMP1 co-

localizes with microtubules, but this co-localization appears to occur in mitosis. Microtubule dynamics in mitosis is rapid when compared to their dynamics in an interphase cell. I have demonstrated microtubule co-localization requires the JMP1 WD-repeats in its amino-terminal end. This is similar to the microtubule association of the p80 subunit of katanin. However, JMP1 was not determined to bind either alpha or beta-tubulin monomers *in vitro*. Although direct binding of JMP1 to microtubules was not demonstrated, the co-localization at the mitotic spindles is evidence that JMP1 either associates with another microtubule associated protein, or direct binding to microtubules occurs only in a stoichiometric balance of components not replicated *in vitro*. JMP1 clearly clusters near the mitotic spindle in dividing cells and this was dependent on intact microtubules. Although we did not detect dynein association, this phenotype suggests that JMP1 is associating with a minus-end microtubule motor protein, or is binding another cargo assembly which is active during cell division. The JIP group of JNK scaffold proteins are capable of binding the microtubule motor protein kinesin at the TPR tripeptide domain of kinesin light chain (Verhey et al., 2001). Determining the nature of JMP1 microtubule association during cell division would help elucidate its function at the mitotic spindles.

JMP1 protein is highly expressed in meiotic spermatocytes. Northern analysis indicates abundant mRNA in testis tissues and immunocytochemistry with an affinity purified anti-JMP1 antibody demonstrates high levels of JMP1 protein is expressed in meiotic spermatocytes. The co-localization of JMP1 at

the mitotic spindles in different cell lines suggests that JMP1 might have a meiotic role in developing spermatocytes. However, there are currently no reliable cell lines replicating mammalian spermatocyte meiosis, and there are no *in vitro* tools to study meiotic systems in mammalian germ cells. Many of the cellular mechanisms used in meiosis are similar to ones found in mitosis. Results obtained from studying mitotic mechanisms might be therefore be valid in meiotic ones. However, there are studies utilizing knock-in ES cells that look promising (Toyooka et al., 2003). When these ES cells were implanted into mouse testis, they differentiated into sperm. Such a ES knock-in system would be a powerful tool in studying JMP1-deficiency *in vivo*.

Given the complexity of developmental signal transduction in the mammalian testis, further examination of a putative meiotic role of JMP1 would be facilitated by the development of a *Jmp1*$^{-/-}$ mouse. JMP1-deficient testis could be analyzed under various stress conditions that activate the SAPK signaling systems (e.g. hyperthermia, vasectomy, chemical alteration of the BTB). Similarly, a JMP1-deficient animal would be useful for the study of its role at the mitotic spindles and its role in the JNK signal transduction pathway.

The complexity of the mammalian testis and its tightly regulated spermatogenesis suggests that investigation of JMP1 biology might be better examined in a more manipulatable organism. Currently, there are no studies or Genbank submissions for JMP1 protein in other organisms, but there are plenty of putative gene submissions with open reading frames (ORFs) that appear to be

JMP1. The *D. melanogaster* JMP1 (geneID 24580959) and *X. laevis* JMP1 (geneID 49899061) have been submitted as predicted proteins. Both of these organisms would be ideal for studying spermatocyte development.

Breeding dysfunction in Jnk3$^{-/-}$ Male Mice

JNK3 has a restricted expression pattern to the heart, brain and testis. There are already well documented phenotypes associated with JNK3 deficiency that affect neuronal apoptosis (Bruckner et al., 2001; Namgung and Xia, 2000; Yang et al., 1997b) and recently evidence of a role in processing of the beta-amyloid precursor protein (Kimberly et al., 2005). It is reasonable to assume that JNK would have a role in cell survival and apoptosis in the testis, but its role has not been fully investigated. The reduction in the number of pups sired by older *Jnk3$^{-/-}$* males is the first breeding phenotype observed with these transgenic animals.

After confirming there was an age-dependent breeding dysfunction in *Jnk3$^{-/-}$* mice, I examined their testis and sperm for morphological or cellular defects that might account for this dysfunction. The morphology of the testis did not have appreciable differences, and sperm motility was unaffected. Apoptosis rates were similarly unaffected. We didn't detect any cellular or morphological defects through these experiments, but have discounted an alteration in testicular apoptosis and sperm motility as causative phenotypes. However, we have not examined for biochemical defects in post-ejaculate sperm and their biology in the female genital tract. Examining the biology of post-ejaculate sperm, the process

of capacitation and *in vitro* fertilization experiments might lead into insight about this JNK3 phenotype (Moore, 2001).

However, that *Jnk3*$^{-/-}$ males are capable of producing normal sized litters suggests that the defect with the older animals might be behavioral, rather than cellular. Although we observed a normal interest in females and mounting behavior with the older JNK3-deficient males, we were unable to determine if this lead to the same number of successful matings as age matched controls. Further study on *Jnk3*$^{-/-}$ reproductive organ may lead into evidence for an age related behavioral dysfunction associated with this genotype.

REFERENCES

Allan, D. J., Harmon, B. V., and Roberts, S. A. (1992). Spermatogonial apoptosis has three morphologically recognizable phases and shows no circadian rhythm during normal spermatogenesis in the rat. Cell Prolif *25*, 241-250.

Altschul, S. F., Gish, W., Miller, W., Myers, E. W., and Lipman, D. J. (1990). Basic local alignment search tool. J Mol Biol *215*, 403-410.

Amato, S. F., Swart, J. M., Berg, M., Wanebo, H. J., Mehta, S. R., and Chiles, T. C. (1998). Transient stimulation of the c-Jun-NH2-terminal kinase/activator protein 1 pathway and inhibition of extracellular signal-regulated kinase are early effects in paclitaxel-mediated apoptosis in human B lymphoblasts. Cancer Res *58*, 241-247.

Andersen, J. S., Wilkinson, C. J., Mayor, T., Mortensen, P., Nigg, E. A., and Mann, M. (2003). Proteomic characterization of the human centrosome by protein correlation profiling. Nature *426*, 570-574.

Ault, J. G., DeMarco, A. J., Salmon, E. D., and Rieder, C. L. (1991). Studies on the ejection properties of asters: astral microtubule turnover influences the oscillatory behavior and positioning of mono-oriented chromosomes. J Cell Sci *99 (Pt 4)*, 701-710.

Baker, S. M., Plug, A. W., Prolla, T. A., Bronner, C. E., Harris, A. C., Yao, X., Christie, D. M., Monell, C., Arnheim, N., Bradley, A., *et al.* (1996). Involvement of mouse Mlh1 in DNA mismatch repair and meiotic crossing over. Nat Genet *13*, 336-342.

Bateman, A., Birney, E., Durbin, R., Eddy, S. R., Howe, K. L., and Sonnhammer, E. L. (2000). The Pfam protein families database. Nucleic Acids Res *28*, 263-266.

Boldt, S., Weidle, U. H., and Kolch, W. (2002). The role of MAPK pathways in the action of chemotherapeutic drugs. Carcinogenesis *23*, 1831-1838.

Bonny, C., Nicod, P., and Waeber, G. (1998). IB1, a JIP-1-related nuclear protein present in insulin-secreting cells. J Biol Chem *273*, 1843-1846.

Borsello, T., Clarke, P. G., Hirt, L., Vercelli, A., Repici, M., Schorderet, D. F., Bogousslavsky, J., and Bonny, C. (2003). A peptide inhibitor of c-Jun N-terminal kinase protects against excitotoxicity and cerebral ischemia. Nat Med *9*, 1180-1186.

Bost, F., McKay, R., Bost, M., Potapova, O., Dean, N. M., and Mercola, D. (1999). The Jun kinase 2 isoform is preferentially required for epidermal growth factor-induced transformation of human A549 lung carcinoma cells. Mol Cell Biol *19*, 1938-1949.

Bowman, A. B., Kamal, A., Ritchings, B. W., Philp, A. V., McGrail, M., Gindhart, J. G., and Goldstein, L. S. (2000). Kinesin-dependent axonal transport is mediated by the sunday driver (SYD) protein. Cell *103*, 583-594.

Brancho, D., Ventura, J. J., Jaeschke, A., Doran, B., Flavell, R. A., and Davis, R. J. (2005). Role of MLK3 in the regulation of mitogen-activated protein kinase signaling cascades. Mol Cell Biol *25*, 3670-3681.

Breitschopf, K., Haendeler, J., Malchow, P., Zeiher, A. M., and Dimmeler, S. (2000). Posttranslational modification of Bcl-2 facilitates its proteasome-dependent degradation: molecular characterization of the involved signaling pathway. Mol Cell Biol *20*, 1886-1896.

Bruckner, S. R., Tammariello, S. P., Kuan, C. Y., Flavell, R. A., Rakic, P., and Estus, S. (2001). JNK3 contributes to c-Jun activation and apoptosis but not oxidative stress in nerve growth factor-deprived sympathetic neurons. J Neurochem *78*, 298-303.

Buchsbaum, R. J., Connolly, B. A., and Feig, L. A. (2002). Interaction of Rac exchange factors Tiam1 and Ras-GRF1 with a scaffold for the p38 mitogen-activated protein kinase cascade. Mol Cell Biol *22*, 4073-4085.

Burgoyne, P. S., and Baker, T. G. (1984). Meiotic pairing and gametogenic failure. Symp Soc Exp Biol *38*, 349-362.

Burke, D. J. (2000). Complexity in the spindle checkpoint. Curr Opin Genet Dev *10*, 26-31.

Carrington, W. A., Lynch, R. M., Moore, E. D., Isenberg, G., Fogarty, K. E., and Fay, F. S. (1995). Superresolution three-dimensional images of fluorescence in cells with minimal light exposure. Science *268*, 1483-1487.

Cassimeris, L. (1999). Accessory protein regulation of microtubule dynamics throughout the cell cycle. Curr Opin Cell Biol *11*, 134-141.

Cassimeris, L., Rieder, C. L., Rupp, G., and Salmon, E. D. (1990). Stability of microtubule attachment to metaphase kinetochores in PtK1 cells. J Cell Sci *96 (Pt 1)*, 9-15.

Cavigelli, M., Dolfi, F., Claret, F. X., and Karin, M. (1995). Induction of c-fos expression through JNK-mediated TCF/Elk-1 phosphorylation. Embo J *14*, 5957-5964.

Cha, H., Dangi, S., Machamer, C. E., and Shapiro, P. (2005). Inhibition of mixed-lineage kinase (MLK) activity during G2-phase disrupts microtubule formation and mitotic progression in HeLa cells. Cell Signal.

Chen, Y. R., Meyer, C. F., and Tan, T. H. (1996). Persistent activation of c-Jun N-terminal kinase 1 (JNK1) in gamma radiation-induced apoptosis. J Biol Chem *271*, 631-634.

Choi, K. Y., Satterberg, B., Lyons, D. M., and Elion, E. A. (1994). Ste5 tethers multiple protein kinases in the MAP kinase cascade required for mating in S. cerevisiae. Cell *78*, 499-512.

Chow, C. W., Rincon, M., Cavanagh, J., Dickens, M., and Davis, R. J. (1997). Nuclear accumulation of NFAT4 opposed by the JNK signal transduction pathway. Science *278*, 1638-1641.

Clarke, D. J., and Gimenez-Abian, J. F. (2000). Checkpoints controlling mitosis. Bioessays *22*, 351-363.

Coghlan, V. M., Perrino, B. A., Howard, M., Langeberg, L. K., Hicks, J. B., Gallatin, W. M., and Scott, J. D. (1995). Association of protein kinase A and protein phosphatase 2B with a common anchoring protein. Science *267*, 108-111.

Cohen, P. (1989). The structure and regulation of protein phosphatases. Annu Rev Biochem *58*, 453-508.

Compton, D. A. (1998). Focusing on spindle poles. J Cell Sci *111 (Pt 11)*, 1477-1481.

Compton, D. A. (2000). Spindle assembly in animal cells. Annu Rev Biochem *69*, 95-114.

Compton, D. A., and Cleveland, D. W. (1994). NuMA, a nuclear protein involved in mitosis and nuclear reformation. Curr Opin Cell Biol *6*, 343-346.

Cuenda, A., and Dorow, D. S. (1998). Differential activation of stress-activated protein kinase kinases SKK4/MKK7 and SKK1/MKK4 by the mixed-lineage kinase-2 and mitogen- activated protein kinase kinase (MKK) kinase-1. Biochem J *333*, 11-15.

Dai, T., Rubie, E., Franklin, C. C., Kraft, A., Gillespie, D. A., Avruch, J., Kyriakis, J. M., and Woodgett, J. R. (1995). Stress-activated protein kinases bind directly to the delta domain of c-Jun in resting cells: implications for repression of c-Jun function. Oncogene *10*, 849-855.

Danial, N. N., and Korsmeyer, S. J. (2004). Cell death: critical control points. Cell *116*, 205-219.

Davis, R. J. (2000). Signal transduction by the JNK group of MAP kinases [In Process Citation]. Cell *103*, 239-252.

Delhalle, S., Duvoix, A., Schnekenburger, M., Morceau, F., Dicato, M., and Diederich, M. (2003). An introduction to the molecular mechanisms of apoptosis. Ann N Y Acad Sci *1010*, 1-8.

Derijard, B., Hibi, M., Wu, I. H., Barrett, T., Su, B., Deng, T., Karin, M., and Davis, R. J. (1994). JNK1: a protein kinase stimulated by UV light and Ha-Ras that binds and phosphorylates the c-Jun activation domain. Cell *76*, 1025-1037.

Derijard, B., Raingeaud, J., Barrett, T., Wu, I. H., Han, J., Ulevitch, R. J., and Davis, R. J. (1995). Independent human MAP-kinase signal transduction pathways defined by MEK and MKK isoforms. Science *267*, 682-685.

Desai, A., Maddox, P. S., Mitchison, T. J., and Salmon, E. D. (1998). Anaphase A chromosome movement and poleward spindle microtubule flux occur At similar rates in Xenopus extract spindles. J Cell Biol *141*, 703-713.

Dickens, M., Rogers, J. S., Cavanagh, J., Raitano, A., Xia, Z., Halpern, J. R., Greenberg, M. E., Sawyers, C. L., and Davis, R. J. (1997). A cytoplasmic inhibitor of the JNK signal transduction pathway. Science *277*, 693-696.

Diviani, D., Langeberg, L. K., Doxsey, S. J., and Scott, J. D. (2000). Pericentrin anchors protein kinase A at the centrosome through a newly identified RII-binding domain. Curr Biol *10*, 417-420.

Dix, D. J., Allen, J. W., Collins, B. W., Mori, C., Nakamura, N., Poorman-Allen, P., Goulding, E. H., and Eddy, E. M. (1996). Targeted gene disruption of Hsp70-2 results in failed meiosis, germ cell apoptosis, and male infertility. Proc Natl Acad Sci U S A *93*, 3264-3268.

Dong, C., Li, Z., Alvarez, R., Jr., Feng, X. H., and Goldschmidt-Clermont, P. J. (2000a). Microtubule binding to Smads may regulate TGF beta activity. Mol Cell *5*, 27-34.

Dong, C., Yang, D. D., Tournier, C., Whitmarsh, A. J., Xu, J., Davis, R. J., and Flavell, R. A. (2000b). JNK is required for effector T-cell function but not for T-cell activation. Nature *405*, 91-94.

Dong, C., Yang, D. D., Wysk, M., Whitmarsh, A. J., Davis, R. J., and Flavell, R. A. (1998). Defective T cell differentiation in the absence of Jnk1. Science *282*, 2092-2095.

Dorow, D. S., Devereux, L., Tu, G. F., Price, G., Nicholl, J. K., Sutherland, G. R., and Simpson, R. J. (1995). Complete nucleotide sequence, expression, and chromosomal localisation of human mixed-lineage kinase 2. Eur J Biochem *234*, 492-500.

Downing, K. H. (2000). Structural basis for the interaction of tubulin with proteins and drugs that affect microtubule dynamics. Annu Rev Cell Dev Biol *16*, 89-111.

Eby, M. T., Jasmin, A., Kumar, A., Sharma, K., and Chaudhary, P. M. (2000). TAJ, a novel member of the tumor necrosis factor receptor family, activates the c-Jun N-terminal kinase pathway and mediates caspase-independent cell death. J Biol Chem *275*, 15336-15342.

Eddy, E. M. (2002). Male germ cell gene expression. Recent Prog Horm Res *57*, 103-128.

Enslen, H., and Davis, R. J. (2001). Regulation of MAP kinases by docking domains. Biol Cell *93*, 5-14.

Essers, M. A., Weijzen, S., de Vries-Smits, A. M., Saarloos, I., de Ruiter, N. D., Bos, J. L., and Burgering, B. M. (2004). FOXO transcription factor activation by oxidative stress mediated by the small GTPase Ral and JNK. Embo J *23*, 4802-4812.

Fanger, G. R., Gerwins, P., Widmann, C., Jarpe, M. B., and Johnson, G. L. (1997). MEKKs, GCKs, MLKs, PAKs, TAKs, and tpls: upstream regulators of the c-Jun amino-terminal kinases? Curr Opin Genet Dev *7*, 67-74.

Faris, M., Kokot, N., Latinis, K., Kasibhatla, S., Green, D. R., Koretzky, G. A., and Nel, A. (1998). The c-Jun N-terminal kinase cascade plays a role in stress-induced apoptosis in Jurkat cells by up-regulating Fas ligand expression. J Immunol *160*, 134-144.

Faux, M. C., and Scott, J. D. (1996a). Molecular glue: kinase anchoring and scaffold proteins. Cell *85*, 9-12.

Faux, M. C., and Scott, J. D. (1996b). More on target with protein phosphorylation: conferring specificity by location. Trends Biochem Sci *21*, 312-315.

Fay, F. S., Carrington, W., and Fogarty, K. E. (1989). Three-dimensional molecular distribution in single cells analysed using the digital imaging microscope. J Microsc *153 (Pt 2)*, 133-149.

Ferrell, J. E., Jr., Wu, M., Gerhart, J. C., and Martin, G. S. (1991). Cell cycle tyrosine phosphorylation of p34cdc2 and a microtubule-associated protein kinase homolog in Xenopus oocytes and eggs. Mol Cell Biol *11*, 1965-1971.

Fuchs, S. Y., Adler, V., Buschmann, T., Yin, Z., Wu, X., Jones, S. N., and Ronai, Z. (1998a). JNK targets p53 ubiquitination and degradation in nonstressed cells. Genes Dev *12*, 2658-2663.

Fuchs, S. Y., Adler, V., Pincus, M. R., and Ronai, Z. (1998b). MEKK1/JNK signaling stabilizes and activates p53. Proc Natl Acad Sci U S A *95*, 10541-10546.

Fuchs, S. Y., Fried, V. A., and Ronai, Z. (1998c). Stress-activated kinases regulate protein stability. Oncogene *17*, 1483-1490.

Gaglio, T., Dionne, M. A., and Compton, D. A. (1997). Mitotic spindle poles are organized by structural and motor proteins in addition to centrosomes. J Cell Biol *138*, 1055-1066.

Gaglio, T., Saredi, A., Bingham, J. B., Hasbani, M. J., Gill, S. R., Schroer, T. A., and Compton, D. A. (1996). Opposing motor activities are required for the organization of the mammalian mitotic spindle pole. J Cell Biol *135*, 399-414.

Galcheva-Gargova, Z., Konstantinov, K. N., Wu, I. H., Klier, F. G., Barrett, T., and Davis, R. J. (1996). Binding of zinc finger protein ZPR1 to the epidermal growth factor receptor. Science *272*, 1797-1802.

Ganiatsas, S., Kwee, L., Fujiwara, Y., Perkins, A., Ikeda, T., Labow, M. A., and Zon, L. I. (1998). SEK1 deficiency reveals mitogen-activated protein kinase cascade crossregulation and leads to abnormal hepatogenesis. Proc Natl Acad Sci U S A *95*, 6881-6886.

Gao, M., Labuda, T., Xia, Y., Gallagher, E., Fang, D., Liu, Y. C., and Karin, M. (2004). Jun turnover is controlled through JNK-dependent phosphorylation of the E3 ligase Itch. Science *306*, 271-275.

Garrington, T. P., Ishizuka, T., Papst, P. J., Chayama, K., Webb, S., Yujiri, T., Sun, W., Sather, S., Russell, D. M., Gibson, S. B., *et al.* (2000). MEKK2 gene disruption causes loss of cytokine production in response to IgE and c-Kit ligand stimulation of ES cell-derived mast cells. Embo J *19*, 5387-5395.

Gill, S. R., Schroer, T. A., Szilak, I., Steuer, E. R., Sheetz, M. P., and Cleveland, D. W. (1991). Dynactin, a conserved, ubiquitously expressed component of an activator of vesicle motility mediated by cytoplasmic dynein. J Cell Biol *115*, 1639-1650.

Gotoh, Y., Masuyama, N., Dell, K., Shirakabe, K., and Nishida, E. (1995). Initiation of Xenopus oocyte maturation by activation of the mitogen-activated protein kinase cascade. J Biol Chem *270*, 25898-25904.

Gotoh, Y., Nishida, E., Matsuda, S., Shiina, N., Kosako, H., Shiokawa, K., Akiyama, T., Ohta, K., and Sakai, H. (1991). In vitro effects on microtubule dynamics of purified Xenopus M phase-activated MAP kinase. Nature *349*, 251-254.

Gupta, S., Barrett, T., Whitmarsh, A. J., Cavanagh, J., Sluss, H. K., Derijard, B., and Davis, R. J. (1996). Selective interaction of JNK protein kinase isoforms with transcription factors. Embo J *15*, 2760-2770.

Haccard, O., Lewellyn, A., Hartley, R. S., Erikson, E., and Maller, J. L. (1995). Induction of Xenopus oocyte meiotic maturation by MAP kinase. Dev Biol *168*, 677-682.

Haccard, O., Sarcevic, B., Lewellyn, A., Hartley, R., Roy, L., Izumi, T., Erikson, E., and Maller, J. L. (1993). Induction of metaphase arrest in cleaving Xenopus embryos by MAP kinase. Science *262*, 1262-1265.

Ham, J., Babij, C., Whitfield, J., Pfarr, C. M., Lallemand, D., Yaniv, M., and Rubin, L. L. (1995). A c-Jun dominant negative mutant protects sympathetic neurons against programmed cell death. Neuron *14*, 927-939.

Hamill, D. R., Howell, B., Cassimeris, L., and Suprenant, K. A. (1998). Purification of a WD repeat protein, EMAP, that promotes microtubule dynamics through an inhibition of rescue. J Biol Chem *273*, 9285-9291.

Hannak, E., Oegema, K., Kirkham, M., Gonczy, P., Habermann, B., and Hyman, A. A. (2002). The kinetically dominant assembly pathway for centrosomal asters in Caenorhabditis elegans is gamma-tubulin dependent. J Cell Biol *157*, 591-602.

Hardwick, K. G. (1998). The spindle checkpoint. Trends Genet *14*, 1-4.

Hartman, J. J., Mahr, J., McNally, K., Okawa, K., Iwamatsu, A., Thomas, S., Cheesman, S., Heuser, J., Vale, R. D., and McNally, F. J. (1998). Katanin, a microtubule-severing protein, is a novel AAA ATPase that targets to the centrosome using a WD40-containing subunit. Cell *93*, 277-287.

Harvey, M., Sands, A. T., Weiss, R. S., Hegi, M. E., Wiseman, R. W., Pantazis, P., Giovanella, B. C., Tainsky, M. A., Bradley, A., and Donehower, L. A. (1993). In vitro growth characteristics of embryo fibroblasts isolated from p53-deficient mice. Oncogene *8*, 2457-2467.

Hecht, N. B. (1987). Gene expression during spermatogenesis. Ann N Y Acad Sci *513*, 90-101.

Hecht, N. B. (1995). The making of a spermatozoon: a molecular perspective. Dev Genet *16*, 95-103.

Hess, P., Pihan, G., Sawyers, C. L., Flavell, R. A., and Davis, R. J. (2002). Survival signaling mediated by c-Jun NH(2)-terminal kinase in transformed B lymphoblasts. Nat Genet *32*, 201-205.

Hikim, A. P., Wang, C., Leung, A., and Swerdloff, R. S. (1995). Involvement of apoptosis in the induction of germ cell degeneration in adult rats after gonadotropin-releasing hormone antagonist treatment. Endocrinology *136*, 2770-2775.

Hirai, S., Noda, K., Moriguchi, T., Nishida, E., Yamashita, A., Deyama, T., Fukuyama, K., and Ohno, S. (1998). Differential activation of two JNK activators, MKK7 and SEK1, by MKN28- derived nonreceptor serine/threonine kinase/mixed lineage kinase 2. J Biol Chem *273*, 7406-7412.

Hirt, L., Badaut, J., Thevenet, J., Granziera, C., Regli, L., Maurer, F., Bonny, C., and Bogousslavsky, J. (2004). D-JNKI1, a cell-penetrating c-Jun-N-terminal kinase inhibitor, protects against cell death in severe cerebral ischemia. Stroke *35*, 1738-1743.

Ho, D. T., Bardwell, A. J., Abdollahi, M., and Bardwell, L. (2003). A docking site in MKK4 mediates high affinity binding to JNK MAPKs and competes with similar docking sites in JNK substrates. J Biol Chem *278*, 32662-32672.

Ho, S. N., Hunt, H. D., Horton, R. M., Pullen, J. K., and Pease, L. R. (1989). Site-directed mutagenesis by overlap extension using the polymerase chain reaction [see comments]. Gene *77*, 51-59.

Hofmann, M. C., Hess, R. A., Goldberg, E., and Millan, J. L. (1994). Immortalized germ cells undergo meiosis in vitro. Proc Natl Acad Sci U S A *91*, 5533-5537.

Inglese, J., Freedman, N. J., Koch, W. J., and Lefkowitz, R. J. (1993). Structure and mechanism of the G protein-coupled receptor kinases. J Biol Chem *268*, 23735-23738.

Inoshita, S., Takeda, K., Hatai, T., Terada, Y., Sano, M., Hata, J., Umezawa, A., and Ichijo, H. (2002). Phosphorylation and inactivation of myeloid cell leukemia 1 by JNK in response to oxidative stress. J Biol Chem *277*, 43730-43734.

Inoue, S., and Salmon, E. D. (1995). Force generation by microtubule assembly/disassembly in mitosis and related movements. Mol Biol Cell *6*, 1619-1640.

Inselman, A., and Handel, M. A. (2004). Mitogen-activated protein kinase dynamics during the meiotic G2/MI transition of mouse spermatocytes. Biol Reprod *71*, 570-578.

Ito, M., Yoshioka, K., Akechi, M., Yamashita, S., Takamatsu, N., Sugiyama, K., Hibi, M., Nakabeppu, Y., Shiba, T., and Yamamoto, K. I. (1999). JSAP1, a novel jun N-terminal protein kinase (JNK)-binding protein that functions as a Scaffold factor in the JNK signaling pathway. Mol Cell Biol *19*, 7539-7548.

Ito, T., Deng, X., Carr, B., and May, W. S. (1997). Bcl-2 phosphorylation required for anti-apoptosis function. J Biol Chem *272*, 11671-11673.

Jacobs, D., Beitel, G. J., Clark, S. G., Horvitz, H. R., and Kornfeld, K. (1998). Gain-of-function mutations in the Caenorhabditis elegans lin-1 ETS gene identify a C-terminal regulatory domain phosphorylated by ERK MAP kinase. Genetics *149*, 1809-1822.

Johnson, A. L., and Howards, S. S. (1975). Intratubular hydrostatic pressure in testis and epididymis before and after vasectomy. Am J Physiol *228*, 556-564.

Jordan, A., Hadfield, J. A., Lawrence, N. J., and McGown, A. T. (1998). Tubulin as a target for anticancer drugs: agents which interact with the mitotic spindle. Med Res Rev *18*, 259-296.

Kallunki, T., Su, B., Tsigelny, I., Sluss, H. K., Derijard, B., Moore, G., Davis, R., and Karin, M. (1994). JNK2 contains a specificity-determining region responsible for efficient c-Jun binding and phosphorylation. Genes Dev *8*, 2996-3007.

Kaneto, H., Nakatani, Y., Miyatsuka, T., Kawamori, D., Matsuoka, T. A., Matsuhisa, M., Kajimoto, Y., Ichijo, H., Yamasaki, Y., and Hori, M. (2004). Possible novel therapy for diabetes with cell-permeable JNK-inhibitory peptide. Nat Med *10*, 1128-1132.

Kasibhatla, S., Brunner, T., Genestier, L., Echeverri, F., Mahboubi, A., and Green, D. R. (1998). DNA damaging agents induce expression of Fas ligand and subsequent apoptosis in T lymphocytes via the activation of NF-kappa B and AP-1. Mol Cell *1*, 543-551.

Kelkar, N., Delmotte, M. H., Weston, C. R., Barrett, T., Sheppard, B. J., Flavell, R. A., and Davis, R. J. (2003). Morphogenesis of the telencephalic commissure requires scaffold protein JNK-interacting protein 3 (JIP3). Proc Natl Acad Sci U S A *100*, 9843-9848.

Kelkar, N., Gupta, S., Dickens, M., and Davis, R. J. (2000). Interaction of a mitogen-activated protein kinase signaling module with the neuronal protein JIP3. Mol Cell Biol *20*, 1030-1043.

Kelkar, N., Standen, C. L., and Davis, R. J. (2005). Role of the JIP4 scaffold protein in the regulation of mitogen-activated protein kinase signaling pathways. Mol Cell Biol *25*, 2733-2743.

Kennedy, N. J., Sluss, H. K., Jones, S. N., Bar-Sagi, D., Flavell, R. A., and Davis, R. J. (2003). Suppression of Ras-stimulated transformation by the JNK signal transduction pathway. Genes Dev *17*, 629-637.

Kesavan, K., Lobel-Rice, K., Sun, W., Lapadat, R., Webb, S., Johnson, G. L., and Garrington, T. P. (2004). MEKK2 regulates the coordinate activation of ERK5 and JNK in response to FGF-2 in fibroblasts. J Cell Physiol *199*, 140-148.

Keyse, S. M. (2000). Protein phosphatases and the regulation of mitogen-activated protein kinase signalling. Curr Opin Cell Biol *12*, 186-192.

Kimberly, W. T., Zheng, J. B., Town, T., Flavell, R. A., and Selkoe, D. J. (2005). Physiological regulation of the beta-amyloid precursor protein signaling domain by c-Jun N-terminal kinase JNK3 during neuronal differentiation. J Neurosci *25*, 5533-5543.

Knight, J. K., and Wood, W. B. (1998). Gastrulation initiation in Caenorhabditis elegans requires the function of gad-1, which encodes a protein with WD repeats. Dev Biol *198*, 253-265.

Kojima, S., Hatano, M., Okada, S., Fukuda, T., Toyama, Y., Yuasa, S., Ito, H., and Tokuhisa, T. (2001). Testicular germ cell apoptosis in Bcl6-deficient mice. Development *128*, 57-65.

Kosako, H., Gotoh, Y., and Nishida, E. (1994a). Mitogen-activated protein kinase kinase is required for the mos-induced metaphase arrest. J Biol Chem *269*, 28354-28358.

Kosako, H., Gotoh, Y., and Nishida, E. (1994b). Requirement for the MAP kinase kinase/MAP kinase cascade in Xenopus oocyte maturation. Embo J *13*, 2131-2138.

Koyano, S., Ito, M., Takamatsu, N., Shiba, T., Yamamoto, K., and Yoshioka, K. (1999). A novel Jun N-terminal kinase (JNK)-binding protein that enhances the activation of JNK by MEK kinase 1 and TGF-beta-activated kinase 1. FEBS Lett *457*, 385-388.

Kozak, M. (1984). Compilation and analysis of sequences upstream from the translational start site in eukaryotic mRNAs. Nucleic Acids Res *12*, 857-872.

Kuan, C. Y., Yang, D. D., Samanta Roy, D. R., Davis, R. J., Rakic, P., and Flavell, R. A. (1999). The Jnk1 and Jnk2 protein kinases are required for regional specific apoptosis during early brain development. Neuron *22*, 667-676.

Kwan, R., Burnside, J., Kurosaki, T., and Cheng, G. (2001). MEKK1 is essential for DT40 cell apoptosis in response to microtubule disruption. Mol Cell Biol *21*, 7183-7190.

Kyriakis, J. M., Banerjee, P., Nikolakaki, E., Dai, T., Rubie, E. A., Ahmad, M. F., Avruch, J., and Woodgett, J. R. (1994). The stress-activated protein kinase subfamily of c-Jun kinases. Nature *369*, 156-160.

Lamb, J. A., Ventura, J. J., Hess, P., Flavell, R. A., and Davis, R. J. (2003). JunD mediates survival signaling by the JNK signal transduction pathway. Mol Cell *11*, 1479-1489.

Lawler, S., Fleming, Y., Goedert, M., and Cohen, P. (1998). Synergistic activation of SAPK1/JNK1 by two MAP kinase kinases in vitro. Curr Biol *8*, 1387-1390.

Le-Niculescu, H., Bonfoco, E., Kasuya, Y., Claret, F. X., Green, D. R., and Karin, M. (1999). Withdrawal of survival factors results in activation of the JNK pathway in neuronal cells leading to Fas ligand induction and cell death. Mol Cell Biol *19*, 751-763.

Lee, J., Richburg, J. H., Shipp, E. B., Meistrich, M. L., and Boekelheide, K. (1999a). The Fas system, a regulator of testicular germ cell apoptosis, is differentially up-regulated in Sertoli cell versus germ cell injury of the testis. Endocrinology *140*, 852-858.

Lee, J., Richburg, J. H., Younkin, S. C., and Boekelheide, K. (1997). The Fas system is a key regulator of germ cell apoptosis in the testis. Endocrinology *138*, 2081-2088.

Lee, R. J., Albanese, C., Stenger, R. J., Watanabe, G., Inghirami, G., Haines, G. K., 3rd, Webster, M., Muller, W. J., Brugge, J. S., Davis, R. J., and Pestell, R. G. (1999b). pp60(v-src) induction of cyclin D1 requires collaborative interactions between the extracellular signal-regulated kinase, p38, and Jun kinase pathways. A role for cAMP response element-binding protein and activating transcription factor-2 in pp60(v-src) signaling in breast cancer cells. J Biol Chem *274*, 7341-7350.

Lei, K., Nimnual, A., Zong, W. X., Kennedy, N. J., Flavell, R. A., Thompson, C. B., Bar-Sagi, D., and Davis, R. J. (2002). The Bax subfamily of Bcl2-related proteins is essential for apoptotic signal transduction by c-Jun NH(2)-terminal kinase. Mol Cell Biol *22*, 4929-4942.

Li, Q., and Suprenant, K. A. (1994). Molecular characterization of the 77-kDa echinoderm microtubule-associated protein. Homology to the beta-transducin family. J Biol Chem *269*, 31777-31784.

Li, R., and Murray, A. W. (1991). Feedback control of mitosis in budding yeast. Cell *66*, 519-531.

Lue, Y., Hikim, A. P., Wang, C., Bonavera, J. J., Baravarian, S., Leung, A., and Swerdloff, R. S. (1997). Early effects of vasectomy on testicular structure and on germ cell and macrophage apoptosis in the hamster. J Androl *18*, 166-173.

MacCorkle-Chosnek, R. A., VanHooser, A., Goodrich, D. W., Brinkley, B. R., and Tan, T. H. (2001). Cell cycle regulation of c-Jun N-terminal kinase activity at the centrosomes. Biochem Biophys Res Commun *289*, 173-180.

MacFarlane, M., Cohen, G. M., and Dickens, M. (2000). JNK (c-Jun N-terminal kinase) and p38 activation in receptor-mediated and chemically-induced apoptosis of T-cells: differential requirements for caspase activation. Biochem J *348 Pt 1*, 93-101.

Maney, T., Hunter, A. W., Wagenbach, M., and Wordeman, L. (1998). Mitotic centromere-associated kinesin is important for anaphase chromosome segregation. J Cell Biol *142*, 787-801.

Maniotis, A., and Schliwa, M. (1991). Microsurgical removal of centrosomes blocks cell reproduction and centriole generation in BSC-1 cells. Cell *67*, 495-504.

Mather, J. P. (1980). Establishment and characterization of two distinct mouse testicular epithelial cell lines. Biol Reprod *23*, 243-252.

Maundrell, K., Antonsson, B., Magnenat, E., Camps, M., Muda, M., Chabert, C., Gillieron, C., Boschert, U., Vial-Knecht, E., Martinou, J. C., and Arkinstall, S. (1997). Bcl-2 undergoes phosphorylation by c-Jun N-terminal kinase/stress-activated protein kinases in the presence of the constitutively active GTP-binding protein Rac1. J Biol Chem *272*, 25238-25242.

McNally, F. J. (1996). Modulation of microtubule dynamics during the cell cycle. Curr Opin Cell Biol *8*, 23-29.

McNally, F. J., and Thomas, S. (1998). Katanin is responsible for the M-phase microtubule-severing activity in Xenopus eggs. Mol Biol Cell *9*, 1847-1861.

McNally, K. P., Bazirgan, O. A., and McNally, F. J. (2000). Two domains of p80 katanin regulate microtubule severing and spindle pole targeting by p60 katanin. J Cell Sci *113*, 1623-1633.

McNeill, R. B., and Colbran, R. J. (1995). Interaction of autophosphorylated Ca2+/calmodulin-dependent protein kinase II with neuronal cytoskeletal proteins. Characterization of binding to a 190-kDa postsynaptic density protein. J Biol Chem *270*, 10043-10049.

Minden, A., Lin, A., Claret, F. X., Abo, A., and Karin, M. (1995). Selective activation of the JNK signaling cascade and c-Jun transcriptional activity by the small GTPases Rac and Cdc42Hs. Cell *81*, 1147-1157.

Minden, A., Lin, A., Smeal, T., Derijard, B., Cobb, M., Davis, R., and Karin, M. (1994). c-Jun N-terminal phosphorylation correlates with activation of the JNK subgroup but not the ERK subgroup of mitogen-activated protein kinases. Mol Cell Biol *14*, 6683-6688.

Minshull, J., Straight, A., Rudner, A. D., Dernburg, A. F., Belmont, A., and Murray, A. W. (1996). Protein phosphatase 2A regulates MPF activity and sister chromatid cohesion in budding yeast. Curr Biol *6*, 1609-1620.

Minshull, J., Sun, H., Tonks, N. K., and Murray, A. W. (1994). A MAP kinase-dependent spindle assembly checkpoint in Xenopus egg extracts. Cell *79*, 475-486.

Mitchison, T., Evans, L., Schulze, E., and Kirschner, M. (1986). Sites of microtubule assembly and disassembly in the mitotic spindle. Cell *45*, 515-527.

Mitchison, T. J. (1989). Polewards microtubule flux in the mitotic spindle: evidence from photoactivation of fluorescence. J Cell Biol *109*, 637-652.

Mochly-Rosen, D. (1995). Localization of protein kinases by anchoring proteins: a theme in signal transduction. Science *268*, 247-251.

Mooney, L. M., and Whitmarsh, A. J. (2004). Docking interactions in the c-Jun N-terminal kinase pathway. J Biol Chem *279*, 11843-11852.

Moore, H. D. (2001). Molecular biology of fertilization. J Reprod Fertil Suppl *57*, 105-110.

Morrison, D. K., and Davis, R. J. (2003). Regulation of MAP kinase signaling modules by scaffold proteins in mammals. Annu Rev Cell Dev Biol *19*, 91-118.

Mountain, V., Simerly, C., Howard, L., Ando, A., Schatten, G., and Compton, D. A. (1999). The kinesin-related protein, HSET, opposes the activity of Eg5 and cross-links microtubules in the mammalian mitotic spindle. J Cell Biol *147*, 351-366.

Mroz, K., Carrel, L., and Hunt, P. A. (1999). Germ cell development in the XXY mouse: evidence that X chromosome reactivation is independent of sexual differentiation. Dev Biol *207*, 229-238.

Musti, A. M., Treier, M., and Bohmann, D. (1997). Reduced ubiquitin-dependent degradation of c-Jun after phosphorylation by MAP kinases. Science *275*, 400-402.

Nagano, M., Brinster, C. J., Orwig, K. E., Ryu, B. Y., Avarbock, M. R., and Brinster, R. L. (2001). Transgenic mice produced by retroviral transduction of male germ-line stem cells. Proc Natl Acad Sci U S A *98*, 13090-13095.

Nagata, K., Puls, A., Futter, C., Aspenstrom, P., Schaefer, E., Nakata, T., Hirokawa, N., and Hall, A. (1998). The MAP kinase kinase kinase MLK2 co-localizes with activated JNK along microtubules and associates with kinesin superfamily motor KIF3. Embo J *17*, 149-158.

Namgung, U., and Xia, Z. (2000). Arsenite-induced apoptosis in cortical neurons is mediated by c-Jun N-terminal protein kinase 3 and p38 mitogen-activated protein kinase. J Neurosci *20*, 6442-6451.

Nateri, A. S., Riera-Sans, L., Da Costa, C., and Behrens, A. (2004). The ubiquitin ligase SCFFbw7 antagonizes apoptotic JNK signaling. Science *303*, 1374-1378.

Neer, E. J., Schmidt, C. J., Nambudripad, R., and Smith, T. F. (1994). The ancient regulatory-protein family of WD-repeat proteins [published erratum appears in Nature 1994 Oct 27;371(6500):812]. Nature *371*, 297-300.

Negri, S., Oberson, A., Steinmann, M., Sauser, C., Nicod, P., Waeber, G., Schorderet, D. F., and Bonny, C. (2000). cDNA cloning and mapping of a novel islet-brain/JNK-interacting protein. Genomics *64*, 324-330.

Nicklas, R. B., Lee, G. M., Rieder, C. L., and Rupp, G. (1989). Mechanically cut mitotic spindles: clean cuts and stable microtubules. J Cell Sci *94 (Pt 3)*, 415-423.

Nishina, H., Fischer, K. D., Radvanyi, L., Shahinian, A., Hakem, R., Rubie, E. A., Bernstein, A., Mak, T. W., Woodgett, J. R., and Penninger, J. M. (1997). Stress-signalling kinase Sek1 protects thymocytes from apoptosis mediated by CD95 and CD3. Nature *385*, 350-353.

Nishina, H., Vaz, C., Billia, P., Nghiem, M., Sasaki, T., De la Pompa, J. L., Furlonger, K., Paige, C., Hui, C., Fischer, K. D., *et al.* (1999). Defective liver formation and liver cell apoptosis in mice lacking the stress signaling kinase SEK1/MKK4. Development *126*, 505-516.

Odorisio, T., Rodriguez, T. A., Evans, E. P., Clarke, A. R., and Burgoyne, P. S. (1998). The meiotic checkpoint monitoring synapsis eliminates spermatocytes via p53-independent apoptosis. Nat Genet *18*, 257-261.

Osborn, M. T., and Chambers, T. C. (1996). Role of the stress-activated/c-Jun NH2-terminal protein kinase pathway in the cellular response to adriamycin and other chemotherapeutic drugs. J Biol Chem *271*, 30950-30955.

Patel, R., Bartosch, B., and Blank, J. L. (1998). p21WAF1 is dynamically associated with JNK in human T-lymphocytes during cell cycle progression. J Cell Sci *111 (Pt 15)*, 2247-2255.

Phelan, D. R., Loveland, K. L., Devereux, L., and Dorow, D. S. (1999). Expression of mixed lineage kinase 2 in germ cells of the testis. Mol Reprod Dev *52*, 135-140.

Posada, J., Sanghera, J., Pelech, S., Aebersold, R., and Cooper, J. A. (1991). Tyrosine phosphorylation and activation of homologous protein kinases during oocyte maturation and mitogenic activation of fibroblasts. Mol Cell Biol *11*, 2517-2528.

Potapova, O., Gorospe, M., Bost, F., Dean, N. M., Gaarde, W. A., Mercola, D., and Holbrook, N. J. (2000a). c-Jun N-terminal kinase is essential for growth of human T98G glioblastoma cells. J Biol Chem *275*, 24767-24775.

Potapova, O., Gorospe, M., Dougherty, R. H., Dean, N. M., Gaarde, W. A., and Holbrook, N. J. (2000b). Inhibition of c-Jun N-terminal kinase 2 expression suppresses growth and induces apoptosis of human tumor cells in a p53-dependent manner. Mol Cell Biol *20*, 1713-1722.

Print, C. G., and Loveland, K. L. (2000). Germ cell suicide: new insights into apoptosis during spermatogenesis. Bioessays *22*, 423-430.

Quarmby, L. (2000). Cellular Samurai: katanin and the severing of microtubules. J Cell Sci *113 (Pt 16)*, 2821-2827.

Raingeaud, J., Gupta, S., Rogers, J. S., Dickens, M., Han, J., Ulevitch, R. J., and Davis, R. J. (1995). Pro-inflammatory cytokines and environmental stress cause p38 mitogen-activated protein kinase activation by dual phosphorylation on tyrosine and threonine. J Biol Chem *270*, 7420-7426.

Raitano, A. B., Halpern, J. R., Hambuch, T. M., and Sawyers, C. L. (1995). The Bcr-Abl leukemia oncogene activates Jun kinase and requires Jun for transformation. Proc Natl Acad Sci U S A *92*, 11746-11750.

Rasmussen, R. K., Ji, H., Eddes, J. S., Moritz, R. L., Reid, G. E., Simpson, R. J., and Dorow, D. S. (1998). Two-dimensional electrophoretic analysis of mixed lineage kinase 2 N- terminal domain binding proteins. Electrophoresis *19*, 809-817.

Rieder, C. L., Davison, E. A., Jensen, L. C., Cassimeris, L., and Salmon, E. D. (1986). Oscillatory movements of monooriented chromosomes and their position relative to the spindle pole result from the ejection properties of the aster and half-spindle. J Cell Biol *103*, 581-591.

Rieder, C. L., and Salmon, E. D. (1994). Motile kinetochores and polar ejection forces dictate chromosome position on the vertebrate mitotic spindle. J Cell Biol *124*, 223-233.

Rieder, C. L., and Salmon, E. D. (1998). The vertebrate cell kinetochore and its roles during mitosis. Trends Cell Biol *8*, 310-318.

Rincon, M., Whitmarsh, A., Yang, D. D., Weiss, L., Derijard, B., Jayaraj, P., Davis, R. J., and Flavell, R. A. (1998). The JNK pathway regulates the In vivo deletion of immature CD4(+)CD8(+) thymocytes. J Exp Med *188*, 1817-1830.

Rodriguez, I., Ody, C., Araki, K., Garcia, I., and Vassalli, P. (1997). An early and massive wave of germinal cell apoptosis is required for the development of functional spermatogenesis. Embo J *16*, 2262-2270.

Sabapathy, K., Hu, Y., Kallunki, T., Schreiber, M., David, J. P., Jochum, W., Wagner, E. F., and Karin, M. (1999). JNK2 is required for efficient T-cell activation and apoptosis but not for normal lymphocyte development. Curr Biol *9*, 116-125.

Sanchez, C., Diaz-Nido, J., and Avila, J. (2000). Phosphorylation of microtubule-associated protein 2 (MAP2) and its relevance for the regulation of the neuronal cytoskeleton function. Prog Neurobiol *61*, 133-168.

Schaeffer, H. J., and Weber, M. J. (1999). Mitogen-activated protein kinases: specific messages from ubiquitous messengers. Mol Cell Biol *19*, 2435-2444.

Schoorlemmer, J., and Goldfarb, M. (2001). Fibroblast growth factor homologous factors are intracellular signaling proteins. Curr Biol *11*, 793-797.

Schoorlemmer, J., and Goldfarb, M. (2002). Fibroblast growth factor homologous factors and the islet brain-2 scaffold protein regulate activation of a stress-activated protein kinase. J Biol Chem *277*, 49111-49119.

Schreiber, M., Kolbus, A., Piu, F., Szabowski, A., Mohle-Steinlein, U., Tian, J., Karin, M., Angel, P., and Wagner, E. F. (1999). Control of cell cycle progression by c-Jun is p53 dependent. Genes Dev *13*, 607-619.

Schroer, T. A., Bingham, J. B., and Gill, S. R. (1996). Actin-related protein 1 and cytoplasmic dynein-based motility - what's the connection? Trends Cell Biol *6*, 212-215.

Scialli, A. R., DeSesso, J. M., and Goeringer, G. C. (1994). Taxol and embryonic development in the chick. Teratog Carcinog Mutagen *14*, 23-30.

Shapiro, P. S., Vaisberg, E., Hunt, A. J., Tolwinski, N. S., Whalen, A. M., McIntosh, J. R., and Ahn, N. G. (1998). Activation of the MKK/ERK pathway during somatic cell mitosis: direct interactions of active ERK with kinetochores and regulation of the mitotic 3F3/2 phosphoantigen. J Cell Biol *142*, 1533-1545.

Sharrocks, A. D., Yang, S. H., and Galanis, A. (2000). Docking domains and substrate-specificity determination for MAP kinases. Trends Biochem Sci *25*, 448-453.

Shiah, S. G., Chuang, S. E., and Kuo, M. L. (2001). Involvement of Asp-Glu-Val-Asp-directed, caspase-mediated mitogen-activated protein kinase kinase 1 Cleavage, c-Jun N-terminal kinase activation, and subsequent Bcl-2 phosphorylation for paclitaxel-induced apoptosis in HL-60 cells. Mol Pharmacol *59*, 254-262.

Shibasaki, F., Price, E. R., Milan, D., and McKeon, F. (1996). Role of kinases and the phosphatase calcineurin in the nuclear shuttling of transcription factor NF-AT4. Nature *382*, 370-373.

Shim, J., Lee, H., Park, J., Kim, H., and Choi, E. J. (1996). A non-enzymatic p21 protein inhibitor of stress-activated protein kinases. Nature *381*, 804-806.

Shiraishi, K., Naito, K., and Yoshida, K. (2001). Vasectomy impairs spermatogenesis through germ cell apoptosis mediated by the p53-Bax pathway in rats. J Urol *166*, 1565-1571.

Shiraishi, K., Yoshida, K., Fujimiya, T., and Naito, K. (2002). Activation of mitogen activated protein kinases and apoptosis of germ cells after vasectomy in the rat. J Urol *168*, 1273-1278.

Shtil, A. A., Mandlekar, S., Yu, R., Walter, R. J., Hagen, K., Tan, T. H., Roninson, I. B., and Kong, A. N. (1999). Differential regulation of mitogen-activated protein kinases by microtubule-binding agents in human breast cancer cells. Oncogene *18*, 377-384.

Sluss, H. K., Barrett, T., Derijard, B., and Davis, R. J. (1994). Signal transduction by tumor necrosis factor mediated by JNK protein kinases. Mol Cell Biol *14*, 8376-8384.

Sluss, H. K., Han, Z., Barrett, T., Davis, R. J., and Ip, Y. T. (1996). A JNK signal transduction pathway that mediates morphogenesis and an immune response in Drosophila. Genes Dev *10*, 2745-2758.

Smith, D. B., and Johnson, K. S. (1988). Single-step purification of polypeptides expressed in Escherichia coli as fusions with glutathione S-transferase. Gene *67*, 31-40.

Sondek, J., Bohm, A., Lambright, D. G., Hamm, H. E., and Sigler, P. B. (1996). Crystal structure of a G-protein beta gamma dimer at 2.1A resolution. Nature *379*, 369-374.

Sorger, P. K., Dobles, M., Tournebize, R., and Hyman, A. A. (1997). Coupling cell division and cell death to microtubule dynamics. Curr Opin Cell Biol *9*, 807-814.

Srayko, M., Buster, D. W., Bazirgan, O. A., McNally, F. J., and Mains, P. E. (2000). MEI-1/MEI-2 katanin-like microtubule severing activity is required for Caenorhabditis elegans meiosis. Genes Dev *14*, 1072-1084.

Stone, A. A., and Chambers, T. C. (2000). Microtubule inhibitors elicit differential effects on MAP kinase (JNK, ERK, and p38) signaling pathways in human KB-3 carcinoma cells. Exp Cell Res *254*, 110-119.

Su, B., Jacinto, E., Hibi, M., Kallunki, T., Karin, M., and Ben-Neriah, Y. (1994). JNK is involved in signal integration during costimulation of T lymphocytes. Cell *77*, 727-736.

Sunayama, J., Tsuruta, F., Masuyama, N., and Gotoh, Y. (2005). JNK antagonizes Akt-mediated survival signals by phosphorylating 14-3-3. J Cell Biol *170*, 295-304.

Swat, W., Fujikawa, K., Ganiatsas, S., Yang, D., Xavier, R. J., Harris, N. L., Davidson, L., Ferrini, R., Davis, R. J., Labow, M. A., *et al.* (1998). SEK1/MKK4

is required for maintenance of a normal peripheral lymphoid compartment but not for lymphocyte development. Immunity *8*, 625-634.

Syntin, P., and Cornwall, G. A. (1999). Immunolocalization of CRES (Cystatin-related epididymal spermatogenic) protein in the acrosomes of mouse spermatozoa. Biol Reprod *60*, 1542-1552.

Takahashi, M., Shibata, H., Shimakawa, M., Miyamoto, M., Mukai, H., and Ono, Y. (1999). Characterization of a novel giant scaffolding protein, CG-NAP, that anchors multiple signaling enzymes to centrosome and the golgi apparatus. J Biol Chem *274*, 17267-17274.

Takenaka, K., Gotoh, Y., and Nishida, E. (1997). MAP kinase is required for the spindle assembly checkpoint but is dispensable for the normal M phase entry and exit in Xenopus egg cell cycle extracts. J Cell Biol *136*, 1091-1097.

Takenaka, K., Moriguchi, T., and Nishida, E. (1998). Activation of the protein kinase p38 in the spindle assembly checkpoint and mitotic arrest. Science *280*, 599-602.

Tanoue, T., Adachi, M., Moriguchi, T., and Nishida, E. (2000). A conserved docking motif in MAP kinases common to substrates, activators and regulators. Nat Cell Biol *2*, 110-116.

Tarapore, P., Horn, H. F., Tokuyama, Y., and Fukasawa, K. (2001). Direct regulation of the centrosome duplication cycle by the p53-p21Waf1/Cip1 pathway. Oncogene *20*, 3173-3184.

Taylor, S. S., and McKeon, F. (1997). Kinetochore localization of murine Bub1 is required for normal mitotic timing and checkpoint response to spindle damage. Cell *89*, 727-735.

Theurkauf, W. E., and Vallee, R. B. (1982). Molecular characterization of the cAMP-dependent protein kinase bound to microtubule-associated protein 2. J Biol Chem *257*, 3284-3290.

Tournier, C., Dong, C., Turner, T. K., Jones, S. N., Flavell, R. A., and Davis, R. J. (2001). MKK7 is an essential component of the JNK signal transduction pathway activated by proinflammatory cytokines. Genes Dev *15*, 1419-1426.

Tournier, C., Hess, P., Yang, D. D., Xu, J., Turner, T. K., Nimnual, A., Bar-Sagi, D., Jones, S. N., Flavell, R. A., and Davis, R. J. (2000). Requirement of JNK for stress-induced activation of the cytochrome c-mediated death pathway. Science *288*, 870-874.

Tournier, C., Whitmarsh, A. J., Cavanagh, J., Barrett, T., and Davis, R. J. (1997). Mitogen-activated protein kinase kinase 7 is an activator of the c-Jun NH2-terminal kinase. Proc Natl Acad Sci U S A *94*, 7337-7342.

Tournier, C., Whitmarsh, A. J., Cavanagh, J., Barrett, T., and Davis, R. J. (1999). The MKK7 gene encodes a group of c-Jun NH2-terminal kinase kinases. Mol Cell Biol *19*, 1569-1581.

Toyooka, Y., Tsunekawa, N., Akasu, R., and Noce, T. (2003). Embryonic stem cells can form germ cells in vitro. Proc Natl Acad Sci U S A *100*, 11457-11462.

Toyoshima, F., Moriguchi, T., and Nishida, E. (1997). Fas induces cytoplasmic apoptotic responses and activation of the MKK7-JNK/SAPK and MKK6-p38 pathways independent of CPP32-like proteases. J Cell Biol *139*, 1005-1015.

Tsuruta, F., Sunayama, J., Mori, Y., Hattori, S., Shimizu, S., Tsujimoto, Y., Yoshioka, K., Masuyama, N., and Gotoh, Y. (2004). JNK promotes Bax translocation to mitochondria through phosphorylation of 14-3-3 proteins. Embo J *23*, 1889-1899.

Ventura, J. J., Cogswell, P., Flavell, R. A., Baldwin, A. S., Jr., and Davis, R. J. (2004). JNK potentiates TNF-stimulated necrosis by increasing the production of cytotoxic reactive oxygen species. Genes Dev *18*, 2905-2915.

Verheij, M., Bose, R., Lin, X. H., Yao, B., Jarvis, W. D., Grant, S., Birrer, M. J., Szabo, E., Zon, L. I., Kyriakis, J. M., *et al.* (1996). Requirement for

ceramide-initiated SAPK/JNK signalling in stress-induced apoptosis. Nature *380*, 75-79.

Verhey, K. J., Meyer, D., Deehan, R., Blenis, J., Schnapp, B. J., Rapoport, T. A., and Margolis, B. (2001). Cargo of kinesin identified as JIP scaffolding proteins and associated signaling molecules. J Cell Biol *152*, 959-970.

Verma, I. M., Stevenson, J. K., Schwarz, E. M., Van Antwerp, D., and Miyamoto, S. (1995). Rel/NF-kappa B/I kappa B family: intimate tales of association and dissociation. Genes Dev *9*, 2723-2735.

Wada, T., Joza, N., Cheng, H. Y., Sasaki, T., Kozieradzki, I., Bachmaier, K., Katada, T., Schreiber, M., Wagner, E. F., Nishina, H., and Penninger, J. M. (2004). MKK7 couples stress signalling to G2/M cell-cycle progression and cellular senescence. Nat Cell Biol *6*, 215-226.

Wall, M. A., Coleman, D. E., Lee, E., Iniguez-Lluhi, J. A., Posner, B. A., Gilman, A. G., and Sprang, S. R. (1995). The structure of the G protein heterotrimer Gi alpha 1 beta 1 gamma 2. Cell *83*, 1047-1058.

Wang, T. H., Popp, D. M., Wang, H. S., Saitoh, M., Mural, J. G., Henley, D. C., Ichijo, H., and Wimalasena, J. (1999). Microtubule dysfunction induced by paclitaxel initiates apoptosis through both c-Jun N-terminal kinase (JNK)-dependent and -independent pathways in ovarian cancer cells. J Biol Chem *274*, 8208-8216.

Wang, T. H., Wang, H. S., Ichijo, H., Giannakakou, P., Foster, J. S., Fojo, T., and Wimalasena, J. (1998). Microtubule-interfering agents activate c-Jun N-terminal kinase/stress-activated protein kinase through both Ras and apoptosis signal-regulating kinase pathways. J Biol Chem *273*, 4928-4936.

Ward, A. C. (1990). Single-step purification of shuttle vectors from yeast for high frequency back-transformation into E. coli. Nucleic Acids Res *18*, 5319.

Waterman, M. S., and Eggert, M. (1987). A new algorithm for best subsequence alignments with application to tRNA-rRNA comparisons. J Mol Biol *197*, 723-728.

Waters, J. C., Mitchison, T. J., Rieder, C. L., and Salmon, E. D. (1996). The kinetochore microtubule minus-end disassembly associated with poleward flux produces a force that can do work. Mol Biol Cell *7*, 1547-1558.

Wertz, I. E., O'Rourke, K. M., Zhang, Z., Dornan, D., Arnott, D., Deshaies, R. J., and Dixit, V. M. (2004). Human De-etiolated-1 regulates c-Jun by assembling a CUL4A ubiquitin ligase. Science *303*, 1371-1374.

Weston, C. R., and Davis, R. J. (2002). The JNK signal transduction pathway. Curr Opin Genet Dev *12*, 14-21.

Whitmarsh, A. J., Cavanagh, J., Tournier, C., Yasuda, J., and Davis, R. J. (1998). A mammalian scaffold complex that selectively mediates MAP kinase activation. Science *281*, 1671-1674.

Whitmarsh, A. J., and Davis, R. J. (1996). Transcription factor AP-1 regulation by mitogen-activated protein kinase signal transduction pathways. J Mol Med *74*, 589-607.

Whitmarsh, A. J., Kuan, C. Y., Kennedy, N. J., Kelkar, N., Haydar, T. F., Mordes, J. P., Appel, M., Rossini, A. A., Jones, S. N., Flavell, R. A., *et al.* (2001). Requirement of the JIP1 scaffold protein for stress-induced JNK activation. Genes Dev *15*, 2421-2432.

Willoughby, E. A., Perkins, G. R., Collins, M. K., and Whitmarsh, A. J. (2003). The JNK-interacting protein-1 scaffold protein targets MAPK phosphatase-7 to dephosphorylate JNK. J Biol Chem *278*, 10731-10736.

Wilson, D. K., Cerna, D., and Chew, E. (2005). The 1.1-angstrom structure of the spindle checkpoint protein Bub3p reveals functional regions. J Biol Chem *280*, 13944-13951.

Wilson, L., and Jordan, M. A. (1994). Microtubules, In Microtubules, J. S. Hyams, and C. W. Lloyd, eds. (New York: John Wiley & Sons), pp. 59-83.

Wisdom, R., Johnson, R. S., and Moore, C. (1999). c-Jun regulates cell cycle progression and apoptosis by distinct mechanisms. Embo J *18*, 188-197.

Wolkowicz, M. J., Coonrod, S. A., Reddi, P. P., Millan, J. L., Hofmann, M. C., and Herr, J. C. (1996). Refinement of the differentiated phenotype of the spermatogenic cell line GC-2spd(ts). Biol Reprod *55*, 923-932.

Wong, C. H., Mruk, D. D., Siu, M. K., and Cheng, C. Y. (2005). Blood-testis barrier dynamics are regulated by {alpha}2-macroglobulin via the c-Jun N-terminal protein kinase pathway. Endocrinology *146*, 1893-1908.

Xia, Y., Makris, C., Su, B., Li, E., Yang, J., Nemerow, G. R., and Karin, M. (2000). MEK kinase 1 is critically required for c-Jun N-terminal kinase activation by proinflammatory stimuli and growth factor-induced cell migration. Proc Natl Acad Sci U S A *97*, 5243-5248.

Xia, Z., Dickens, M., Raingeaud, J., Davis, R. J., and Greenberg, M. E. (1995). Opposing effects of ERK and JNK-p38 MAP kinases on apoptosis. Science *270*, 1326-1331.

Xu, X., Heidenreich, O., Kitajima, I., McGuire, K., Li, Q., Su, B., and Nerenberg, M. (1996). Constitutively activated JNK is associated with HTLV-1 mediated tumorigenesis. Oncogene *13*, 135-142.

Yamamoto, K., Ichijo, H., and Korsmeyer, S. J. (1999). BCL-2 is phosphorylated and inactivated by an ASK1/Jun N-terminal protein kinase pathway normally activated at G(2)/M. Mol Cell Biol *19*, 8469-8478.

Yang, D., Tournier, C., Wysk, M., Lu, H. T., Xu, J., Davis, R. J., and Flavell, R. A. (1997a). Targeted disruption of the MKK4 gene causes embryonic death, inhibition of c-Jun NH2-terminal kinase activation, and defects in AP-1 transcriptional activity. Proc Natl Acad Sci U S A *94*, 3004-3009.

Yang, D. D., Conze, D., Whitmarsh, A. J., Barrett, T., Davis, R. J., Rincon, M., and Flavell, R. A. (1998). Differentiation of CD4+ T cells to Th1 cells requires MAP kinase JNK2. Immunity *9*, 575-585.

Yang, D. D., Kuan, C. Y., Whitmarsh, A. J., Rincon, M., Zheng, T. S., Davis, R. J., Rakic, P., and Flavell, R. A. (1997b). Absence of excitotoxicity-induced apoptosis in the hippocampus of mice lacking the Jnk3 gene. Nature *389*, 865-870.

Yang, J., Lin, Y., Guo, Z., Cheng, J., Huang, J., Deng, L., Liao, W., Chen, Z., Liu, Z., and Su, B. (2001). The essential role of MEKK3 in TNF-induced NF-kappaB activation. Nat Immunol *2*, 620-624.

Yasuda, J., Whitmarsh, A. J., Cavanagh, J., Sharma, M., and Davis, R. J. (1999). The JIP group of mitogen-activated protein kinase scaffold proteins. Mol Cell Biol *19*, 7245-7254.

Yen, T. J., and Schaar, B. T. (1996). Kinetochore function: molecular motors, switches and gates. Curr Opin Cell Biol *8*, 381-388.

Yujiri, T., Fanger, G. R., Garrington, T. P., Schlesinger, T. K., Gibson, S., and Johnson, G. L. (1999). MEK kinase 1 (MEKK1) transduces c-Jun NH2-terminal kinase activation in response to changes in the microtubule cytoskeleton. J Biol Chem *274*, 12605-12610.

Yujiri, T., Sather, S., Fanger, G. R., and Johnson, G. L. (1998). Role of MEKK1 in cell survival and activation of JNK and ERK pathways defined by targeted gene disruption. Science *282*, 1911-1914.

Yujiri, T., Ware, M., Widmann, C., Oyer, R., Russell, D., Chan, E., Zaitsu, Y., Clarke, P., Tyler, K., Oka, Y., *et al.* (2000). MEK kinase 1 gene disruption alters cell migration and c-Jun NH2-terminal kinase regulation but does not cause a measurable defect in NF-kappa B activation. Proc Natl Acad Sci U S A *97*, 7272-7277.

Zanke, B. W., Boudreau, K., Rubie, E., Winnett, E., Tibbles, L. A., Zon, L., Kyriakis, J., Liu, F. F., and Woodgett, J. R. (1996). The stress-activated protein kinase pathway mediates cell death following injury induced by cis-platinum, UV irradiation or heat. Curr Biol *6*, 606-613.

Zecevic, M., Catling, A. D., Eblen, S. T., Renzi, L., Hittle, J. C., Yen, T. J., Gorbsky, G. J., and Weber, M. J. (1998). Active MAP kinase in mitosis: localization at kinetochores and association with the motor protein CENP-E. J Cell Biol *142*, 1547-1558.

Zhang, D., and Nicklas, R. B. (1995). The impact of chromosomes and centrosomes on spindle assembly as observed in living cells. J Cell Biol *129*, 1287-1300.